

REPORT DOCUMENTATION PAGE				Form Approved OMB No. 0704-0188	
<p>The public reporting burden for this collection of information is estimated to average 1 hour per response, including the time for reviewing instructions, searching existing data sources, gathering and maintaining the data needed, and completing and reviewing the collection of information. Send comments regarding this burden estimate or any other aspect of this collection of information, including suggestions for reducing the burden, to the Department of Defense, Executive Service Directorate (0704-0188). Respondents should be aware that notwithstanding any other provision of law, no person shall be subject to any penalty for failing to comply with a collection of information if it does not display a currently valid OMB control number.</p> <p>PLEASE DO NOT RETURN YOUR FORM TO THE ABOVE ORGANIZATION.</p>					
1. REPORT DATE (DD-MM-YYYY) 30-11-2014		2. REPORT TYPE FINAL		3. DATES COVERED (From - To) 9-1-2012 to 8-31-2014	
4. TITLE AND SUBTITLE Fine Scale Modeling and Forecasts of Upper Atmospheric Turbulence for Operational Use.				5a. CONTRACT NUMBER FA9550-12-C-0067	
				5b. GRANT NUMBER FA9550-12-C-0067	
				5c. PROGRAM ELEMENT NUMBER N/A	
6. AUTHOR(S) Mahalov, Alex, PhD., Mackenzie, Timothy. Shaffer, Stephen, PhD.				5d. PROJECT NUMBER N/A	
				5e. TASK NUMBER N/A	
				5f. WORK UNIT NUMBER N/A	
7. PERFORMING ORGANIZATION NAME(S) AND ADDRESS(ES) IntelliWare LLC 8540 E McDowell Road Unit #16 Mesa, AZ 85207-1430				8. PERFORMING ORGANIZATION REPORT NUMBER FINAL	
9. SPONSORING/MONITORING AGENCY NAME(S) AND ADDRESS(ES) AFOSR/RSE Dr. A Nachman 875 N Randolph Road Suite 325, Room 3112 Arlington, VA 22203				10. SPONSOR/MONITOR'S ACRONYM(S) N/A	
				11. SPONSOR/MONITOR'S REPORT NUMBER(S)	
12. DISTRIBUTION/AVAILABILITY STATEMENT Approved for public release.					
13. SUPPLEMENTARY NOTES					
14. ABSTRACT Final status and results of the high resolution mesoscale/microscale modeling and forecasting system with advanced upper troposphere and lower stratosphere physics and fast computational algorithms are described. The Upper Troposphere and Lower Stratosphere (UTLS)-2 v1.0 software, designed to forecast the presence of turbulence in UTLS, demonstrates the utility of the software to generate predictions of turbulent areas and to provide information needed to make a fly or no-fly rating. The UTLS-2 software is now positioned to be transitioned into an operational state for customer-specific applications and operational scenarios that have been identified in this development phase. Models can be adapted to solve other complex problems in complex terrain or urban areas such as biological, chemical, and radiological dispersion.					
15. SUBJECT TERMS numerical weather prediction, modeling, atmospheric processes, turbulence, gravity waves, upper troposphere and lower stratosphere(UTLS).					
16. SECURITY CLASSIFICATION OF:			17. LIMITATION OF ABSTRACT UU	18. NUMBER OF PAGES	19a. NAME OF RESPONSIBLE PERSON Dr. Alex Mahalov
REPORT U	ABSTRACT U	THIS PAGE U			19b. TELEPHONE NUMBER (include area code) (480) 226-2730

20150202030

IntelliWare STTR Phase 2 Final Report, November 2014

Authors: A. Mahalov, T. Mackenzie, S. Shaffer

Executive Summary

Final status and results of the Small Business Technology Transfer Program (STTR) Phase 2 development effort are described, including the High Resolution Mesoscale/Microscale Modeling System with advanced UTLS physics and fast computational algorithms, Upper Troposphere and Lower Stratosphere (UTLS)-2 v1.0 software designed to forecast presence of Turbulence in UTLS. The problem space, transition from the Phase 1 effort, state of the UTLS-2 v1.0 software and other results of this phase of development as well as how the project is positioned for future phases, are reported.

The products developed during Phase 2 demonstrate the utility of the software to generate predictions of turbulent areas and to provide information needed to make a fly or no-fly rating. It also demonstrates analysis for the rotational shear stratified turbulence generation mechanism (polarized Richardson number, variable turbulent Prandtl number), which is new to operational UTLS turbulence forecasting products.

The software is now being transitioned into an operational state for customer-specific applications and operational scenarios that have been identified in this development phase.

Essentially all current operational models de-emphasize UTLS: (1) current models have very low vertical resolution near the tropopause; (2) current operational models use the same equation solving methods at all levels of the model and incorrect 'boundary layer' physics at UTLS altitudes.

UTLS-2 software uses targeted physics based modeling, fast and accurate computational techniques that take into account the shear-stratified turbulence physics, therefore the outcome is superior UTLS products and forecasts.

Introduction

Forecast of Clear Air Turbulence (CAT) is an ongoing challenge for both commercial and military flights. High impact CAT in the Upper Troposphere and Lower Stratosphere (UTLS) region can impact the safety of personnel and the equipment as well as the successful operation of the aircraft, airborne remote sensing platforms, weapons, and communication systems. For example, flying through CAT can cause the autopilot to begin pitch oscillations that seriously degrade photographic and synthetic aperture radar performance as well as put the platform itself at risk. High altitude CAT is a major challenge to the safety, controllability and flight path optimization of the U2, Predator, Global Hawk and other Unmanned Aerial Vehicles (UAVs) and Platforms.

As CAT cannot be visually detected by pilots, timely creation of predictions both of location and intensity of such CAT is an important component in flight track and other planning activities. As such, this software has been developed to assist in rapid analysis and generation of predictions for CAT, using generation mechanisms and flexibility not supported in contemporary analysis software. The UTLS-2 software uses High Resolution Mesoscale/Microscale (HRMM) simulation data to produce various metrics and allows an operator to perform further analysis in order to generate such predictions.

The software aims to answer these two main questions:

- Is the presence of CAT predicted in a particular point or geographic region of interest at a particular time?
- And, if CAT is predicted, what are the defining characteristics such as time, latitude, longitude, altitude, flight level, and intensity?

Addressing Limitations of Contemporary Software

Contemporary software and technologies were researched in this phase to understand existing capabilities and limitations as well as relevant interfaces. While an exhaustive review of such options is outside of the scope of this report, a brief overview of selected limitations is presented here to provide context for the needs that this software addresses.

Contemporary turbulence metrics and analysis products are constrained in their domain size and spatial resolution, as well as the time resolution. For example, the Aviation Weather Center Digital Data Service (ADDS) [<http://www.aviationweather.gov/adds>, <http://weather.aero/>] Graphical Turbulence Guidance product, GTG-2.5 [<http://www.aviationweather.gov/turbulence>], produces CONUS forecast updates every hour for several different snapshot times up to 12 hours in advance. These outputs are limited to a fixed altitude range, a 12.5km horizontal grid, and approximately 700 feet per vertical level. In addition, the product explicitly states that the snapshots are valid for the specified time, not for any range of times. As such, many planning scenarios cannot be fully validated using that product.

Two typical planning categories are strategic, for about 24h advance to plan the routing for the next day, and tactical, which might be for a 20 minute window to support hazard avoidance for

short time horizon mission planning. Both of these types of planning are difficult with current forecast tools and available data because the spatial and temporal resolution of automatically generated data sets may be too low, and the time to generate on-demand forecasts may exceed the available time for the planning window. The UTLS-2 software seeks to mitigate these planning difficulties.

One particular advantage of the UTLS-2 software is that it has the flexibility for creating a domain anywhere in the world, with full control over the horizontal grid size, vertical level spacing, and temporal resolution. It can focus on a small area with a fine grid to improve accuracy of predictions. Combined with the ability to perform analysis with higher temporal resolution, meaning nesting in time, this software can support a much more detailed analysis of a region of interest.

Since large domains typically have coarse spatial grid resolution, the dynamic phenomena which can be explicitly resolved is limited. By using an HRMM with vertical nesting capability, such limitations can be overcome for limited areas using available computational resources. The ability to tailor the region and resolution of analysis of the input HRMM is critical to identifying shorter duration CAT anomalies which may be false negatives by other methods. This software has the capability to interrogate thin layers - on the order of 10's to 100's of meters thick, and horizontal extents below a few kilometers.

Beyond the additional flexibility, this software introduces an analysis process for detecting a shear stratified turbulence generation mechanism, polarized Richardson number and variable turbulent Prandtl number are new to operational UTLS turbulence forecasting products, known as rotational shear instability. Through data display and analysis tools, this software allows a user to determine a likely location for CAT, and then generate predictions of rotational shear instability that would indicate the presence or absence of CAT.

This software also has the capability to perform analysis of other commonly used metrics for instability to assist in analyzing the region of interest. This can support performing a more complete assessment of the conditions as well as a comparison between the available metrics and turbulence generation mechanisms to generate a final prediction.

For external reporting, the PIREP User Interface (UI) investigation led to an internal report that informed the Turbulence Report (TR) format, as described in the *Turbulence Report* section. Being voluntarily self-reported by pilots, PIREP data is only available for the times and locations of flights, with limited completeness in reported events. Furthermore, PIREP data are not always shared between collecting agencies and companies, even when collection is prioritized. Since this existing PIREP data does not currently provide a comprehensive picture of turbulence in a region, the Turbulence Report is designed to support creating outputs compatible with PIREP reporting systems to enhance flight planning operations.

Goals of This Software

The broad goal of this project (through all phases) is to complete the phase 2 development of a technologically superior modeling system, in support of success of the operational outcomes of the warfighter, and to improve safety for the Federal Aviation Administration and aviation industry. This modeling system is also intended for adaptation to resolve forecasting problems in complex terrain or urban areas for biological, chemical, and radiological dispersion. Applications for these adapted models will be useful to the Department of Homeland Security, and the growing field of wind energy producers. Shaffer and Mahalov have developed novel techniques based on fractional land cover representation in computational grid cells and performed evaluation of subgrid land use information. These methods improved accuracy of forecasting in complex terrain and urban areas.

To support the broad goal and primary questions indicated above during Phase 2 of the project, several more specific software goals were defined to support an analysis workflow. The following summarizes the more detailed software goals and internal requirements developed in support of implementation of the UTLS-2 v1.0 software, as described further in the Software Architecture and other sections in this report:

- View vertical cross sections of HRMM data and derived data as well as profiles therein to observe metrics indicative of UTLS turbulence (e.g. polarized Richardson number and variable turbulent Prandtl number) for the purpose of identifying a subset of the simulation domain or region of interest within which to run the CAT Solver for further analysis.
- Configure and launch the Solver to predict CAT resulting from rotational shear instability.
- Determine predicted presence and characteristics of CAT by inspecting Solver results for the presence of instabilities predicted using the polarized Richardson number threshold.
- Save displayed figures (such as cross sections, vertical profile plots, and hodographs) with associated displayed metadata for reference or further analysis.
- Produce an easy-to-read report of turbulence predictions from the Solver which can be saved for further analysis or used in conjunction with external turbulence reporting systems.

A 'fly' or 'no-fly' rating for a particular point, region, or route is not prescribed by the v1.0 software. Such a decision needs to be informed by variables such as customer thresholds for allowable turbulence, the type of aircraft, the type of flight path, the cargo, and if any in-flight operations need to be accounted for. These details can cause a significant variance with a fly or no-fly rating for the same predicted turbulence, so the v1.0 software limits assessment to the prediction of existence of turbulence and gives the operator the information to make fly or no-fly decisions.

This report covers the technology background, additional internal goals developed to complete the software, the software architecture (both internal and user interface components), and the infrastructure required by the project to perform ongoing design and development. It covers the data set used in the baseline workflow and describes the workflow itself. Finally, it covers plans

for moving into the operational phase, and then wraps up in summary. Supplementary material is located in the appendices.

The first-stage of processing takes existing global or regional weather analysis data sets, such as data from the National Center for Environmental Prediction (NCEP) Final Operational Model Global Tropospheric Analysis (FNL) <http://rda.ucar.edu/datasets/ds083.2> , ECMWF T799L91 (25km horizontal resolution and 91 vertical levels) or High Resolution Rapid Refresh (HRRR) <http://ruc.noaa.gov/hrrr> , and performs a simulation for a region of interest at the desired horizontal resolution (e.g. 1 km) and vertical resolution (arbitrary). This is where the location and resolution can be tailored to provide a higher level of detail than available national or global models provide. As resolution is correlated with processing time and required hardware, criteria for the specific application can inform the selection of resolution.

Examples of compatible HRMM data sources include but are not limited to Weather Research and Forecasting mesoscale model (WRF) such as WRF ARW and WRF NMM, Unified Model [Andrew Brown, Sean Milton, Mike Cullen, Brian Golding, John Mitchell, and Ann Shelly (2012), <http://www.metoffice.gov.uk/research/modelling-systems/unified-model> , developed by the UK Met Office, doi: <http://dx.doi.org/10.1175/BAMS-D-12-00018.1>

Following the generation of the simulation data, further analysis is performed to assess the risk of turbulence. In the UTLS-2 v1.0 software, this analysis is performed both by viewing the simulation data to identify a region of interest, and also by performing a second processing step using the Solver to produce more detailed predictions using a new metric.

Software Architecture

The UTLS-2 v1.0 software is composed of three major UI components:

- The Cross-Section Viewer (CSV), which allows analyzing and visualizing both variables typically packaged with the HRMM simulation data source as well as variables derived from those included variables.
- The Solver Configuration Interface (SCI), which configures and runs the CAT Solver
- The Solver Output Viewer (SOV), which allows viewing hodographs and supporting data generated by the Solver. This final step shows if CAT is predicted by the rotational shear generation mechanism, as measured by the polarized Richardson number, and provides additional data to assist in validation efforts.
- Turbulence Report (TR) - this report, aligned with PIREP data fields, describes existence and nature of turbulence predicted by the solver.

Additional sub-components accessed through the main UI components described above:

- Clear Air Turbulence (CAT) Solver - this processing engine has no graphical UI, and is configured through the Solver Configuration Interface to run one of the available solver methods.

Refer to Figure 1 for a workflow showing the interaction between these UI components.

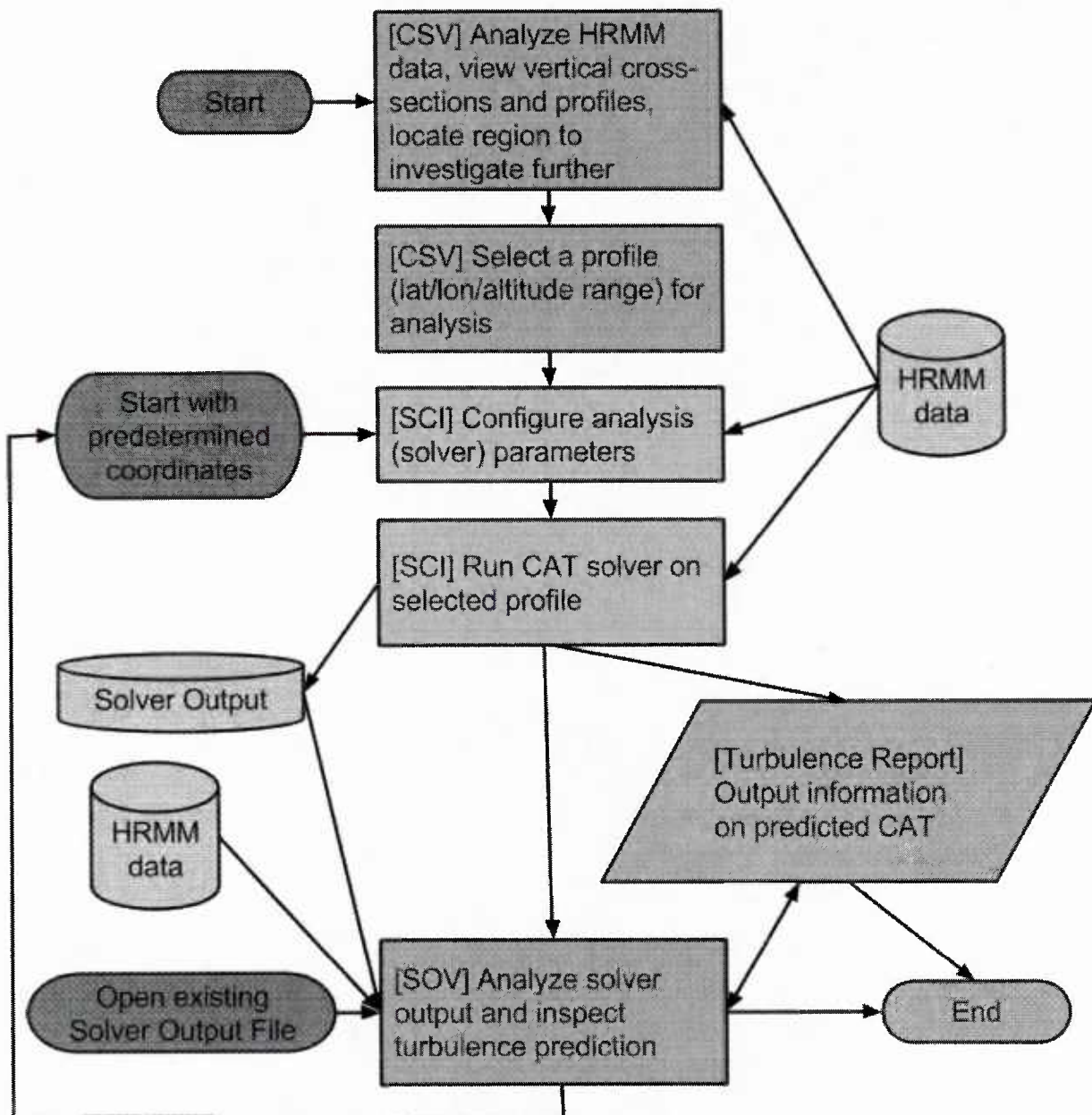


Figure 1: Simplified Analysis Workflow

Legend

CSV	Cross Section Viewer
SCI	Solver Configuration Interface
SOV	Solver Output Viewer
HRMM	High Resolution Mesoscale/Microscale

Figure 2: Legend for Simplified Workflow

The end result of the analysis workflow is a prediction of the existence of CAT in a particular region, described in terms of standard flight levels. This enables the predicted CAT data to be used in the generation of outputs that conform to the pilot report, or PIREP, of turbulence standard. Discovery of potential CAT hazards not predicted by contemporary analysis methods can help make the forecast more complete and accurate, which makes this data useful in conjunction with, rather than instead of, contemporary data sources.

Top Level Components

Cross-Section Viewer (CSV)

The CSV, shown in Figure 3, is the first interface when starting analysis without predetermined coordinates. It allows visualizing and analyzing both variables typically packaged with the HRMM simulation data source as well as variables derived from those included variables, as both 2D vertical cross-sections and 1D vertical profiles. This includes the polarized Richardson number index used by this process as an indicator of instability and shear-stratified turbulence in UTLS.

Variables derived from typical HRMM variables, known as User Defined Variables (UDVs), are a way to extend this analysis framework to include other metrics, such as those used in contemporary turbulence forecasting systems. Beyond the Polarized Richardson Number criteria (Ri_c), additional variables are described in Appendix C: UDV table. While many of these metrics are not considered current best indicators of turbulence, they are available to allow comparing various metrics and analysis systems.

After loading an HRMM data file, the CSV UI presents controls to adjust

- The selected simulation data file
- The variable to display
- The variable orientation and vertical range (on load)
- The frame and vertical profile index (resulting in the lat/lon for display)
- Feature toggles such as the vertical profile bounding box, the scale lock, and colorbar-related controls
- The “Jump To Location” button
- The “Capture Screen” button
- The solver launcher controls

Additionally, the CSV displays information such as

- Variable metadata such as the units and the direction
- The vertical profile plot with the terrain line and threshold value, when appropriate
- The cross-section image
- The lat/lon coordinates corresponding to the selected frame and vertical profile index
- The colorbar scale

For annotated images of these figures, refer to Appendix C.

After selecting a point of interest, the SCI can be directly invoked to configure and run the Solver for further analysis.

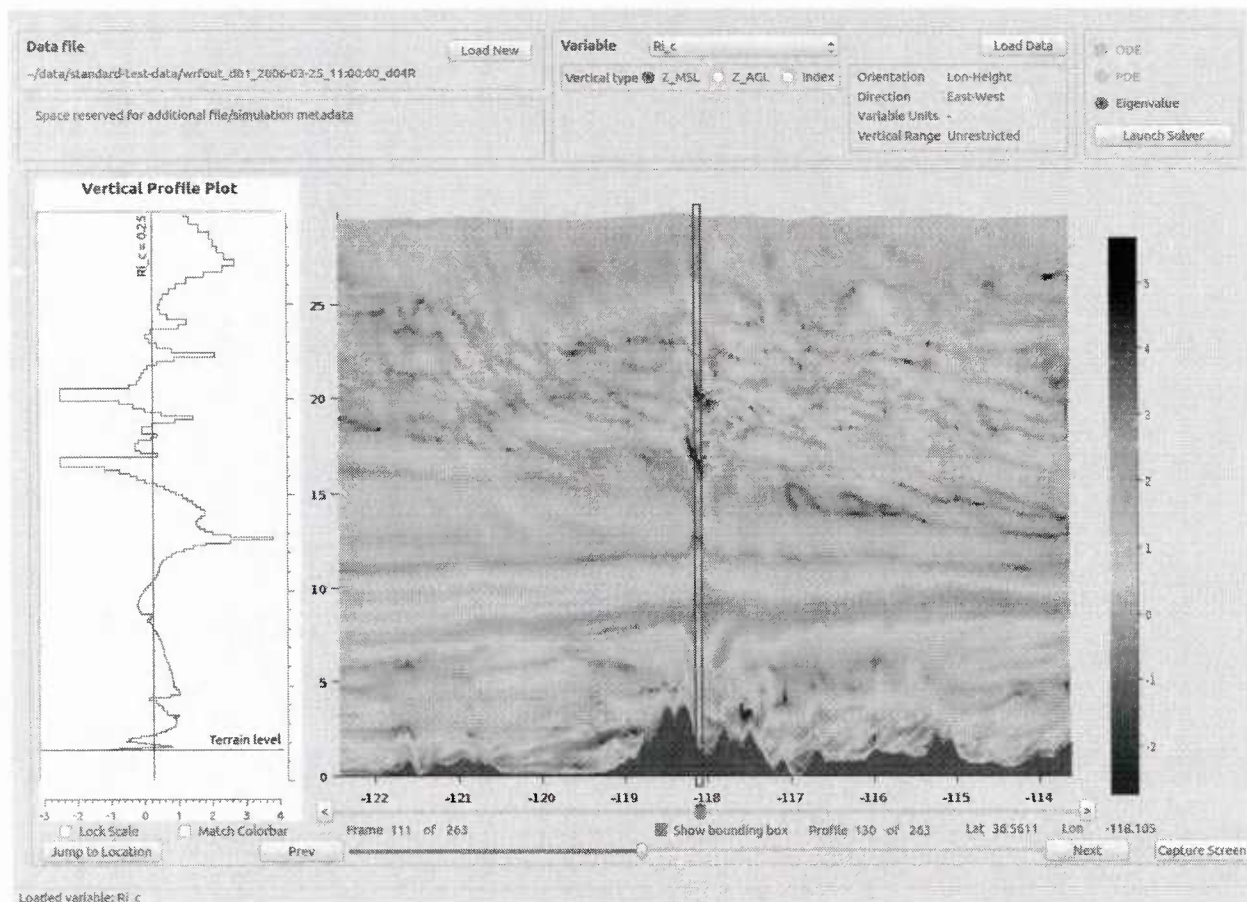


Figure 3: CSV

Solver Configuration Interface (SCI)

The SCI, shown in Figure 4, allows configuring and launching the Solver based on a location of interest selected through analysis using the CSV, or an alternative starting point when the analysis coordinates are predetermined.

Inputs to the SCI are grouped as such:

- **Input Details** - the simulation file as well as time and location for which to perform the analysis
- **Processing Details** - the machine used to perform processing and the output file to store the results in
- **Method Details** - the method to perform analysis with and the number of vertical levels to employ.
- **Solver Details** - the altitude range as well as parameters for the solver algorithm to use
- **Map** - an HRMM map as well as a Google map (when available)

Appendix E contains an annotated version of this figure and associated descriptions.

The input details are automatically populated when the location information is transferred from the CSV. If this has not occurred, the simulation file as well as the latitude and longitude must be selected to configure the region of analysis.

Next, the Processing Details section allow selecting the target machine to do the processing (currently limited to the local machine), and the number of cores to use. In some cases it may be preferable to use less than the maximum number of processor cores on the local machine to allow other processes to operate simultaneously. When cluster processing is enabled, configuring the number of processor cores to use will be essential for batch processing management.

In the Method Details section, the number of vertical levels (NX3) can be selected, and in conjunction with the altitude range selections in the Solver Details section this controls the vertical distance covered by each vertical level. For example, with 200 levels between 5 km and 15 km MSL the solver's vertical resolution is 50 meters. Typical values for vertical levels in the solver output are 50 to 200, depending upon analysis altitude range or desired resolution, with a minimum of 4 levels.

The Solver Details section contains a number of parameters that affect how the solver will apply the selected method. The NK1 and NK2 values can be automatically selected from presets, or manually adjusted. These values affect the resolution of the analysis and affect the processing time and output file size, as well as the probability of capturing every instability in the region of analysis. Next the K1 and K2 min and max values can be configured either as k or λ , wavenumber or wavelength, respectively. These affect the same factors as the resolution. Finally, the MSL min and max entries allow restricting the altitude range for analysis. In conjunction with the number of vertical levels as described above, this affects the vertical distance covered by each vertical level. In addition, this range can limit or include phenomena at specific altitudes, so when higher altitude (e.g. above 20 km) phenomena are being investigated from the CSV, the range should be adjusted to include all altitudes with potential instabilities. Alternatively, this range can be used to exclude regions of known instabilities that are not of interest to the current analysis.

To provide context, the final section of the SCI provides two map options. The default map option requires no internet connection, and uses the HRMM simulation data to construct a terrain map, and displays a marker at the selected latitude and longitude. A second option displays Google Maps content for the selected region, with a pin at the selected latitude and longitude. This display includes zoom controls as well as overlay options including map, terrain, and satellite. The Google Map display requires an active internet connection, and will not display any map data when in offline mode.

Once the Solver has been run, the confirmation dialog shows a summary and gives the option to view the TR or launch the SCI to view the Solver Output File (SOF) created by the Solver.

Input Details

Input File

~/data/standard-test-data/wrfout_d01_2006-03-25_11:00:00_d04R

Change

Latitude

36.5611

130

Longitude

-118.105

111

Time

2006-03-25 11:00:00

Domain

d01

x3 [min, max]

1

179

Solver Details

NK1/NK2 presets

[30, 60] medium-resolution

NK1

NK2

30

60

k

lambda

k1 min

0.25 km⁻¹

25.133 km

k1 max

10.00 km⁻¹

0.628 km

k2 min

0.25 km⁻¹

25.133 km

k2 max

10.00 km⁻¹

0.628 km

msl min

0.00 km

msl max

22.00 km

Processing Details

Processor cores

8

Machine

Local

Change

Output location

/home/iwdev1/data

Change

Method Details

Method

Eigenvalue

Change

Vertical Levels

50

☒ Show Map

Google

HRMM

Start Solver

Capture Screen

Loaded file: ~/data/standard-test-data/wrfout_d01_2006-03-25_11:00:00_d04R

Figure 4: SCI

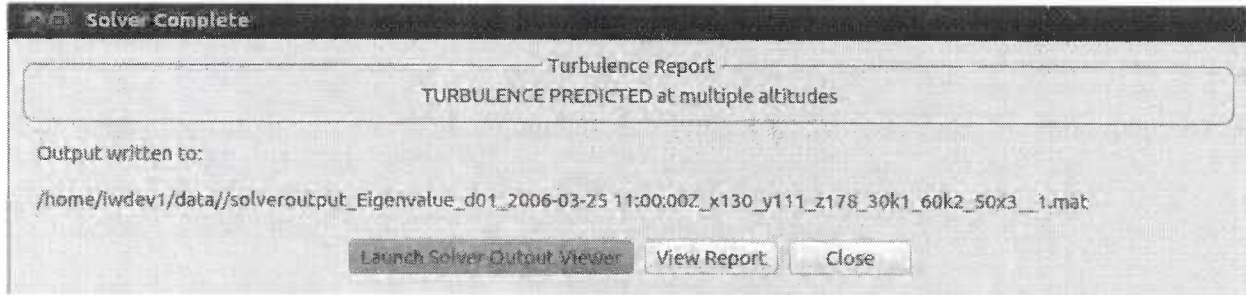


Figure 5: SCI Solver Complete dialog

Solver Output Viewer (SOV)

The final phase of analysis is performed using the SOV, shown in Figure 6, which supports several types of analysis of the data in the Solver Output File generated by the CAT Solver. If launched from the SCI, the SOF is automatically loaded and displayed. These files are saved to disk, and can also be loaded manually in the SOV.

Refer to Appendix E for an annotated figure describing the controls.

The SOV has controls to select the SOF and once loaded has controls to view the parameters used for the solver. The TR summary is expanded to the full report with the Turbulence Report button.

The Vertical Profile Plot can be configured to show various metrics as well as a red bar to show instability bands. The instabilities match the altitude ranges described in the Turbulence report, so this display offers a different way to visualize the results.

The Hodograph display can select between three different modes:

- The profiles of horizontal velocity components U and V
- Wavenumber and wavelength derived from the maximum unstable eigenvalue at each vertical level of solver output
- The most unstable eigenvalue at each vertical level for all wavenumber pairs used within the solver.

These plots allow investigating if CAT is predicted by the rotational shear generation mechanism, as measured by the polarized Richardson number, and provides additional data to assist in validation efforts.

The X3 slider and Jump-To button allow selection of a vertical level to focus on, which causes the corresponding point on the hodograph to be highlighted with a bounding box as well as an arrow originating at the center of the graph, if those options are enabled. In addition, the hodograph colorbar displays a marker at the selected vertical altitude to help correlate the colorbar value to the point for the selected vertical level.

A final component is the Horizontal Slices viewer for algorithm and solver validation purposes. This display can be selected in place of the hodograph display.

As with the other UI components, the Capture Screen button can be used to capture the display for reporting or further analysis.

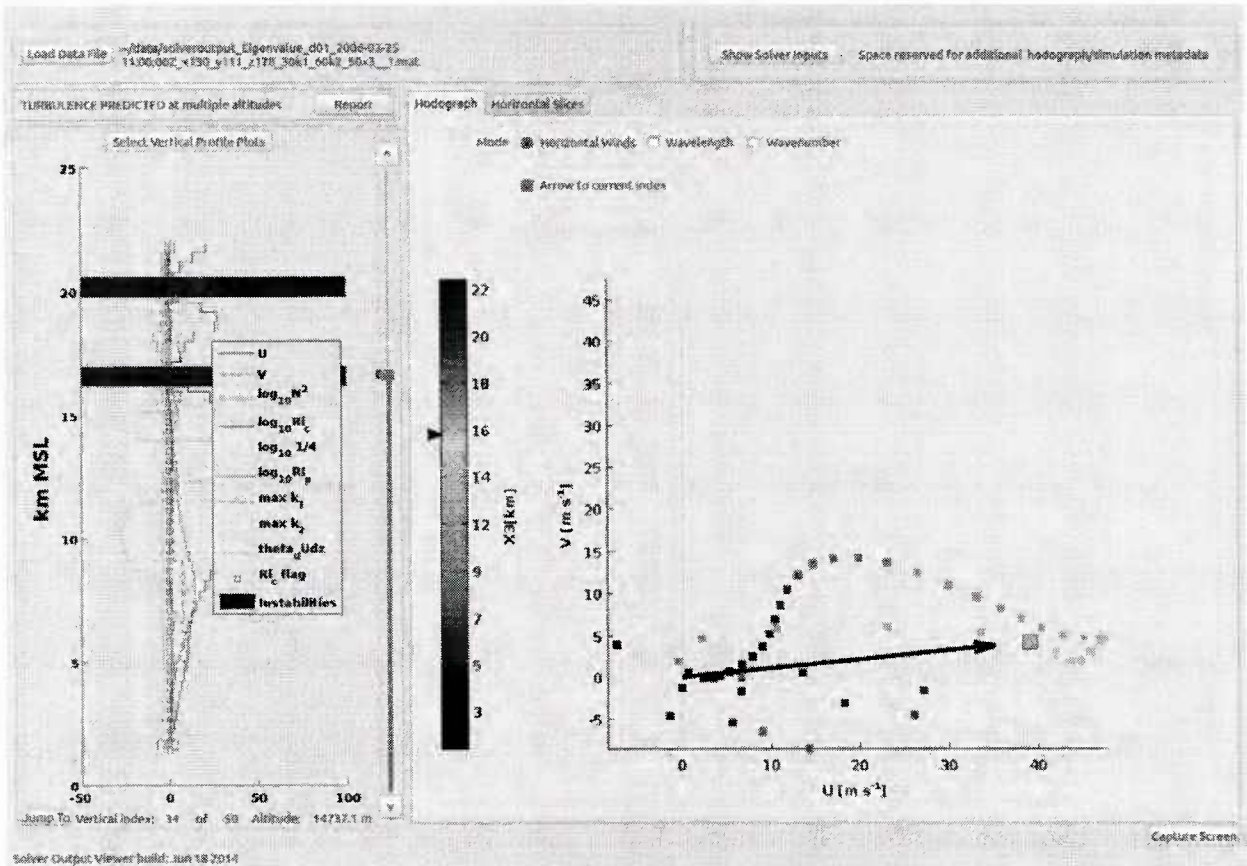


Figure 6: SOV

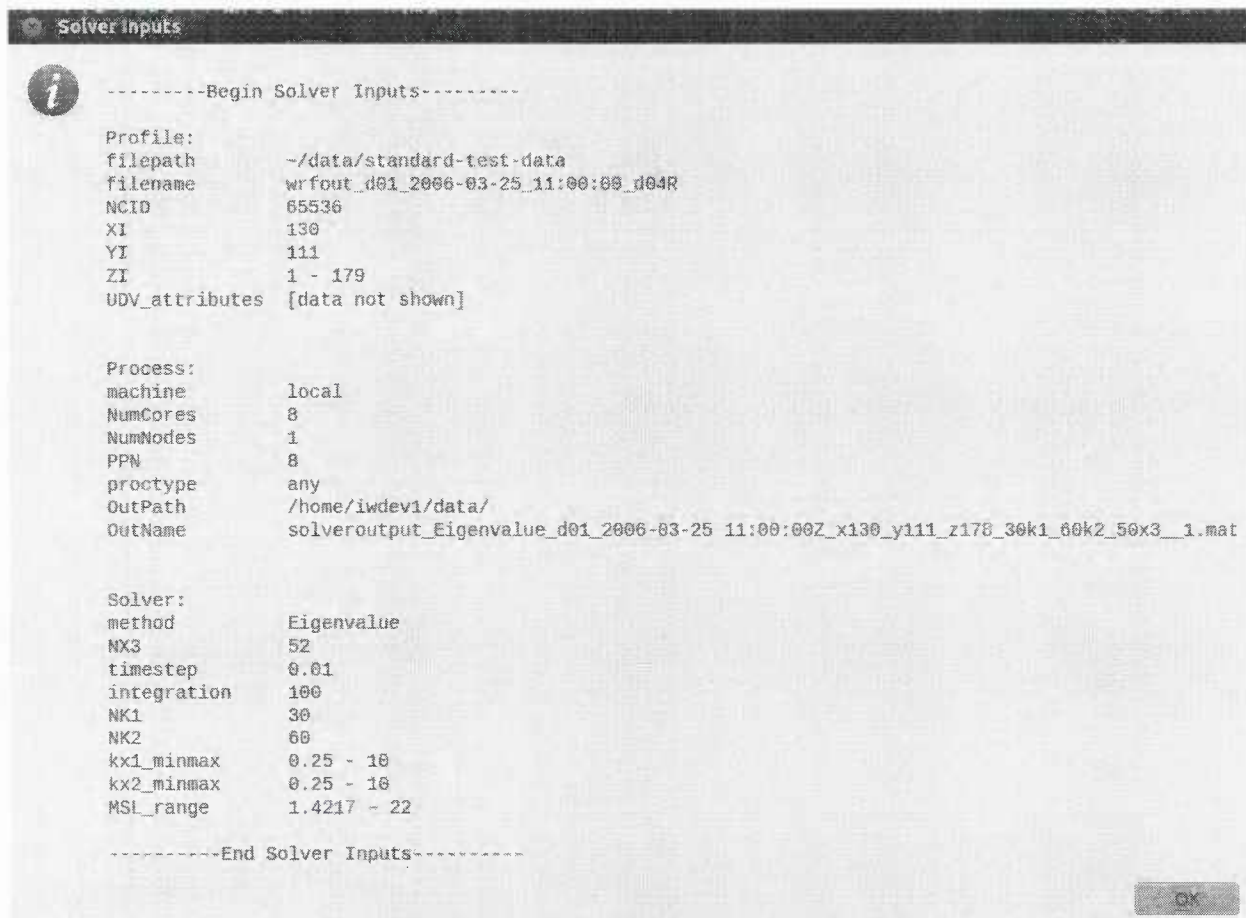


Figure 7: SOV Inputs

Turbulence Report (TR)

The TR is a streamlined textual report of predicted turbulence with additional data to characterize the predictions.

The TR has two components - the summary and the detailed report. The summary is more compact and is visible directly in the SCI and SOV without further interaction. When desired, the detailed report can be opened for inspection, analysis, and export.

The current format of the Turbulence Report, seen in Figure 8, shows:

1. The single-profile Solver Output File that the report describes
2. Latitude, Longitude, and time being analyzed
3. Altitude range that the solver used in producing the Solver Output File
4. Turbulence Summary - one of:
 - a. No turbulence predicted
 - b. Turbulence predicted at a single altitude
 - c. Turbulence predicted at multiple altitudes
5. Turbulence details, with adjacent detections described as a range
 - a. Number of adjacent levels included in each detection
 - b. Altitude in meters MSL

- c. Estimated corresponding Standard Flight Levels
- d. Growth factor for the instability in 20 minutes

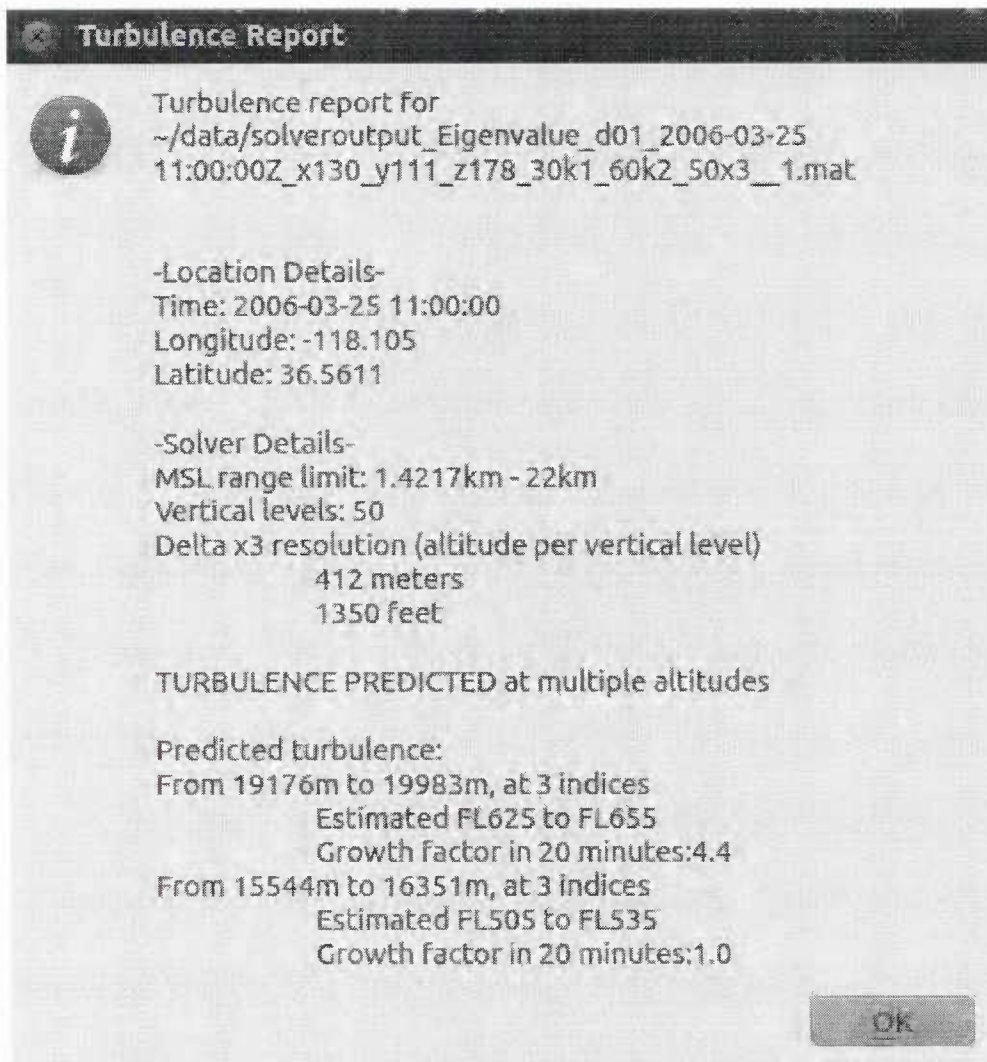


Figure 8: Turbulence Report

The intention for the current format and content of the Turbulence Report is to allow the full report or any portion to be selected and copied for use in documentation or to communicate with parties interested in the results of the analysis. This report is designed to be able to assemble multiple types of data generated by this software into a coherent output so as to support current CAT analysis methods, results of contemporary analysis methods, and results of methods scheduled for future releases of the UTLS software.

The Turbulence Report is available immediately after the SCI completes running the solver, with the short report summarizing the solver findings, shown in the Solver Complete Dialog seen in Figure 5. The user can opt to view the detailed Turbulence Report, close the dialog and continue interfacing with the SCI to run the solver again, or proceed directly to the SOV.

Parameter sensitivity can be investigated by configuring and running the Solver for different settings and investigating the detailed results within the SOV.

The Turbulence Report is available in the SOV, as shown in Figure 6, to support three capabilities. First, this allows opening previously generated Solver Output Files and viewing all relevant data. Inclusion of the Solver Inputs display aims to enable reproducibility of the experiment by giving the parameters that were used to generate the Solver Output File. Second, having the report available assists with analyzing and correlating the hodograph, vertical slice data, and the vertical profile plot. Finally, the report itself contains a condensed and formatted output that can be used to communicate the results of analysis to external parties through formats such as email, written reports, and potentially through established PIREP compatible reporting mechanisms.

The internal PIREP UI report investigated contemporary reporting mechanisms and relevant data that is of use in communicating turbulence. It has informed the format and content of the TR available in UTLS-2 v1.0, as described above.

Sub-Components

Clear Air Turbulence (CAT) Solver

The Clear Air Turbulence (CAT) Solver performs processing of input HRMM meteorological data using parameters supplied by the SCI. The resulting output is a Solver Output File which encapsulates the input parameters, analysis results and associated data, and the Turbulence Report. Analysis of the outputs is described in the *SOV* and *TR* sections.

Performance and Parallelization

The solver can independently process each wavenumber pair (or wavevector), as well as each meteorological profile. This means that the solver can be scaled to run on a high performance computing cluster because it is completely parallelizable. For a fixed set of hardware, processing time can be controlled by selection of the available number of processors and other parameters in the SCI. See the *SCI* section for discussion of input parameters.

Project Infrastructure

Additional infrastructure has been both designed and created to provide support for the continuing software development and testing of the deliverable software. Separate from the software specifications that defines the deliverable software, this infrastructure includes processes and additional software, and is a necessary component of the software development process. This section summarizes some of the critical infrastructure efforts.

Task Management

A cloud-based project task management site has been used to track unimplemented features, known bugs to be fixed, and other issues to investigate. This system allows a lightweight way to manage multiple priority timeframes, assign implementers to tasks, and capture both discussions and relevant data for each issue. Bugs that require more thorough investigation are tracked in the bug tracker. This tracker is based in the cloud with the project documentation and captures more specific details such as software versions tested, who is assigned to investigate,

screen captures showing the issue, and data files required to recreate the problem. Both the task management site and the bug tracker support archiving closed issues, which allows for review of previous issues when necessary.

Prioritization and scheduling of these tasks has allowed tracking remaining work expected for target versions such as the v1.0 software. Additional target versions were identified to separate short-term and longer-term goals and priorities. The task list was highly dynamic as issues were resolved, new ones were discovered through testing, and priorities were adjusted.

Data Size

The simulation output is data intensive, and requires storage and retrieval of a large amount of information.

The anticipated data is expected to be a 4 dimensional grid (3 spatial dimensions and 1 time dimension), each with a resolution, N , between 400 and 2000 data points. An evaluation upper limit treated variables as being of size $(N_{\max})^4$ to ensure scalability of results, with the cross-section data to be extracted as an array of 2 dimensional slices. The 2-D cross-sections and hodograph cross-sections have similar data needs and thus are treated similarly.

Each point represents a 64-bit data value, which corresponds to 8 bytes. Generating images with full color depth for $N_{\max} = 2000$ results in the following maximum size information:

- 2-D cross-section images at $N_{\max} \times N_{\max}$ in size would be 30.5 MB in size,
- A full set of N_{\max} cross-section images would be 59.6 GB,
- A set of N_{\max} vertical profile data points for a set of cross-sections would be 30.5 MB.

Computing Hardware

CAT hazard detection, at a high level, involves two separate processor-intensive steps. First, a HRMM simulation is run on current conditions to create the simulation files needed by our unique software. Next, the CAT Solver creates the detailed forecasts.

Hardware requirements including storage space and processing power were evaluated to ensure that the development environments could support the expected workloads. In addition, the workflow was evaluated to determine acceptable performance time for each step and ensure that the selected hardware is expected to meet these expectations.

Data requirements, deployment environment, and performance expectations were assessed to evaluate the suitability of various languages and architectures for software development.

Operational criteria used for evaluating technology and architecture were:

- Loading each cross-section is a synchronous activity but does not need to be immediate, and should occur within a reasonable amount of time.
- Iterating through vertical profile data for a cross section is a synchronous activity and should be seamless.
- Generating simulation data and running algorithms such as the CAT solver are highly processing speed dependent, and do not need to occur synchronously with user interaction.

- Loading a new slice of a previously generated Solver output data set is a synchronous activity and should occur within a reasonable amount of time.

Our software also takes advantage of the faster processing speed of C++ and the rapid cross-platform-compatible UI capabilities of Qt.

Internal Documentation

These documentation components were essential to ensure that initial development met project goals and enabled scalability as the software grew in scope.

The specification documents provide information such as:

- The purpose of this component
- Preconditions for this component to operate
- Details of how this component operates and interacts with other components
- Description of data storage format and data interchange with other components
- The workflow, or sequence of events that this component/system is involved in
- Performance expectations
- Scope restrictions, describing functionality that is out of scope for the current phase
- Output produced by this component (such as data or interaction with other components)

The project also retained records such as the Release Log, which tracks the changes between internal releases. The Release Log will also support creating a summary change log for major releases after v1.0.

In addition, procedural documentation has been maintained including:

- The *Build Methodology* procedure, which describes how the internal and external deliverable software is built from the software sources
- The *Baseline Test* procedure, which performs the standard regression test for each build to ensure that all components function properly and that no new issues have been introduced.
- Development and operational machine setup and maintenance instructions

Internal Software

Internal software, which is not included in the deployment packages, has been developed for tasks such as creating the deployment package for internal builds and the deliverable software.

Software has also been developed to prepare the target machine to run the software and enables rapid deployment of builds to test and operational machines. This software is included in the deployment package.

Additional Technology Infrastructure

Data integrity and safety is ensured by a process for backups and redundancy.

- Documentation is maintained in the cloud as well as backed up periodically to local media.
- All developed software is backed up both locally and within a remote versioned repository.

Local software version control is handled with Git <http://git-scm.com> , and is also maintained remotely with BitBucket software tools. This allows a lightweight method to keep the developer repositories synchronized as well as to provide safety in case updates need to be reverted or investigated further. Increased protection has been provided by ensuring that this code is stored in a separate versioned repository and never transmitted over the internet or stored on an external server in an unencrypted state. An encrypted transport mechanism has been developed and deployed, and is in use between development machines.

Testing

Unit testing was completed by the developers to validate proper operation of the code in isolation of other functionality, and was performed during development. Internal builds, which were generally created bi-weekly, contain a snapshot of the current versions of all software components on a specific date. Internal builds were versioned and archived, which enables tracking revision history at a higher level than tracked by the software repository, as well as providing a reference of previous software for use when resolving issues.

Each build receives a more thorough test by different members of the team to verify the most recent changes. The *Baseline Test* procedure, seen in Appendix D, is part of the evolving regression test and was established to maintain consistency of evaluation across builds. Unstructured component testing was also employed. After testing, comments and all discovered issues were discussed with the UI developer to process into tasks and to determine priority and schedule.

Current Software Capabilities

At present, the UTLS-2 v1.0 software helps answer the two primary questions identified at the outset, both to identify and to characterize potential CAT hazards in a region of interest at a specific time. The analysis workflow utilizes the CSV, SCI and SOV to locate a region of interest to perform further analysis and then generates a prediction of turbulence.

The Baseline Test illustrates the workflow required for an operator to use the software to perform this analysis. While the interface and outputs at several steps can be captured for further evaluation as well as recreation of the analysis state, the primary output is the Turbulence Report, which contains a summary of the predicted turbulence and related details. The TR can be used to produce outputs compatible with the PIREP standard as well as to inform fly or no-fly decisions.

Data source: Validation and Verification

The performance of HRMM/UTLS-2 software was tested against the fine-scale meteorological data sets, aircraft measurements and PIREPs. Terrain Induced Rotor Experiment (T-REX)

[https://www.eol.ucar.edu/field_projects/t-rex], was chosen to demonstrate extension of real-time forecasting tools within specific regional-scale domains in complex terrains. The HRMM simulation outputs overlap with the Intensive Observational Periods (IOPs), making it possible to validate simulation results against measured inputs. Analyses of turbulence cases also included reports of turbulence provided by pilots of commercial airlines (pilot reports, PIREPs). The selection of cases in 2012-2013 was based mostly on the height of the (severe) turbulence being at least 30,000 feet AGL. Details are given in Appendix E.

Baseline Workflow

While there are many scenarios that the v1.0 feature set and goals can address, the primary scenario used in analysis is described by the Baseline Test. This test involves analyzing a known location of potential instability within the HRMM dataset and assessing the probability that turbulence exists in that region.

The software is used to locate the most appropriate location to analyze further, to generate a prediction, and to assess if the predicted conditions match the defined threshold for a region of CAT. This assessment is accomplished by using the CSV to iterate through generated cross-sections of selected metrics over a region of interest to locate a specific location that merits further investigation. The Solver (accessed through the SCI) generates the Solver Output File and the Turbulence Report, which can be assessed through the SOV and the Turbulence Report viewer to determine if the selected location and time represent a predicted region of CAT.

The end result of this scenario is information to help make a decision - typically fly or no-fly rating for a particular region. This information presented in the TR is formatted and ready to disseminate externally to allow a third party to make the fly or no-fly decision.

The *Baseline Workflow* procedure is described in full in *Appendix B* as the Baseline Test.

Considerations for Operational Phase

The UTLS-2 v1.0 software produced in Phase 2 demonstrates some of the potential uses of the analysis software and the new instability generation mechanism that it can detect. It presents an opportunity to springboard into some of the already-defined operational scenarios.

Forecasting timeframes fall into several categories:

- 'Next Day Planning' or 'Strategic' - routine, ongoing planning for 24h in advance that may cover a large area
- 'Extreme Event' Planning, where an abnormal weather event necessitates precise planning over a short period with short notice in order to avoid unexpected turbulent areas
- 'Hot Spot' planning where a region periodically requires additional attention due to intermittent conditions
- 'Tactical' planning, where frequent short-term prediction updates may be needed for the upcoming 20 minutes

Each of these time frames require different processing hardware, personnel, and systems to both configure the simulations and to disseminate the resulting predictions.

Some of the anticipated scenarios driven by customer decision needs include:

1. Generation of a dichotomous “fly” versus “no-fly” rating for a point or region to ensure avoidance of turbulence above a critical threshold
2. Production of a regionally informative map, showing intensity and location of turbulence for various metrics such as categorizing as light, moderate, or severe (with lower spatial and temporal resolution as required for larger spatial domains)
3. Support for special operation such as high spatial and temporal resolution over a limited area during specific time frame, with full characterization of any predicted turbulence

Each of these scenarios may be applicable for several of the timeframe categories, so there are quite a number of different configurations may need to be addressed. These and other operational scenarios can be pursued now that the v1.0 software workflow has been developed and evaluated.

Summary

The software developed during Phase 2 demonstrates the utility of the software to discover a region of interest and to perform further analysis, to generate a prediction of turbulence for this region, and to provide information needed to make a fly or no-fly rating for this region and selected UTLS altitudes. It also demonstrates analysis for the rotational shear turbulence generation mechanism, which is new to operational turbulence forecasting products.

Support for UDV's allows this software to demonstrate metrics and analysis used in contemporary forecasting software, using simulation data potentially at a much higher spatial resolution and with a smaller time step for the region of interest. In addition, the design of the TR supports generation of PIREP-compatible outputs for integration with external systems.

This progress during Phase 2 brings the prototype software from Phase 1 into a functional software package capable of performing analysis and answering the central questions. It also presents the opportunity to continue further development of software and infrastructure to enable efficient operational application. As there are multiple potential operational scenarios with different needs, the exact set of enhancements to be developed and required infrastructure will be determined by the nature of each operational scenario.

Datasets from campaigns of measurements (T-REX, Hawaii), 2012-2013 PIREPS and ensembles of runs with varying resolution are used for validation&verification of computational results (Appendix E).

Appendix A: List of Acronyms and Abbreviations

ADDS - Aviation Weather Center Digital Data Service

ARW-WRF - Advanced Research WRF

CAT - Clear Air Turbulence

CSV - Cross Section Viewer

ECMW – European Centre for Medium Range Weather Forecasts

FNL - NCEP final operational model global tropospheric analysis

GTG - Graphical Turbulence Guidance

HRMM - High Resolution Mesoscale/Microscale

ICD - Interface Control Document

IDE - Integrated Development Environment

NCEP - National Center for Environmental Prediction

NCAR - National Center for Atmospheric Research

Phase 2 - STTR Phase 2, for which this document is the final report

PIREP - Pilot Report (of turbulence)

SCI - Solver Configuration Interface

SOF - Solver Output File

SOV - Solver Output Viewer

STTR - Small Business Technology Transfer Program

TR - Turbulence Report

UAV - Unmanned Aerial Vehicle

UDV - User Defined Variable

UI - User Interface

UM – UK Met Office Unified Model

UTLS - Upper Troposphere and Lower Stratosphere

WRF - Weather Research & Forecasting Model

Appendix B - Baseline Test v1.0

1. After installation of software, start the CSV
 - a. Wait for loading dialog to complete
2. 'Load New'
 - a. Load either:
 - i. data/standard-test-data/wrfout_d01_2006-03-24_11:00:00_d04R
 - ii. data/standard-test-data/wrfout_d01_2006-03-25_11:00:00_d04R
3. Select variable 'Ri_c' from 'Select variable' drop-down
4. Click 'Load Data' then 'Open' (accepting defaults)
 - a. Wait for data to display (no loading dialog is shown)
5. Use the frame slider (lower) to move to around to a few places, e.g frame 200
6. Use the "Jump To" button to change frame to 109 of 263
7. Use the 'Next' and 'Previous' buttons to move to frame 111
8. Click the 'Show bounding box' checkbox
9. Move the profile slider (upper slider) to index 130
10. Observe that the bounding box covers two red spots
11. Observe that the bounding box is over terrain, and that the terrain line is shown on the side plot at the point of terrain at the center of the bounding box
12. Observe that the side plot crosses to the left of the 0.25 line at the two vertical points that are red inside the bounding box.
13. Change the vertical type to Z_AGL and then Index
 - a. Verify in each case that the side plot adjusts and that there are still two points where the vertical profile plot crosses left of the 0.25 mark, and that these two crossing points match up to the vertical level of the red spots in the bounding box.
14. Click the 'Launch Solver' button
 - a. Wait for loading dialog to complete
15. Observe
 - a. The input filename, latitude index, and longitude index are populated
 - b. The maps display the selected location
 - i. Google Maps, only if online
 - ii. Domain map, with red cross at selected location
16. Under 'Processing Details', configure output location if necessary
17. Under 'Solver Details',
 - a. Change NX1/NX2 presets to medium resolution
 - b. Change msl max to 32km
18. Click 'Start Solver'
 - a. Wait for processing to complete
 - b. Observe that the 'Turbulence Report' summary on the processing completion dialog

- i. Shows multiple detections
- c. Click the 'View Report' button and observe the two reported altitude ranges with turbulence
- d. Click 'OK' to close the dialog
- 19. Click 'Launch Solver Output Viewer'
 - a. Wait for SOV loading dialog to complete and for hodograph to load
- 20. Observe
 - a. The instability lines in the side plot
- 21. Change the x3 (vertical) slider to the position of the lower instability, and observe the value for this vertical level
 - a. on the hodograph for each of the three hodograph types
 - i. Horizontal Winds
 - ii. Wavelength
 - iii. Wavenumber
 - b. Shown both as
 - i. Border on point
 - ii. Arrow to point
- 22. Click 'Show Solver Inputs' to view the options selected in the solver, then close the dialog.
- 23. Click the 'Report' button and observe the same plain English Turbulence Report as from the 'Solver Complete' dialog
 - a. Observe that the instability lines are visually approximate to the altitudes shown in the report
 - b. Click in the dialog, then press ctrl-a, then ctrl-c to copy all text from the report.
 - c. Click 'OK' to close the dialog
- 24. Completion
 - a. Close all apps, saving screenshots if necessary to capture observed anomalies if this was not already done.

If any anomalies are observed, use the screen capture button in the UI (or the system print screen if necessary to capture the entire screen) to capture what is seen for analysis.

Appendix C: Annotated UI Figures

The following figures match the earlier figures with the same number (after the appendix label, e.g. C.3 matches figure 3), with the addition of annotations.

Cross-Section Viewer

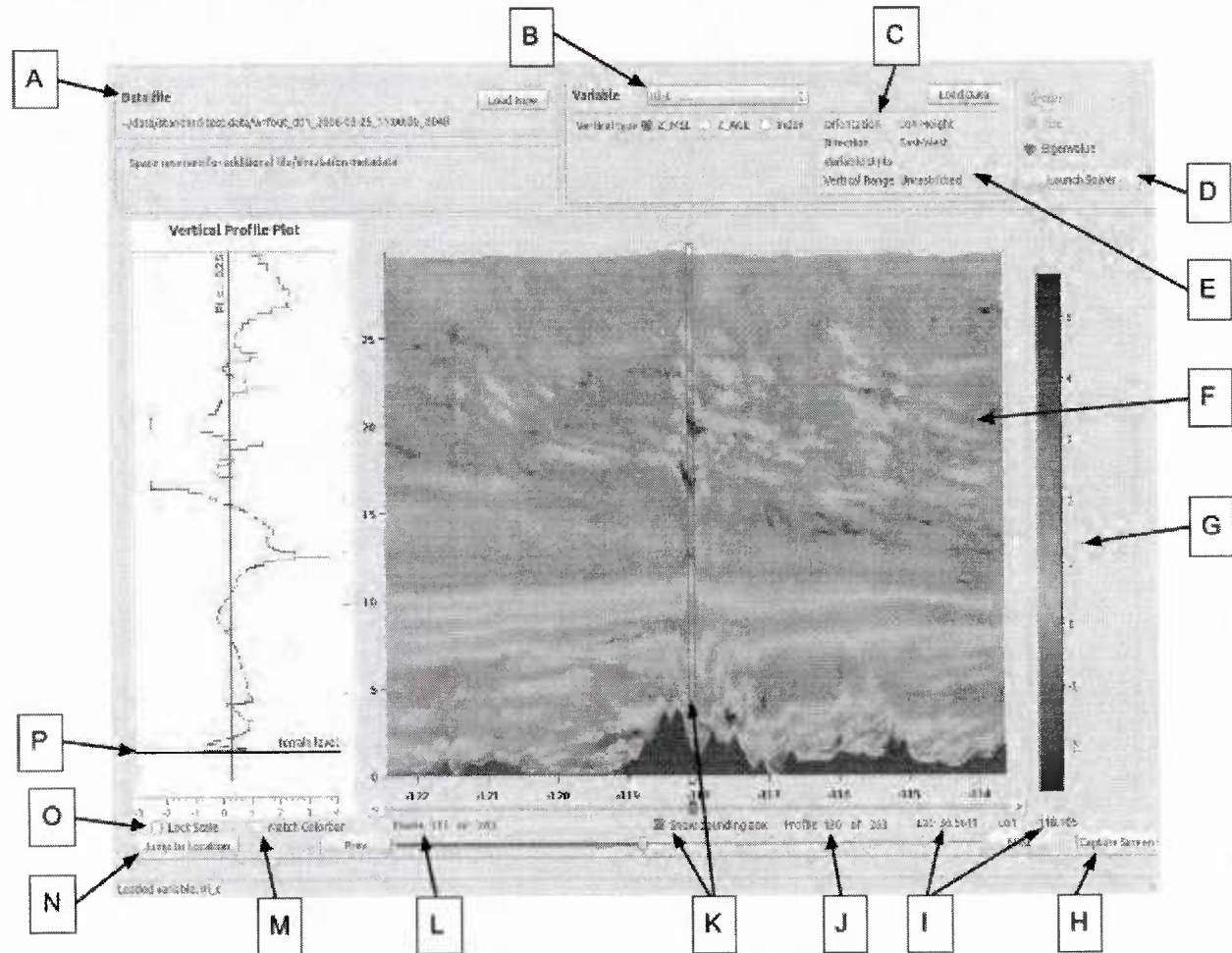


Figure C.3: CSV with annotation given below

The CSV UI presents:

- A. Controls to load a simulation file and display of the selected file name
- B. The variable to display
- C. The variable orientation and vertical range (after loading)
- D. The solver launcher controls
- E. Variable metadata such as the units and the direction
- F. The cross-section image
- G. The colorbar scale
- H. The "Capture Screen" button

- I. The lat/lon coordinates corresponding to the selected frame and vertical profile index
- J. The vertical profile index (resulting in the lat/lon for display, along with the frame)
- K. The 'Show bounding box' feature toggles to show the vertical profile bounding box
- L. The frame (resulting in the lat/lon for display, along with the vertical profile index)
- M. The 'Match Colorbar' feature toggle
- N. The 'Jump To Location' button
- O. The 'Lock Scale' feature toggle
- P. The vertical profile plot with the terrain line and threshold value, when appropriate

Solver Configuration Interface

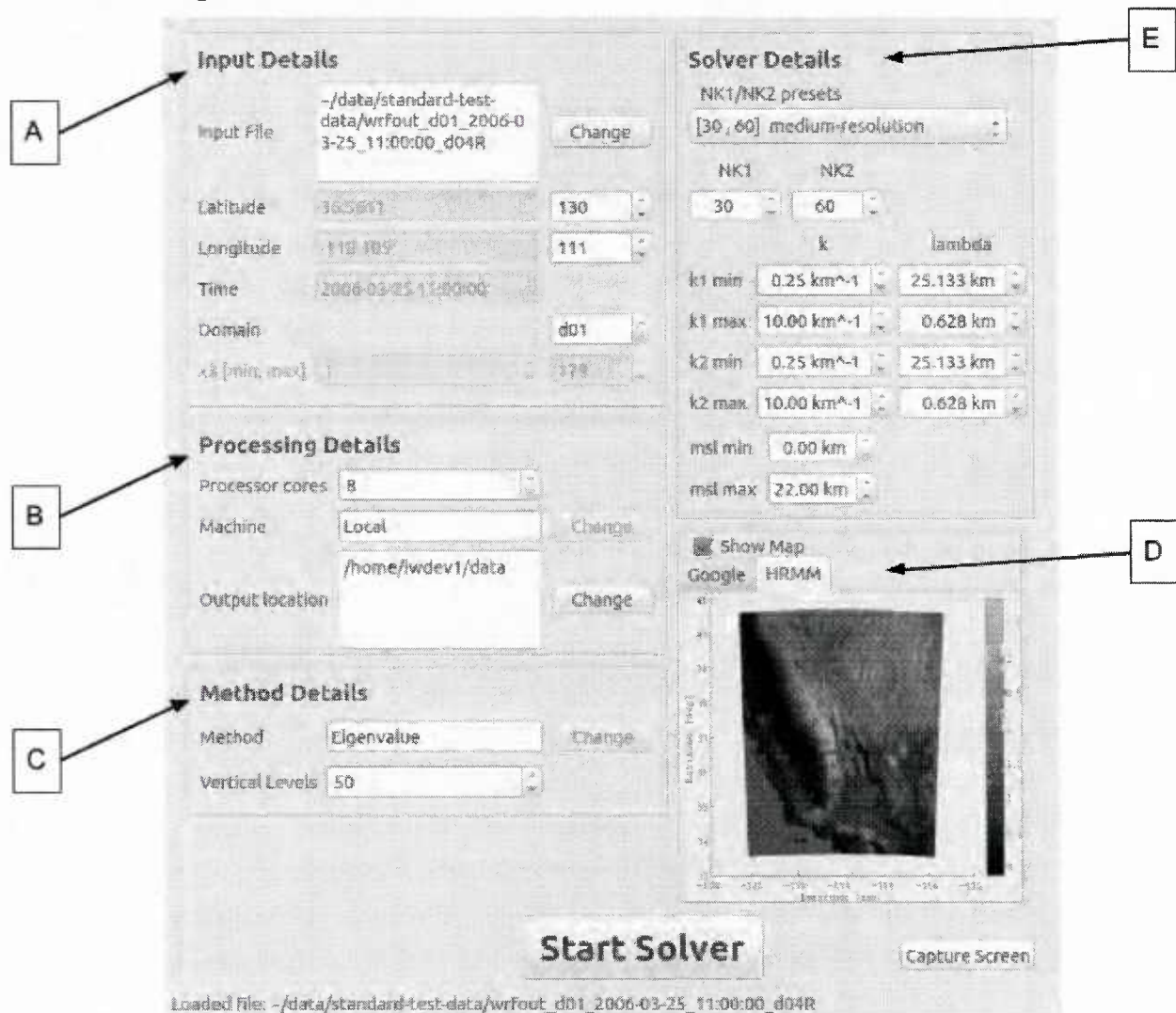


Figure C.4: SCI with annotation given below

- A. Input Details - the simulation file as well as time and location for which to perform the analysis
- B. Processing Details - the machine used to perform processing and the output file to store the results in
- C. Method Details - the method to perform analysis with (currently limited to eigenvalue method) and the number of vertical levels to employ.

- D. Map - an HRMM map as well as a Google map (when available)
- E. Solver Details - the altitude range as well as parameters for the solver algorithm to use

Solver Output Viewer

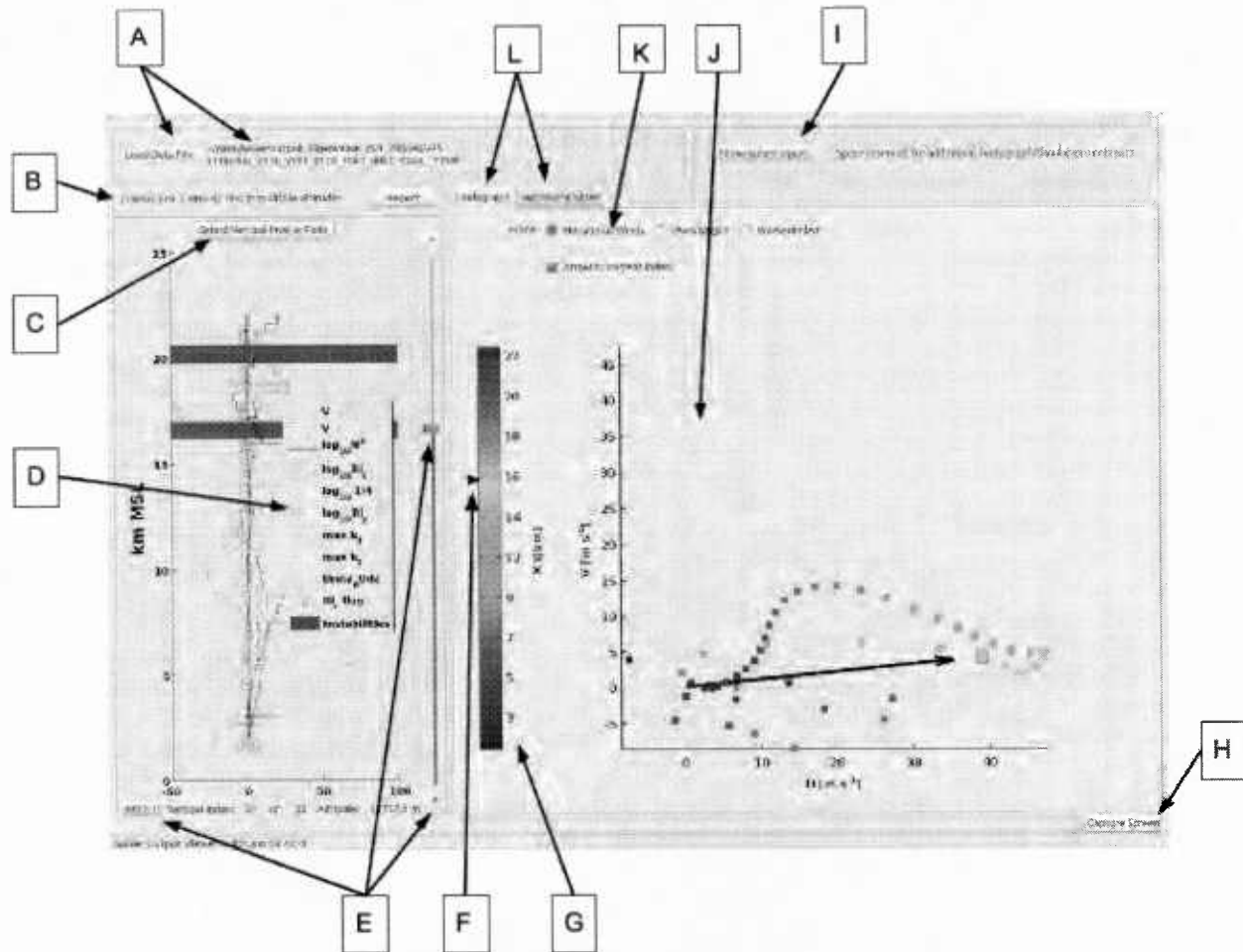


Figure C.6: SOV with annotation given below

- A. Data file selection
- B. Turbulence report summary and button to load full report
- C. Selection control for vertical profile plot variables
- D. Legend for vertical profile plot
- E. Vertical index selection controls
- F. Vertical index indicator on hodograph colorbar
- G. Hodograph colorbar
- H. Capture Screen button
- I. Solver Inputs display button
- J. Hodograph
- K. Hodograph type selector
- L. Hodograph or Horizontal Slices tab selection

Turbulence Report

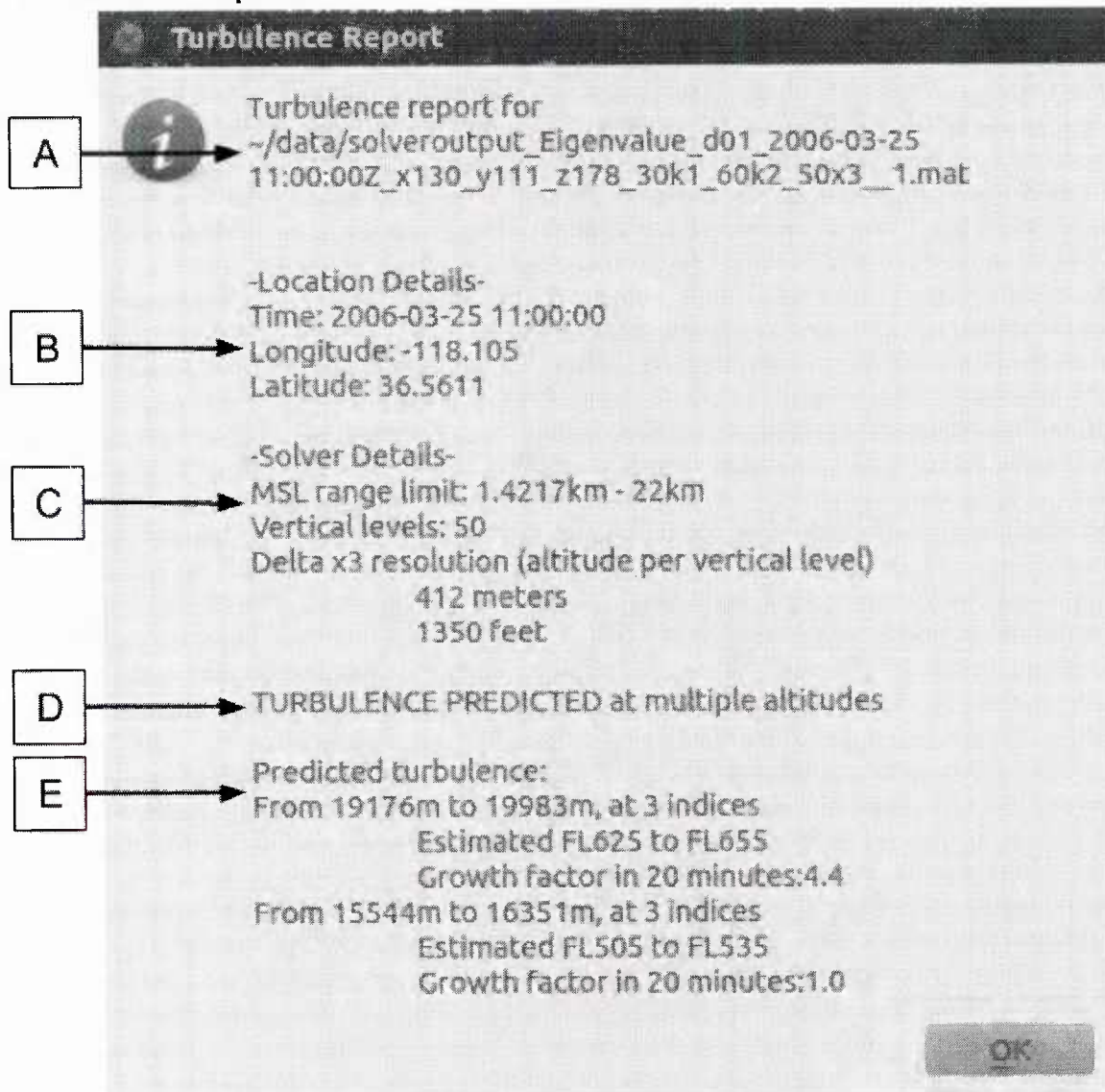


Figure C.8: Turbulence Report with annotations given below

- A. The single-profile Solver Output File that the report describes
- B. Latitude, Longitude, and time being analyzed
- C. Altitude range that the solver used in producing the Solver Output File, number of vertical levels, and resulting vertical spacing
- D. Turbulence Summary - one of:
 - No turbulence predicted
 - Turbulence predicted at a single altitude
 - Turbulence predicted at multiple altitudes
- E. Turbulence details, with adjacent detections described as a range
 - Number of adjacent levels included in each detection
 - Altitude in meters MSL
 - Estimated corresponding Standard Flight Levels
 - Growth factor for the instability in 20 minutes

Appendix D: References and Links

- Delta Airlines Meteorology Website, http://www.lattery.com/dalmetro/domestic_turb.php (last accessed November 2014).
- FAA (2013). U.S. Department of Transportation Federal Aviation Administration, Order JO 7110.10W CHG1 (release date 8-22-2013), subpara 9-2-7a. Available at: <http://www.faa.gov/documentlibrary/media/order/fss.pdf>.
- NOAA Technical Implementation Notices - <http://www.nws.noaa.gov/os/notif.htm#tin> (last accessed November 2014).
- FAA Pilot Weather Report change order describing PIREP http://www.faa.gov/air_traffic/publications/atpubs/fss/fss0902.html
- Aviation Weather Digital Data Service (ADDS) <http://www.aviationweather.gov/adds/>
- ADDS Turbulence site (with GTG 2.5 data) <http://www.aviationweather.gov/turbulence>
- ADDS Experimental site <http://weather.aero/>
- NCEP FNL data - <http://rda.ucar.edu/datasets/ds083.2/>
- High Resolution Rapid Refresh <http://ruc.noaa.gov/hrrr/>
- WRF site <http://www.wrf-model.org>
- NCAR - <http://ncar.ucar.edu>
- WRF-ARW user site <http://www2.mmm.ucar.edu/wrf/users/>
- T-REX experiment https://www.eol.ucar.edu/field_projects/t-rex
- <http://www.metoffice.gov.uk/research/modelling-systems/unified-model> , Unified Model (UM) developed by the UK Met Office.
- Andrew Brown, Sean Milton, Mike Cullen, Brian Golding, John Mitchell, and Ann Shelly, 2012: Unified Modeling and Prediction of Weather and Climate: A 25-Year Journey. *Bull. Amer. Meteor. Soc.*, **93**, 1865–1877. doi: <http://dx.doi.org/10.1175/BAMS-D-12-00018.1>
- References in Appendix E below.

Appendix E: Final Report Presentation

AFWA, Omaha, Nov 19, 2014

**AFOSR STTR:
Fine Scale Modeling and Forecasts of
Upper Atmospheric Turbulence for Operational Use**

**ALEX MAHALOV (PI)
Wilhoit Foundation Dean's Distinguished Professor
Arizona State University**

Tim Mackenzie and Stephen Shaffer

STTR Partners: IntelliWare LLC and Arizona State University

State of the Science: UTLS Turbulence

Current Operational Forecasting

STTR UTLS-2: Findings and Products

Selected Refereed Publications Turbulence (Mahalov et al)

Multiscale modeling and nested simulations of three-dimensional ionospheric plasmas: Rayleigh-Taylor turbulence and nonequilibrium layer dynamics at fine scales, *Phys. Scr.* 89 (22pp) 098001 (2014).

Observation and simulation of wave breaking in the southern hemispheric stratosphere during VORCORE, *Annales Geophysicae*, 31 (4), p. 675-687 (2013).

3D Dynamics and Turbulence Induced by Mountain and Inertia-Gravity Waves in the Upper Troposphere and Lower Stratosphere (UTLS), American Institute of Aeronautics and Astronautics (AIAA), 41st AIAA Fluid Dynamics Conference, Invited Paper AIAA 2011-3930 (2011).

Numerical Studies of Mountain Waves in the Upper Troposphere and Lower Stratosphere (UTLS), *Atmospheric Chemistry and Physics*, vol. 11, p. 5123-5139 (2011).

Characterization of Optical Turbulence for Laser Propagation, *Laser and Photonics Reviews*, p. 144-159, vol. 4, No. 1, Special Issue: 50 Years of Laser (2010).

Vertically Nested Nonhydrostatic Model for Multi-Scale Resolution of Flows in the Upper Troposphere and Lower Stratosphere, *Journal of Computational Physics*, vol. 228, p. 1294-1311 (2009).

Multi-Scale Resolution of Polarized Inertia-Gravity Waves: *Theor. Comput. Fluid Dyn.* vol. 21, p. 399-422 (2008).

Stochastic 3D Rotating Navier-Stokes Equations: Averaging, Convergence and Regularity, *Archive for Rational Mechanics and Analysis*, vol. 205, p. 195-237 (2012).

Instabilities in Non-Parallel Shear-Stratified Flows, *Kinetic and Related Models*, vol. 2, No. 1, p. 215-229 (2008).

Selected Refereed Publications Turbulence (Mahalov et al)

Variability of Turbulence and Its Outer Scales in a Nonuniformly Stratified Tropopause Jet, J. Atmos. Sci., vol. 41, p. 524-537 (2008).

Cirrus Cloud Diagnosis Using Numerical Weather Prediction Model and Comparison with Observations, Special Volume on Lasers and Applications in Science and Engineering. Atmospheric Propagation of Electromagnetic Waves', International Society for Optical Engineering, Vol. 7200, pp. 72000A-72000A-10, 2009.

Lagrangian Dynamics in Stochastic Inertia-Gravity Waves, Physics of Fluids, vol. 22, 126601. doi: 10.1063/1.3518137 (2011).

Multiscale Nesting and High Performance Computing Simulations of Limited Area Atmospheric Environments, Handbook of Environmental Fluid Dynamics, Invited Chapter, Published by Taylor and Francis Co. (2013).

The Effect of the Jet-Stream on the Intensity of Laser Beams Propagating Along Slanted Paths in the Upper Layers of the Turbulent Atmosphere, Waves in Random and Complex Media, vol. 19, No. 4, p. 692-702, (2009).

Atmospheric Characterization and Ensemble Forecasting of Multi-Scale Flows in the Upper Troposphere and Lower Stratosphere (UTLS), American Institute of Aeronautics and Astronautics, Invited Paper AIAA 2009-110, p. 1-6, (2009).

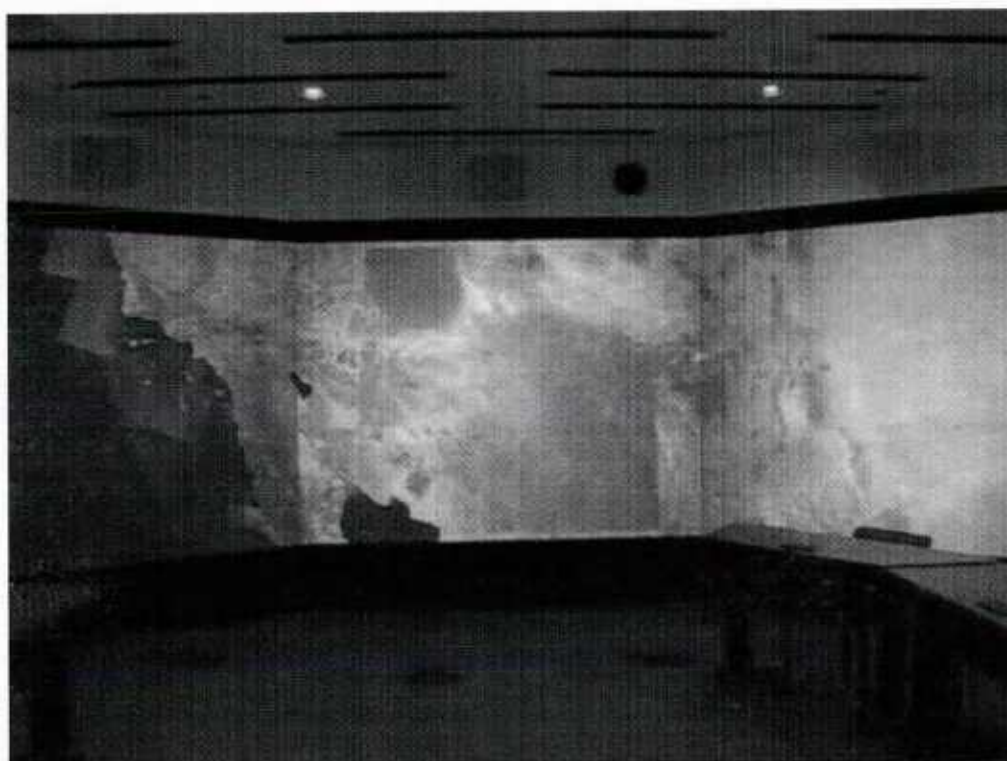
Multi-Scale Predictability of High-Impact Upper Tropospheric Ice Clouds, IEEE Comp. Soc. J., Special Issue on HPC, p. 267-273, (2008).

ASU Resources

Arizona Advanced Computing Center (A2C2): 3,000 CPUs, 215 TB high-speed disk, 11TB RAM; National Lambda Rail and Internet 2 network access.

ASU Resources

Decision Theater (DT) : seven screen immersive environment allows to look at complex data, models and visualizations. The DT is designed for collaborative decision making (3D immersive environment built with cutting edge graphics technologies).



Physics Based Predictive Modeling of UTLS

- *Non-Kolmogorov shear stratified UTLS turbulence: inhomogeneous, anisotropic and patchy, non-Gaussian statistics*
- *Conventional turbulence models (RANS, k - ϵ , $Pr=1$) fail to resolve waves/nonlinear multi-scale UTLS dynamics*
- *Physics based predictive modeling and subgrid scale parameterizations: polarized Richardson number, variable turbulent Prandtl number*
- *3D Navier-Stokes Equations + waves: novel multi-scale computational methods are needed to resolve shear stratified UTLS dynamics*

Physics Based Predictive Modeling of UTLS

- *Microscale nesting (space and time) and novel implicit relaxation techniques*
- *Boundary conditions from high resolution global/mesoscale datasets*
- *Multi-scale operator splitting computational methods and turbulence models customized for UTLS*
- *Targeted fine scale modeling and forecasts, nested simulations*

UTLS Dynamics and Stratospheric Turbulence

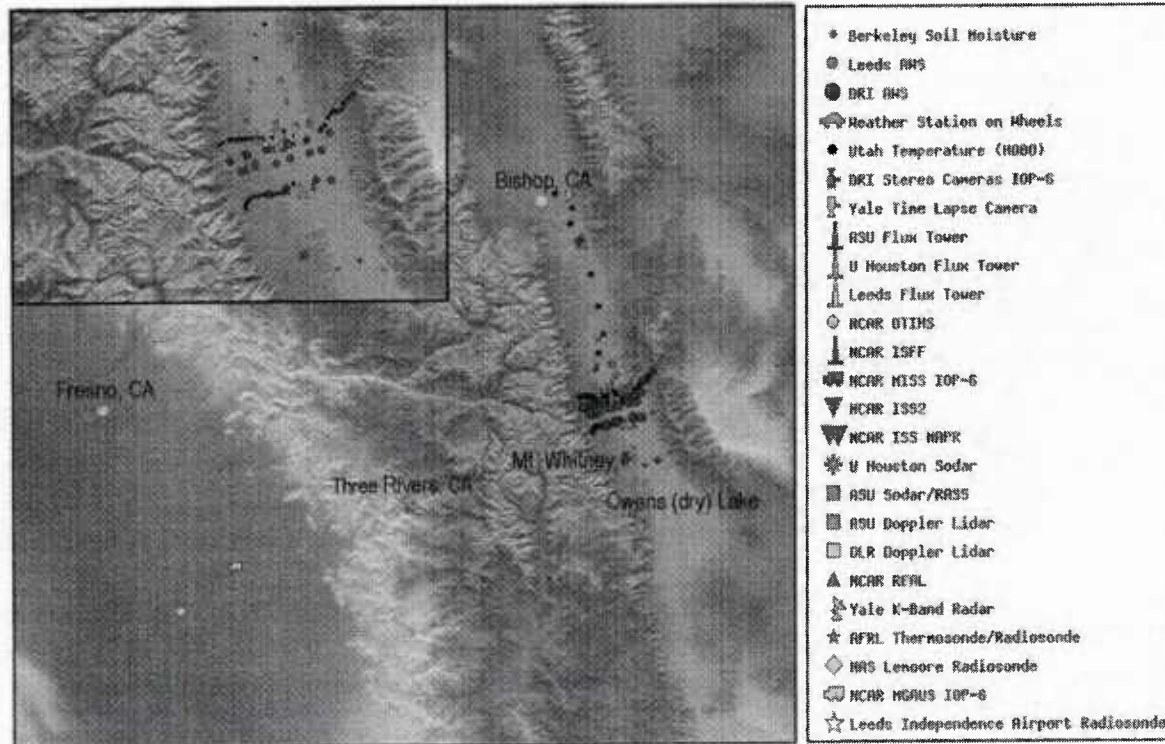
Sources: mountain waves, jetstreams,
convective storms, clouds

Mountain Waves in UTLS

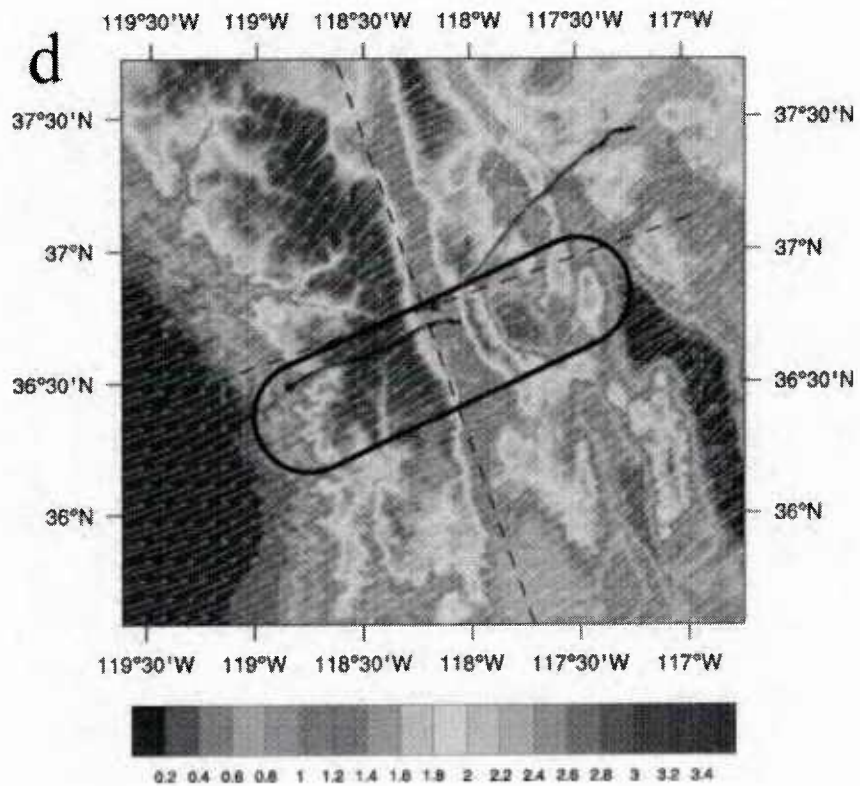
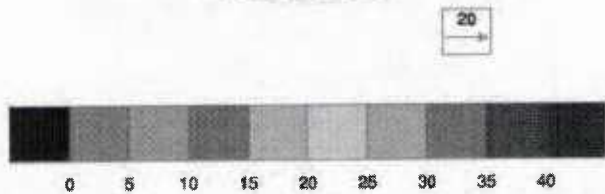
Fine Scale Modeling: **Validation and Verification**

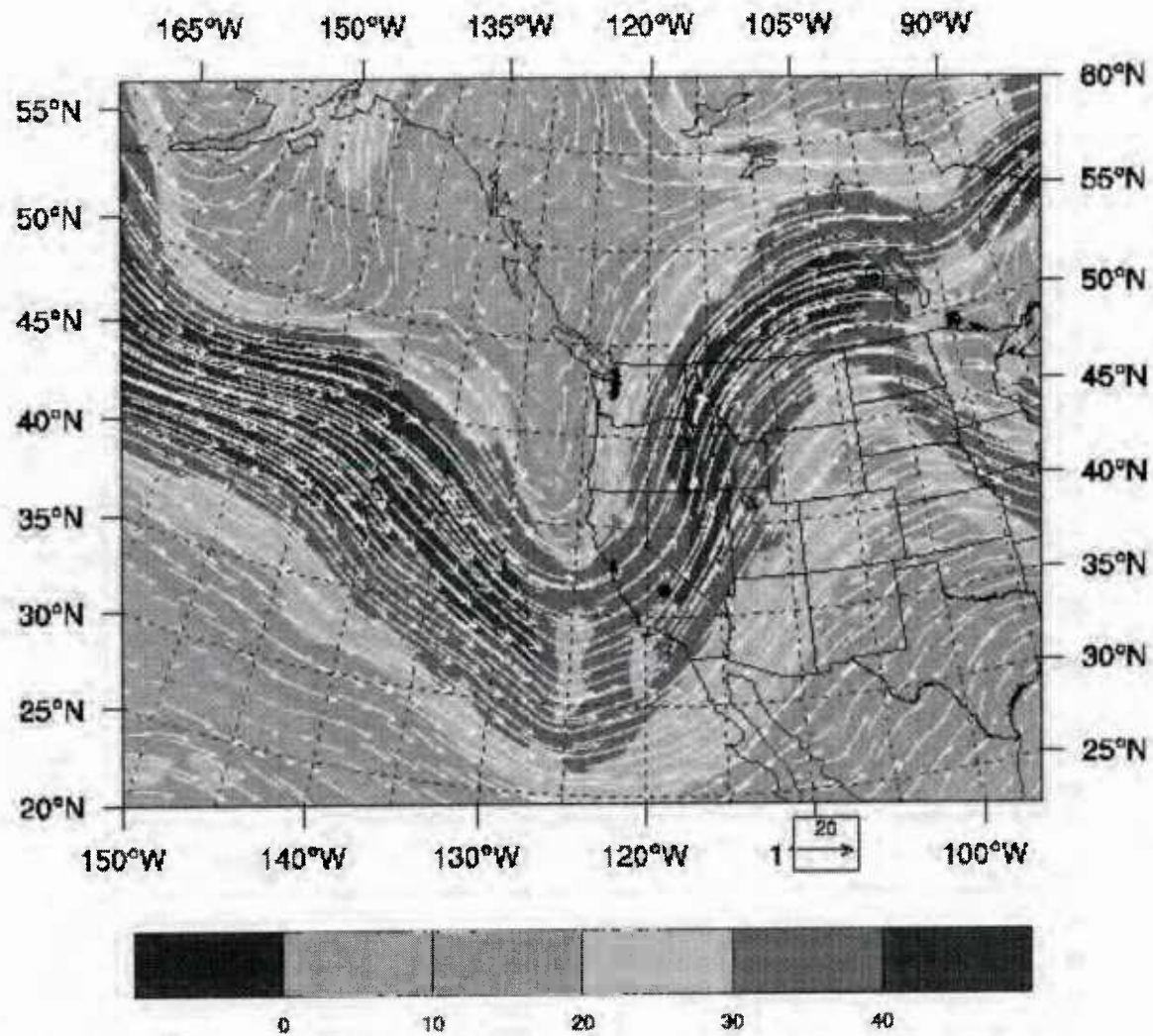
Physics Based Predictive Modeling of UTLS: Validation and Verification

**Terrain-induced Rotor Experiment (T-REX) campaign of
measurements, *Owens Valley, CA*, March-April 2006
Targeted Simulations: IOPs of the T-REX campaign**



Global data and targeted microscale domain
showing National Center for Atmospheric
Research (NCAR) research aircraft and
balloon trajectories



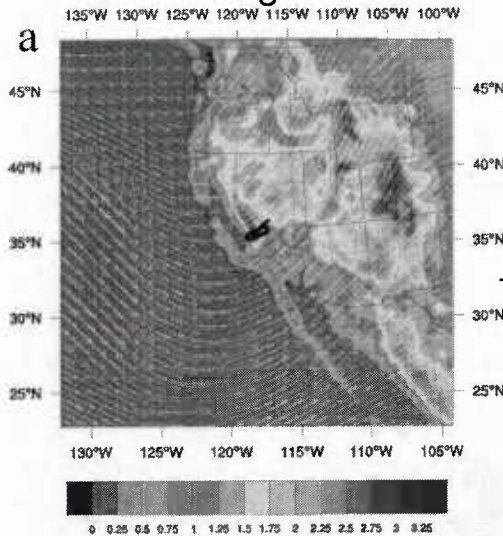


Distributions of vector wind speed fields on 320 K isentrope on April 1, 2006.
The dot indicates the location of balloon launching site.

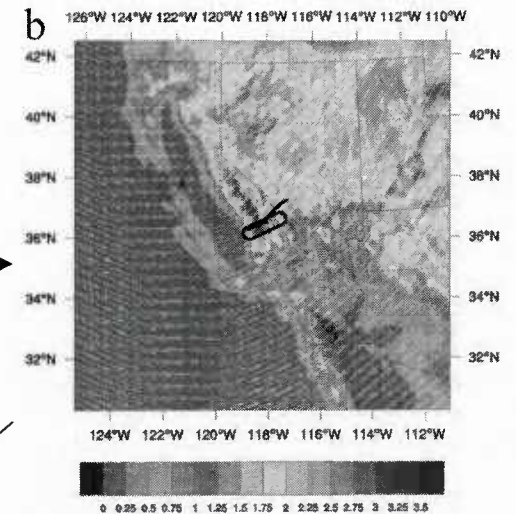
Global model data



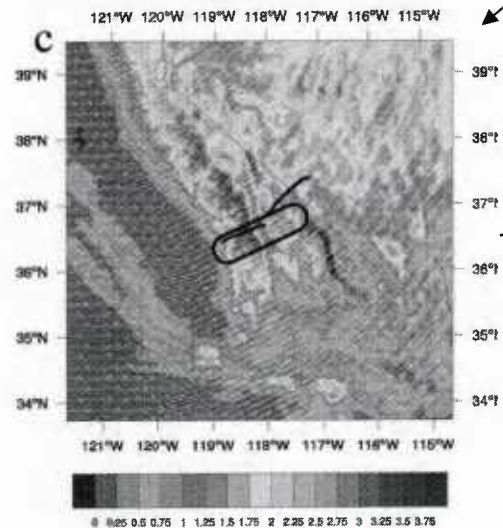
Domain 1: Nested to the global model



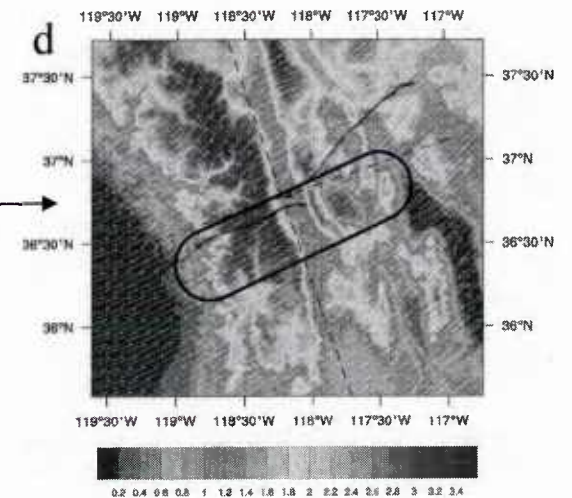
Domain 2: Nested to domain 1



Domain 3: Nested to domain 2



Domain 4: Nested to domain 3



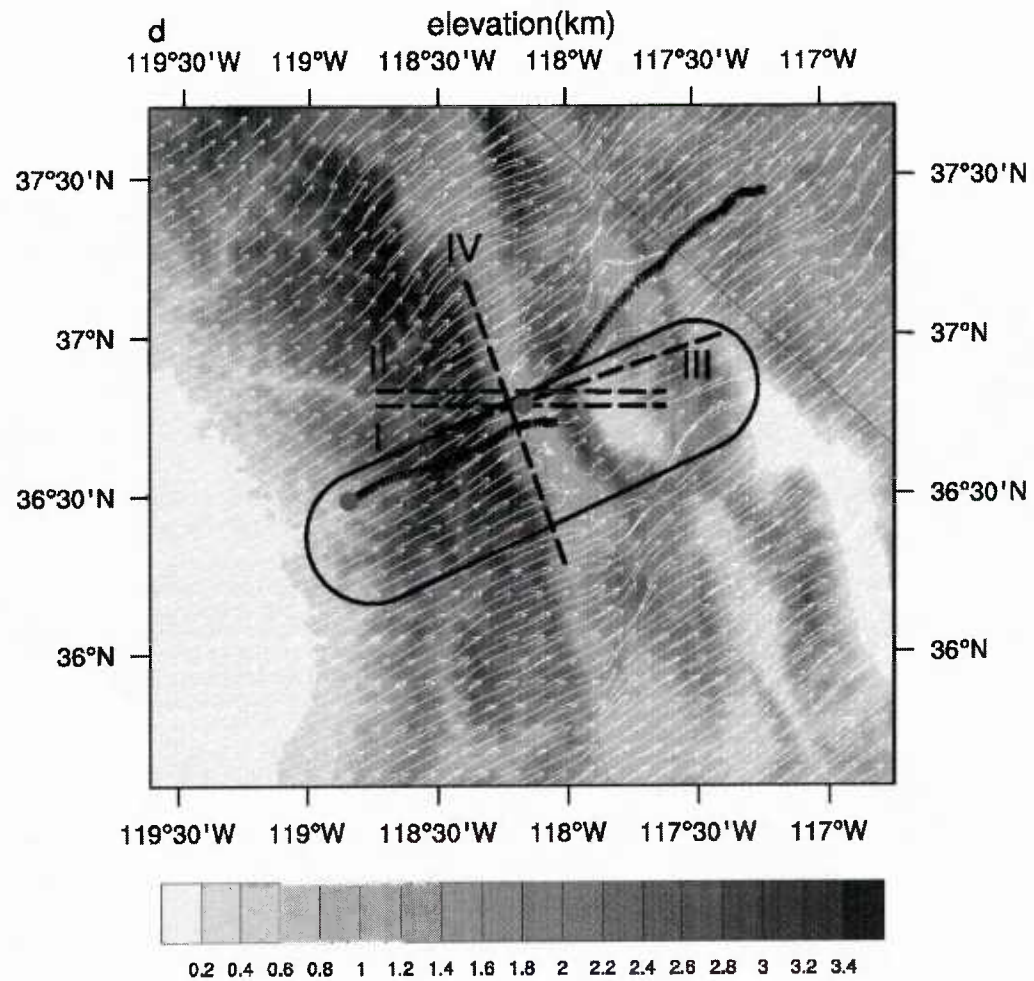
❖ Nested simulations are initialized with analysis from ECMWF, GFS.

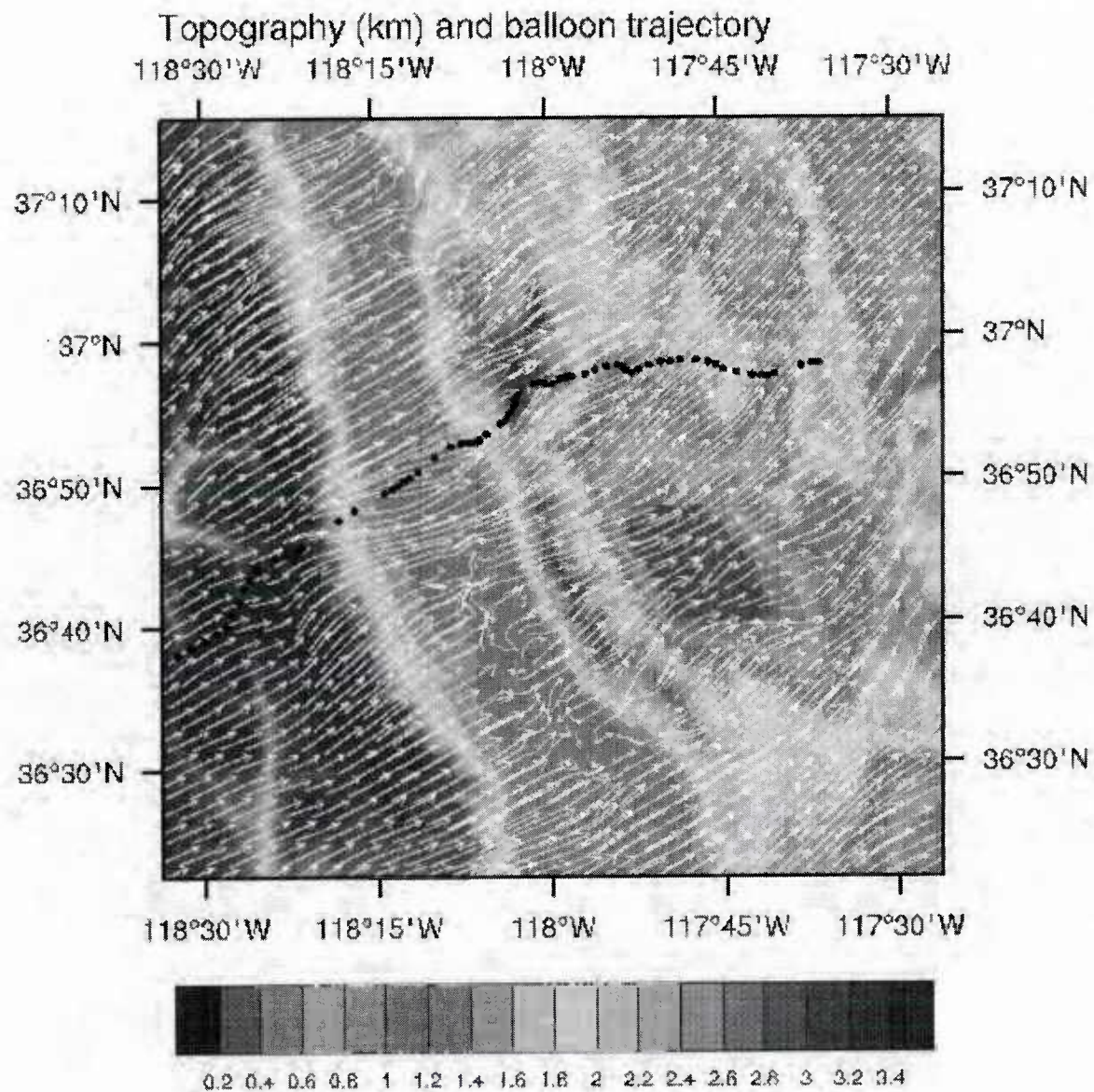
❖ 4 nested domains with horizontal gridding of 27km, 9km, 3km (61 vertical levels) and 1km (181 vertical levels).

NCAR Research Aircraft and Two Balloons

❖ Topography and wind vector fields simulated on April 1, 2006 at 8 UTC (altitude $z = 12\text{km}$).

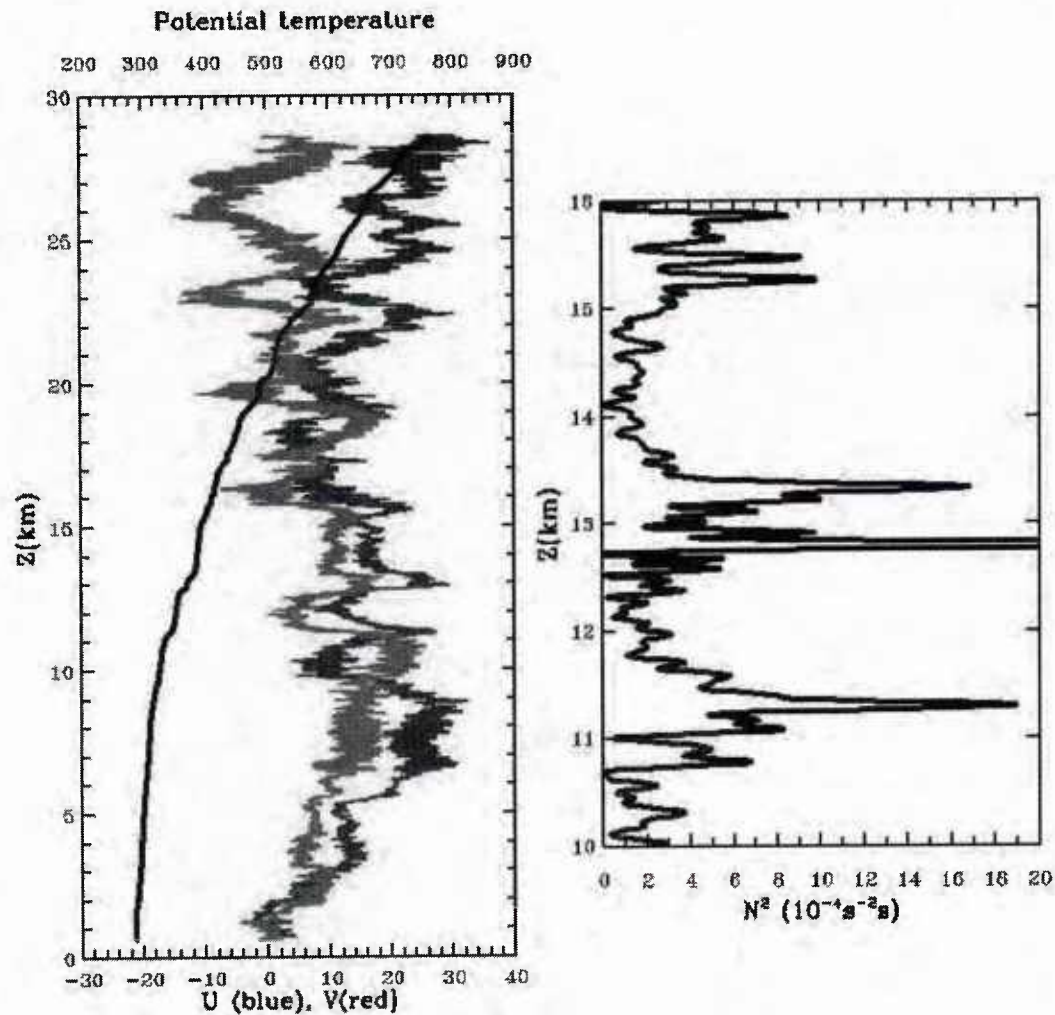
❖ The balloons are launched from Three Rivers (36.49 N, 118.84 W) and Owens Valley (36.78 N, 118.17 W). The curve shaped like an ellipse is the trajectory of the research aircraft (NCAR HIAPER). The dashed lines indicate the locations where various vertical cross-sections are taken.



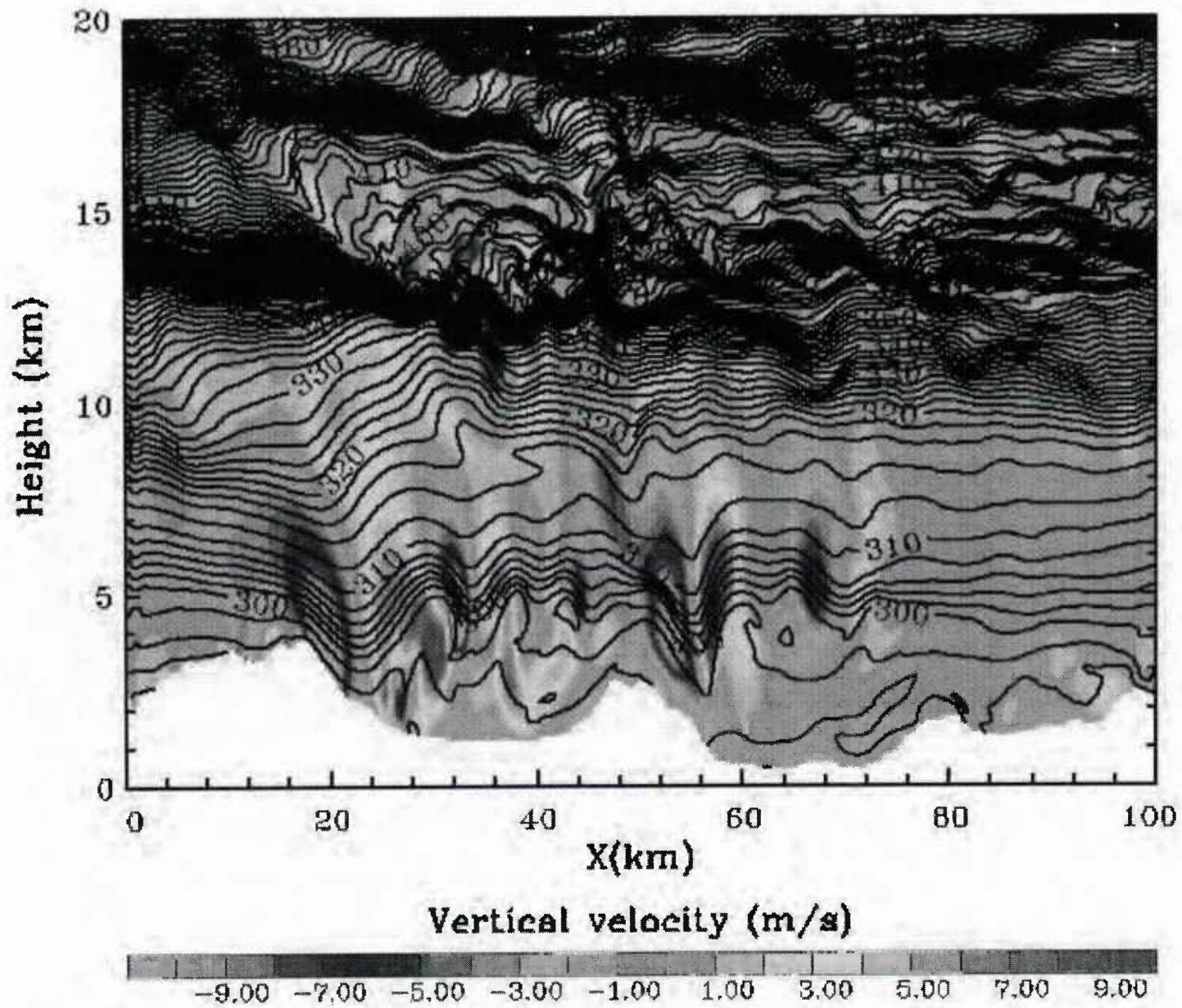


Topography and wind vector fields at 12 km altitude. The black curve shows the trajectory of balloon launched at (36.49 N, 118.84 W) on April 1, 2006 at 7:50 UTC

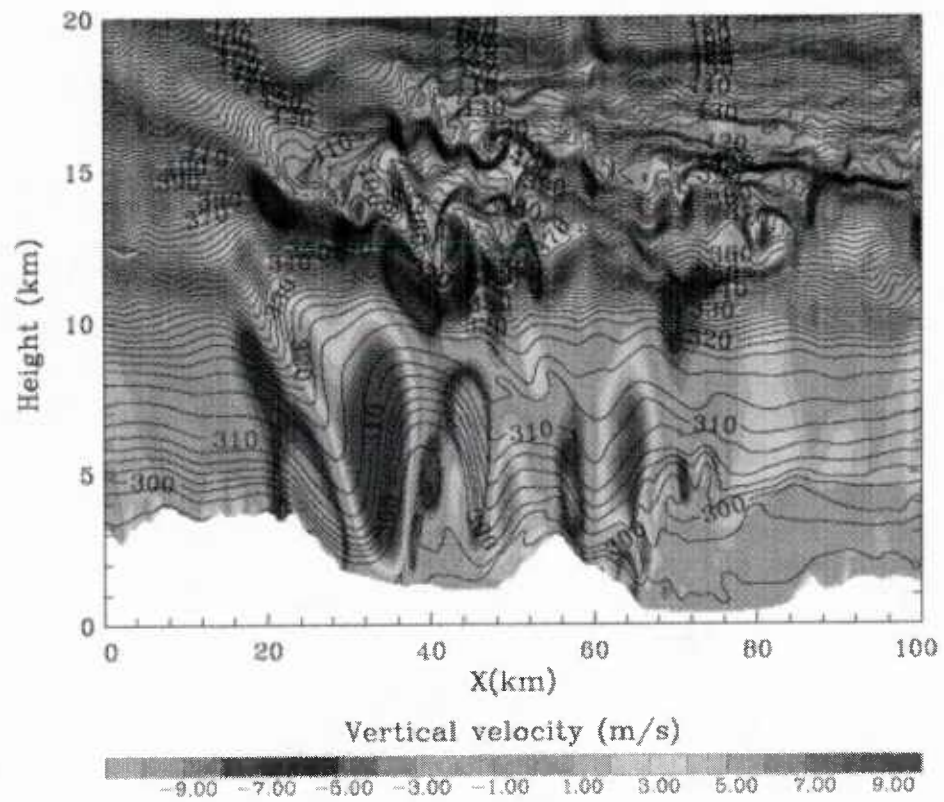
Terrain-induced Rotor Experiment (T-REX) campaign of measurements, *Owens Valley, CA*, March-April 2006



Potential temperature (black), eastward wind (blue), and northward wind (red) from balloon measurements during T-REX. The balloon was launched at (36.49 N, 118.84 W) on April 1, 2006 at 7:50 UTC.

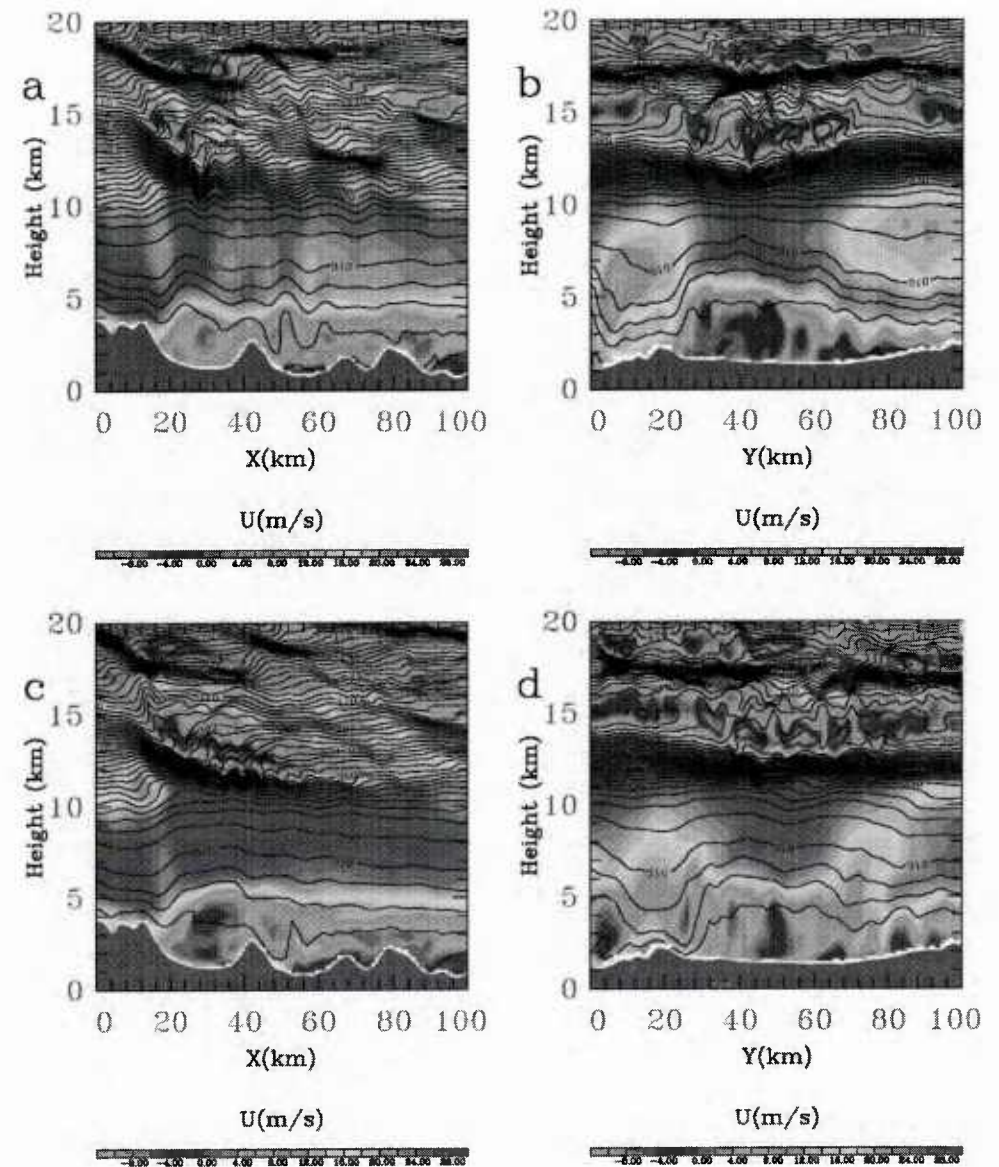


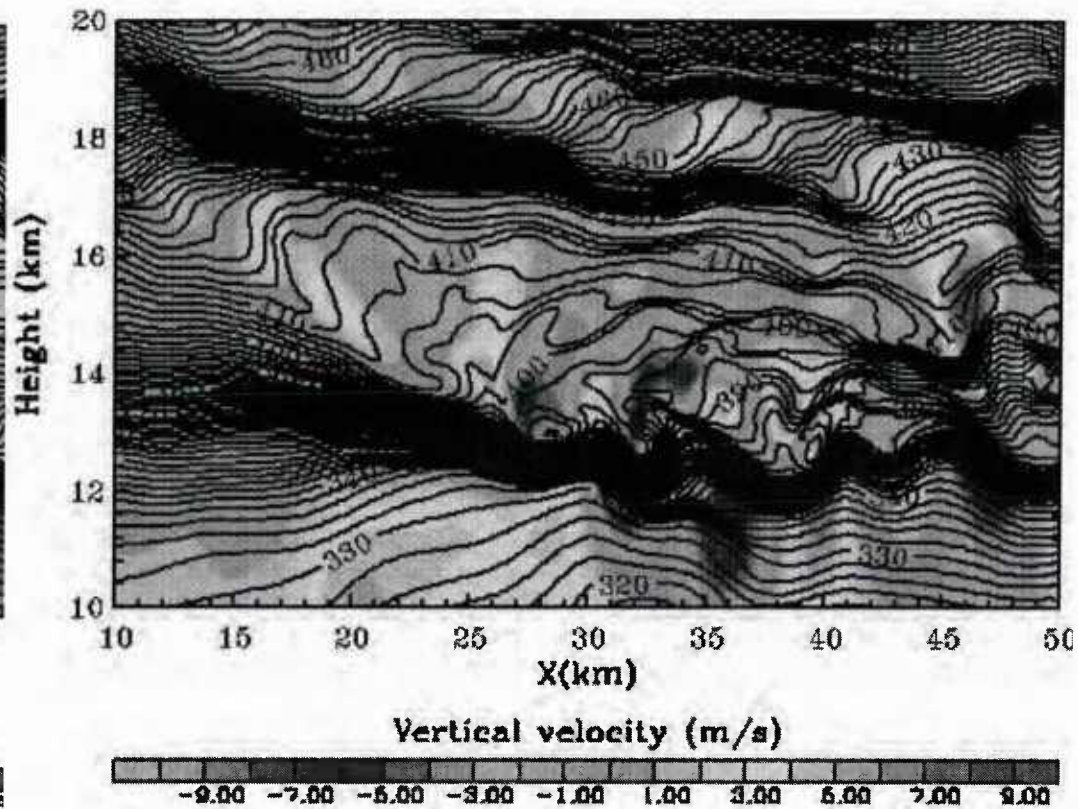
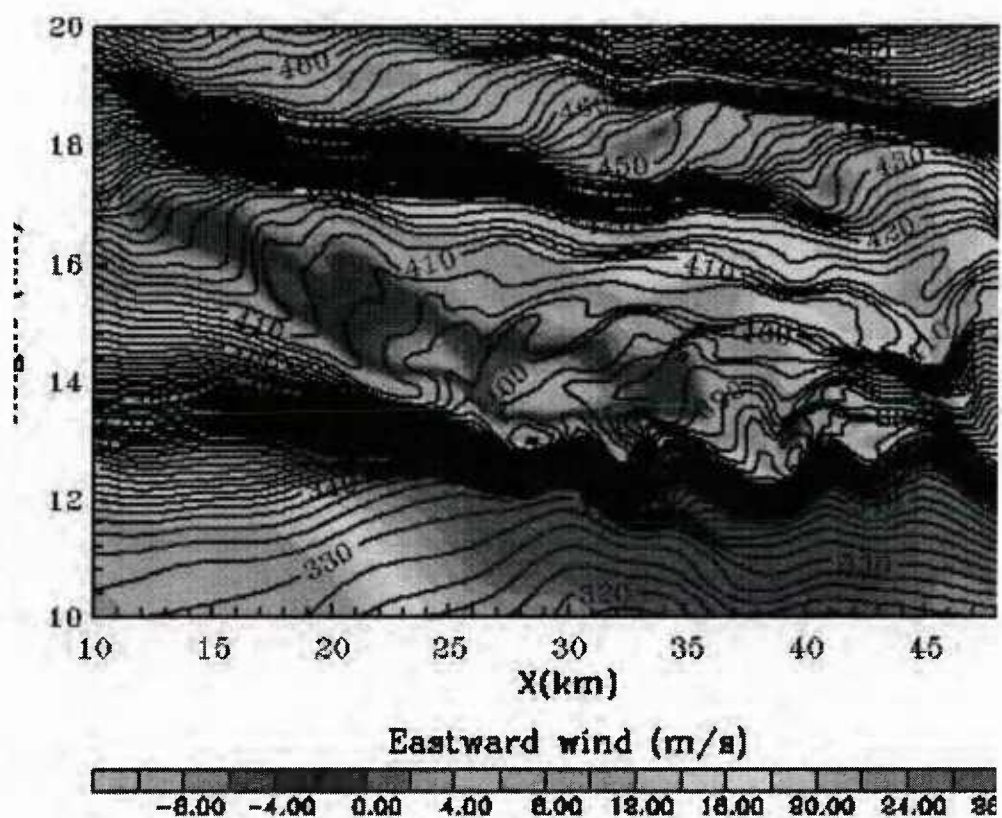
TREX campaign Owens Valley, CA. Longitude (118.56 W, 117.42 W)-altitude cross-section at latitude 36.82 N for potential temperature (contour) and vertical velocity (color) for the microscale domain.



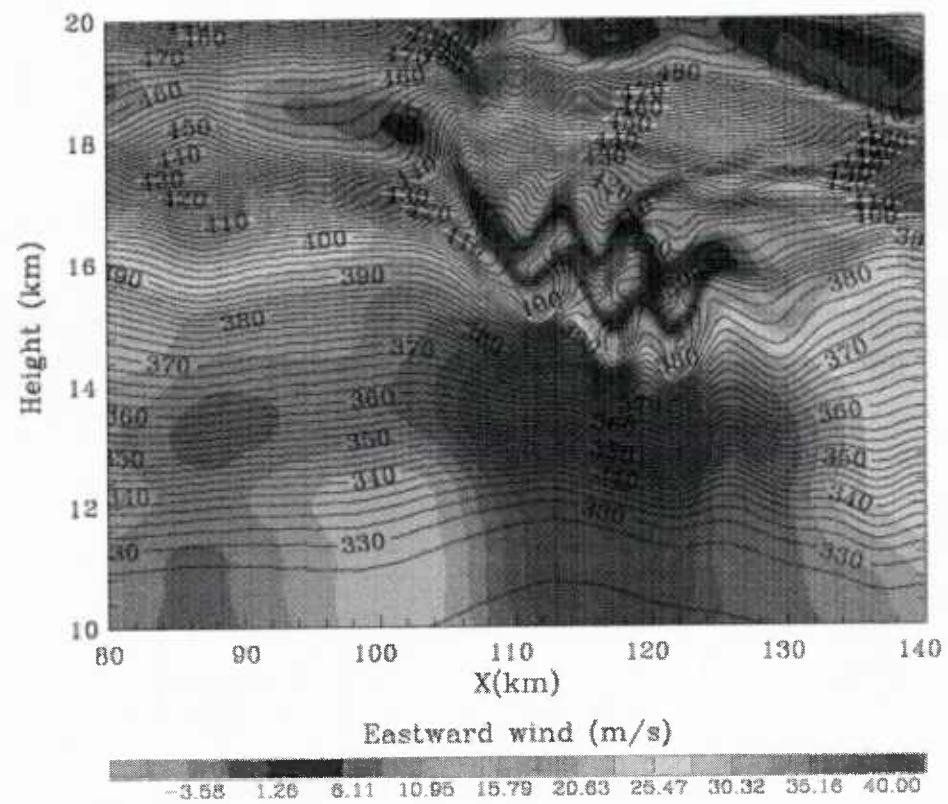
❖ Vertical cross-sections of horizontal wind component transverse to the valley (color, m/s) and potential temperature (K) on April 1, 2006 at 8 UTC: (a) across and (b) along the valley. (c) and (d) are the same as (a) and (b) respectively but at 6 UTC.

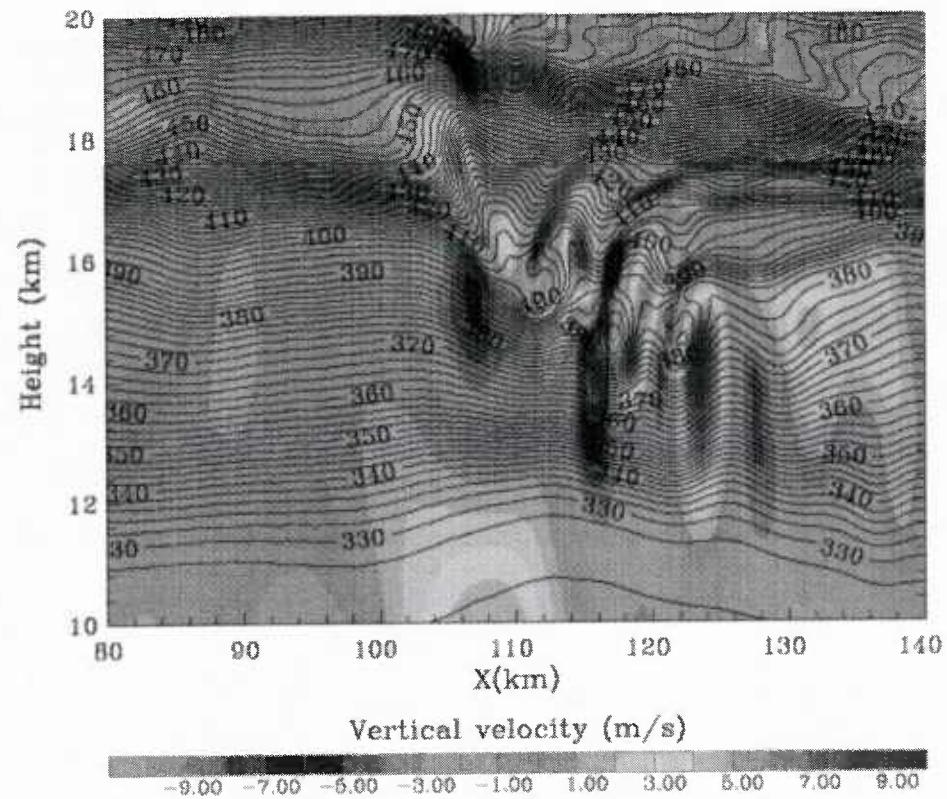
❖ The horizontal axes X and Y indicate the distance with respect to the location (36.70 N, 118.50 W) and (36.29 N, 118.01 W) respectively.



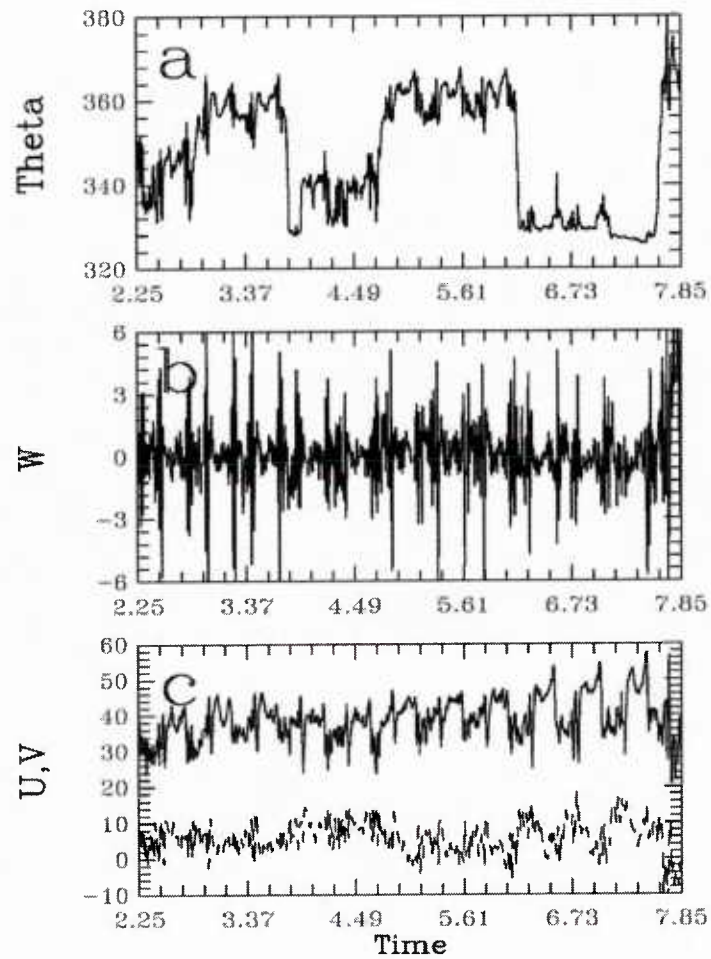


Longitude-altitude cross-sections. Left panel: potential temperature (contour) and eastward wind (color); right panel: potential temperature (contour) and vertical velocity from the microscale domain.

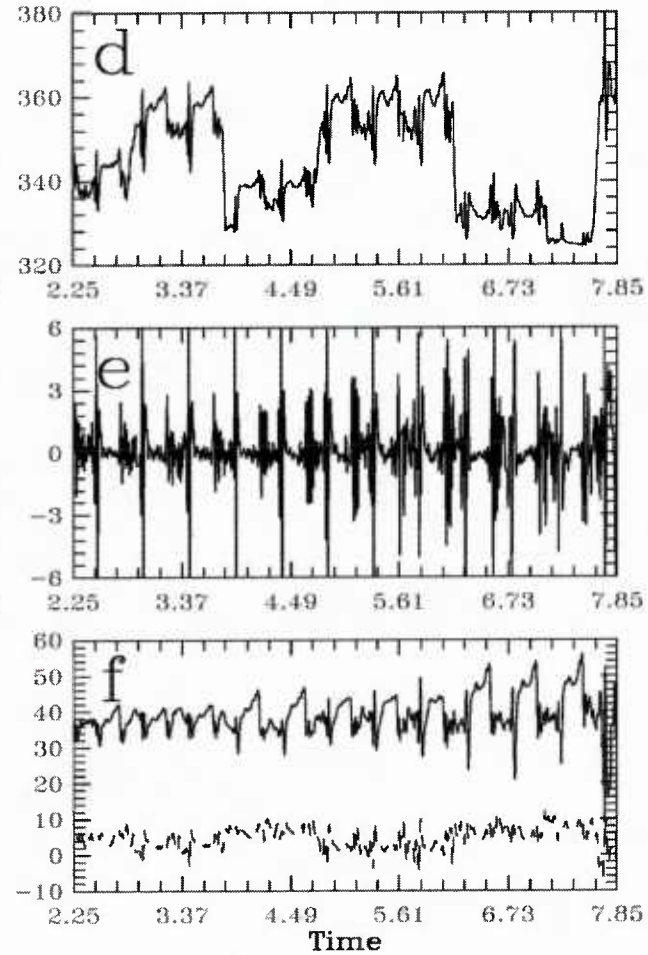




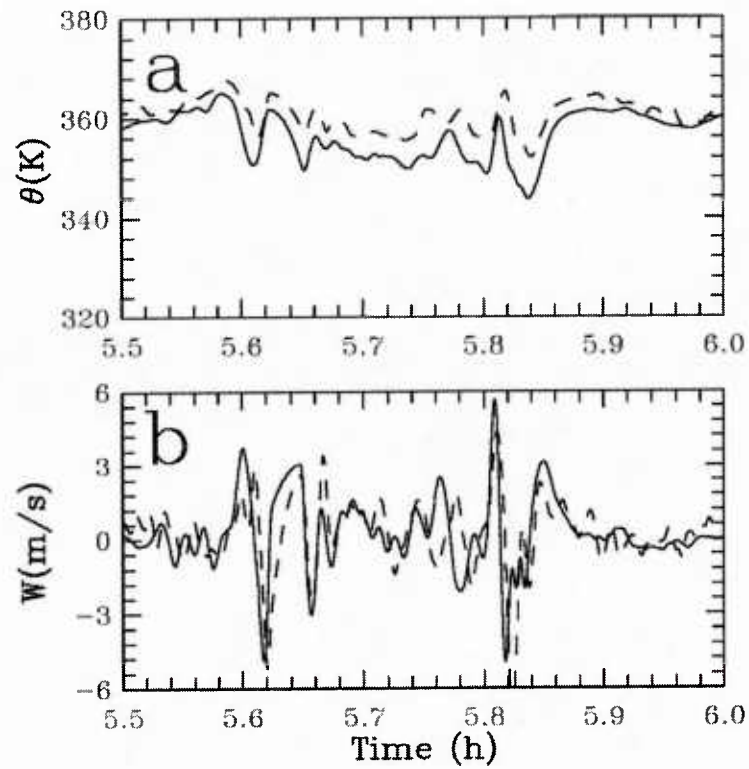
observations



simulations



Time series of (a) potential temperature, (b) vertical velocity, and (c) eastward (solid) and northward (dashed) winds from aircraft measurements. (d)-(f) are the same as (a)-(c) but from simulations.

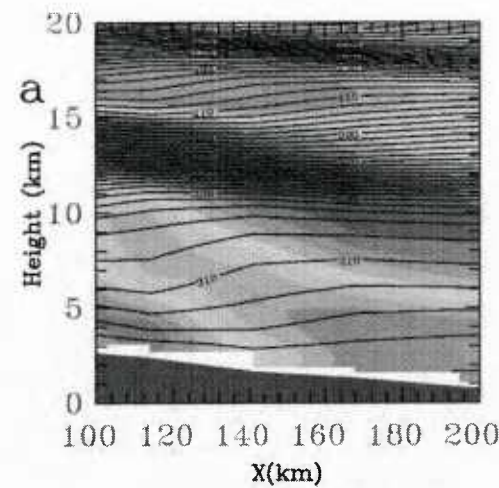


Zooms of time series for (a) potential temperature and (b) vertical velocity from NCAR research aircraft HIAPER observations/measurements (dashed) and from simulations (solid).

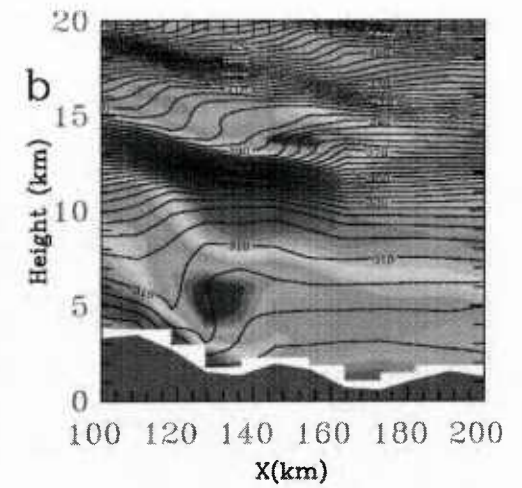
❖ **Horizontal Resolutions:**
15km, 9km, 3km, 1km, 333m.

❖ Vertical cross-sections of
potential temperature (contour, K)
and eastward wind (color, m/s).

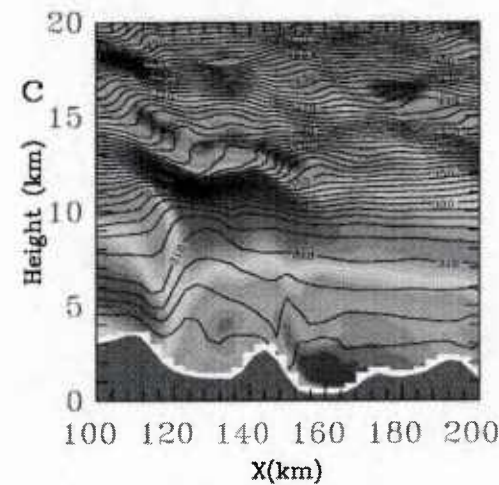
❖ The horizontal axis indicates
the distance with respect to the
location (36.79 N, 118.73 W).



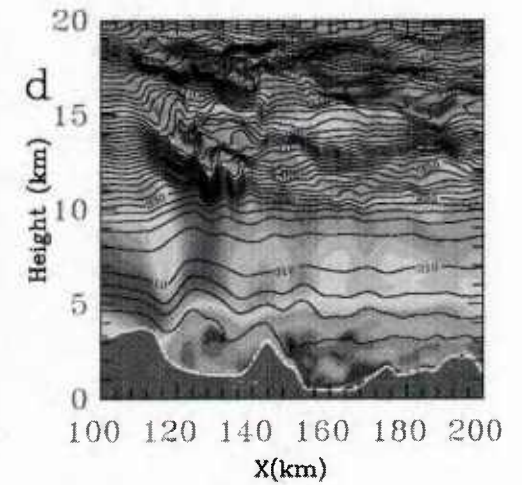
Eastward wind (m/s)



Eastward wind (m/s)

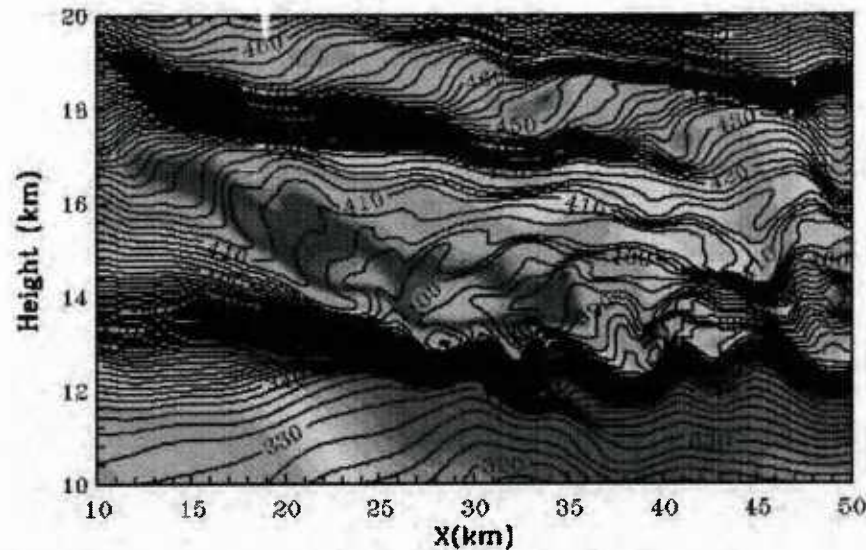


Eastward wind (m/s)

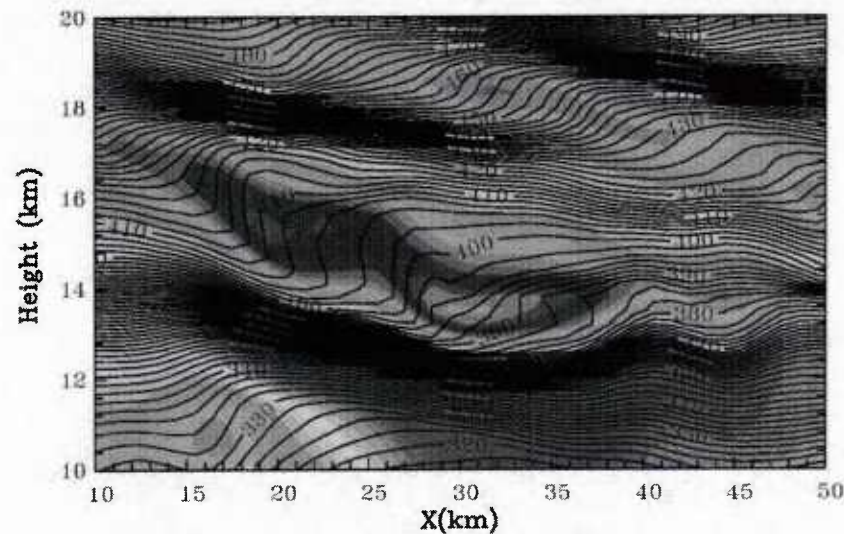
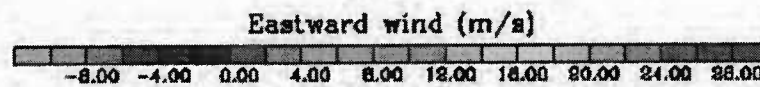


Eastward wind (m/s)

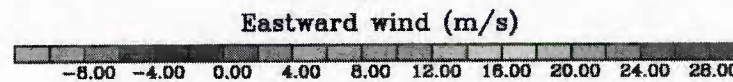




450 vertical levels (from the ground to 30km altitude)



150 vertical levels (from the ground to 30km altitude)



Longitude-altitude cross-sections for: potential temperature and eastward wind.

Global/Mesoscale Datasets

**NOAA GFS, ECMWF T799L91, T1023 L91,
NOAA/NCEP Rapid Refresh (RAP)**

T799L91: 25km horiz res and 91 vertical levels

NOAA RAP: 13km horiz res, 50 vertical levels

Stratospheric Turbulent Layers Triggered by *Helical (Directional) Shear* Associated with Velocity Fields of Polarized Inertia Gravity Waves (Radiated by Jetstreams and VPMW)

Stratospheric Turbulence (altitudes 45,000-90,000 feet)

- **Stratospheric Mechanical Turbulence (15-30 km):** patchy high frequency fluctuations in the stratospheric wind fields and long-lived energetic eddies with several hundred meters/1km scales; pitch oscillations induced by CAT.
- How do Gravity Waves with large horizontal wavelengths (few hundred km) generate thin CAT layers (few hundred meters/1km scales) ?
- Dynamically unstable Jet Streams (around 10 -12 km) radiate polarized inertia-gravity waves and refract mountain waves into the stratosphere (15-30 km); transfer of turbulent energy from the Jet to the dispersive, polarized and non-monochromatic waves.
- As mountain and gravity waves are transmitted across tropopause and jet, they become polarized and undergo significant spectral shift to lower wavenumbers, larger horizontal scales.
- Thin stratospheric long lived CAT layers are induced by high helical (directional) shear associated with helical velocity field of such polarized waves: **rapid change of horizontal wind direction is a precursor of instabilities and formation of turbulent layers.**
- Propagation of polarized waves into the lower stratosphere (non-uniform background stratification): *collapse of stability inside thin CAT layers.*
- Characterization of fully three dimensional instability mechanisms and turbulent dynamics: conventional turbulence indices and numerical models are not applicable (ie Lighthill-Ford, Ellrod, Ellrod-Knox).

Challenges of Fine Scale Modeling and Forecasting of Stratospheric Turbulence

non-Kolmogorov, multi-scale, inhomogeneous, anisotropic, shear-stratified and patchy, non-Gaussian statistics.

Stratospheric environment: strongly vertically variable gravity wave frequencies, mean horizontal wind velocity profiles with stiff vertical variability.

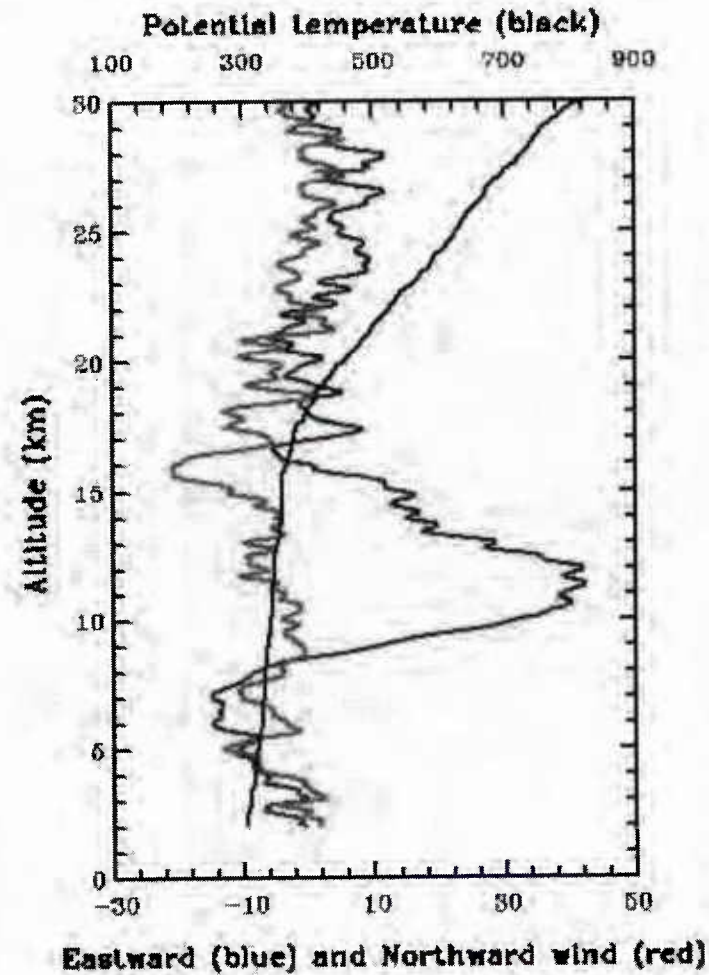
Standard numerical approaches do not capture the strong horizontal and vertical variability of the turbulent Prandtl number, the momentum and thermal eddy diffusivity coefficients, polarized Richardson number, heat /momentum fluxes and other turbulent parameters.

Conventional turbulence models cannot accurately predict intense turbulent layers in the stratosphere, as they are based on the flawed turbulent Prandtl number $Pr=1$ assumptions.

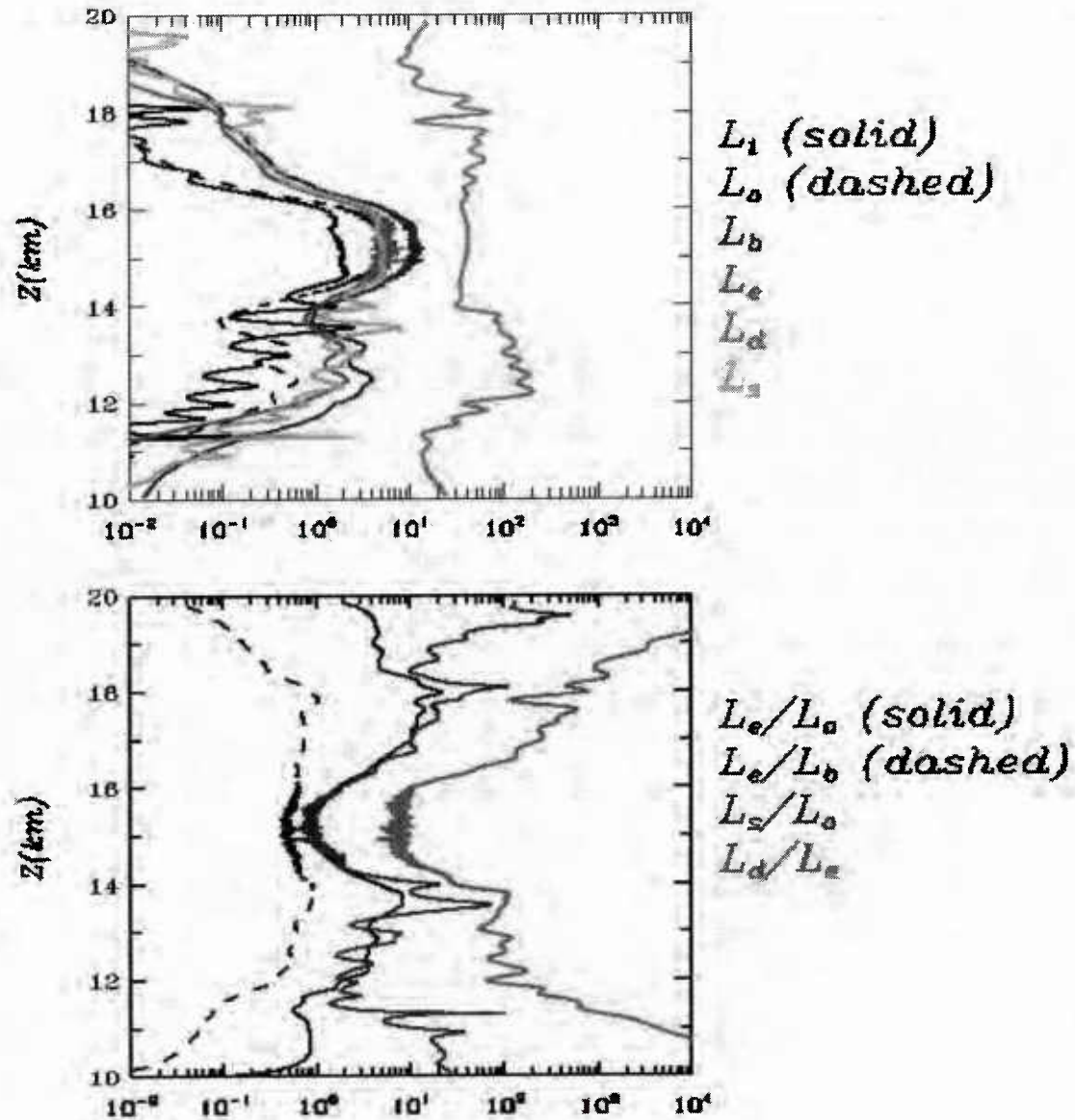
Conventional turbulence models (RANS, LES, $k-\epsilon$) do not properly incorporate oscillations (waves) and dependence of density/pressure on altitude (stable stratification). Standard numerical approaches including RANS fail to resolve waves+turbulence stratospheric physics phenomena.

Reynolds Averaged Navier-Stokes (RANS) methods are based on comparison of magnitudes/sizes of various terms but they are unable to resolve oscillations and wave dynamics.

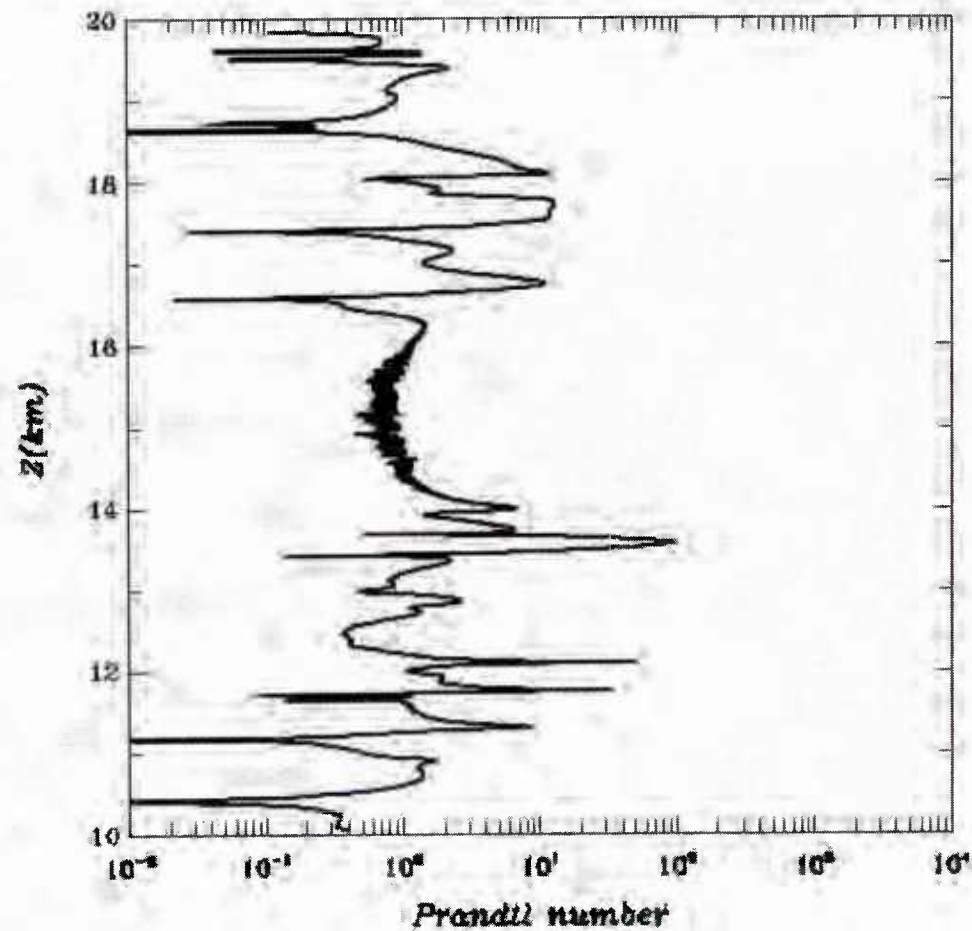
Phases, polarization, resonances and other wave effects are not captured by standard turbulence modeling numerical approaches (RANS, LES, $k-\epsilon$).



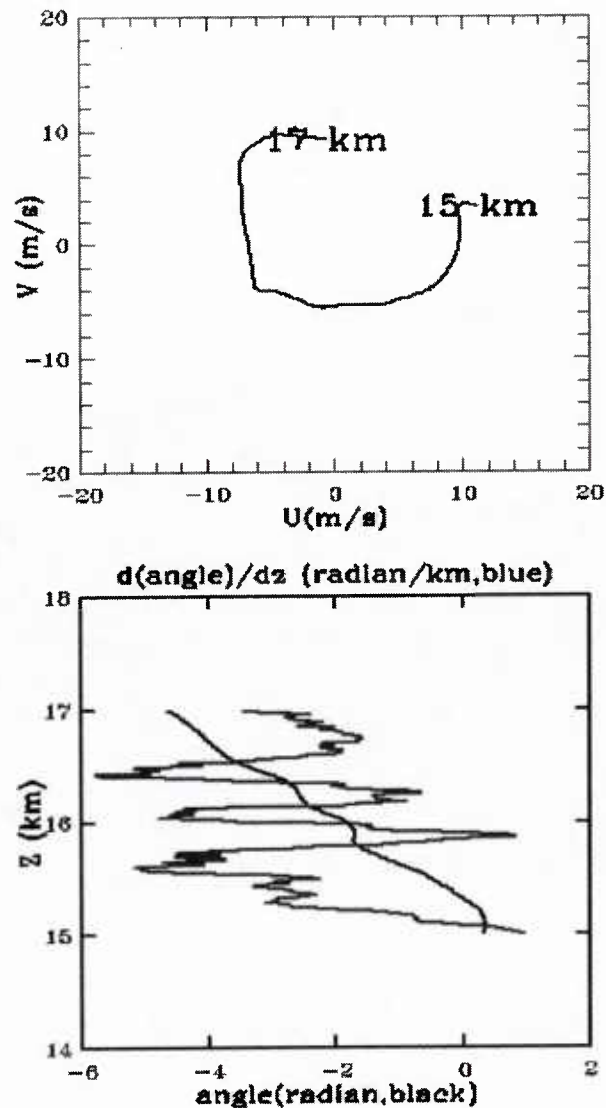
Vertical profiles of eastward wind (blue), northward wind (red), and potential temperature from a sounding at Hawaii (155.3 W, 19.5 N) on 12 December 2002 at 5 UTC



Upper panel: Vertical profiles of length scales: Tatarski (solid), Ozmidov (dashed), buoyancy (blue), Ellison (red), dissipation (purple), and shear (green); lower panel: ratio between various scales. Strong vertical variability of ratios of scales is insensitive to increased vertical resolution beyond a threshold. Variable length scales are used in sub-grid parameterizations of non homogeneous shear stratified turbulence. They control size and distribution of stratospheric turbulent layers.



Vertical profile of turbulent Prandtl number from 10km to 20km altitudes over Hawaii's Big Island (155.3W, 19.5N) on 12 December 2002. Non-Kolmogorov, layered, inhomogeneous shear-stratified turbulence in the lower stratosphere is characterized by strong vertical variability of the turbulent Prandtl number.



Upper panel: hodograph of the horizontal wind above the tropopause; lower panel: angle (u,v) (black) and the variation of the angle with altitude (blue). Thin stratospheric long lived CAT layers are induced by high helical (directional) shear coupled with reduced stability associated with helical velocity field of such polarized waves. Rapid change of horizontal wind direction triggers instabilities and formation of turbulent layers in the stratosphere.

THE POLARIZED RICHARDSON NUMBER

- (a) The polarized Ri is associated with the velocity fields of three dimensional nonlinear polarized inertia- gravity waves.**
- (b) The polarized Ri takes into account horizontal anisotropy and the angle between horizontal wave vectors and wind vectors at each vertical level (altitude).**
- (c) The polarized Ri and hodographs of polarized wind fields are needed to develop strategies for CAT detection at stratospheric altitudes (45,000-90,000 feet).**

$N(x_3)$: Brunt-Väisälä wave frequency profile

$\mathbf{U} = (U, V, W)$; $\mathbf{k} = (k_1, k_2, k_3)$.

$\alpha(x_3)$ denotes the angle between vectors

$d\mathbf{U}_h(x_3)/dx_3 = (dU(x_3)/dx_3, dV(x_3)/dx_3)$ and

$\mathbf{k}_h = (k_1, k_2)$.

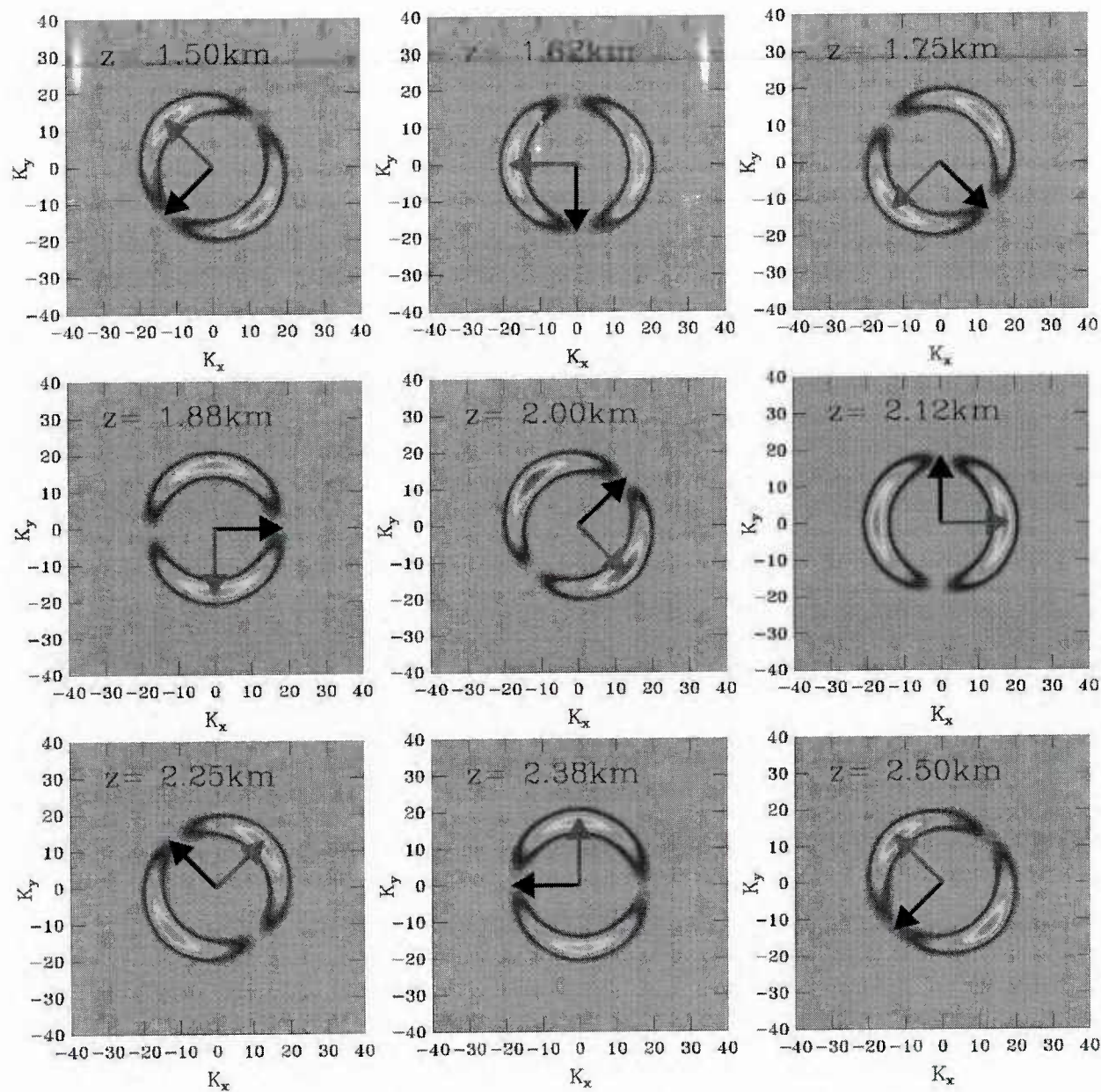
The Polarized Richardson Number:

$$Ri_p(x_3) = \frac{N^2(x_3)}{\left(\left(\frac{dU}{dx_3} \right)^2 + \left(\frac{dV}{dx_3} \right)^2 \right) \cos^2(\alpha(x_3))}.$$

For parallel shear flows ($V = 0$) we recover

definition of classical Richardson number

$$Ri = N^2/(dU/dx_3)^2.$$



Spectral components for divergence at different altitudes relative to the tropopause. The black and the red arrows indicate the direction of the helical wind, and the horizontal wavenumber of the most unstable mode respectively. Note that the wavenumber of the most unstable mode is perpendicular to the wind field and rotates in the same direction as the polarized wind field with increasing altitude.

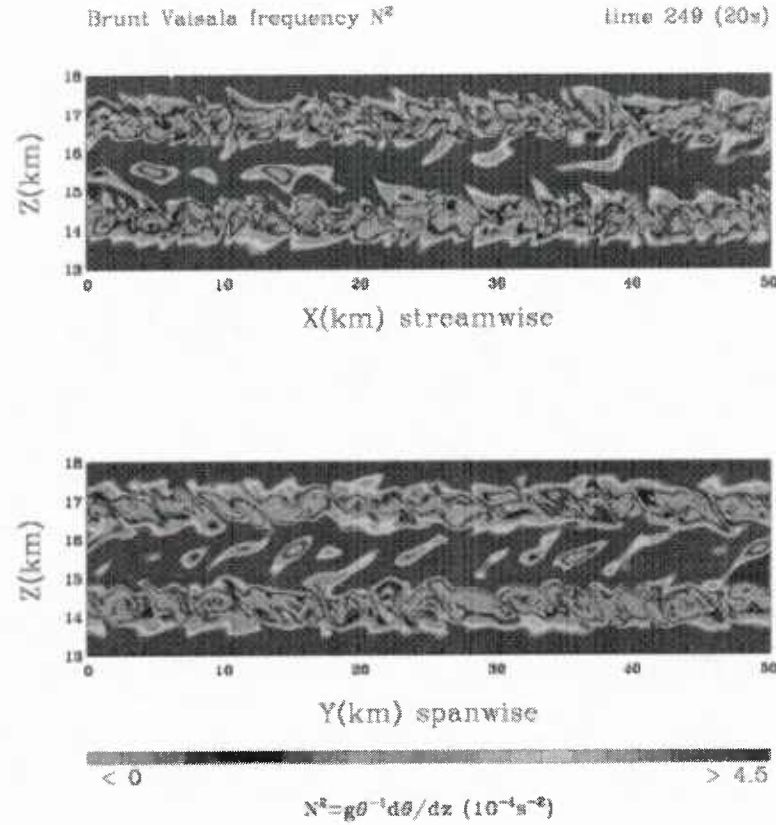


Fig. 1: upper panel: (streamwise-altitude) cross section of Brunt Vaisala frequency at $y=25$ km and $t=1.39$ h. lower panel: (spanwise-altitude) cross section of Brunt Vaisala frequency at $x=25$ km and $t=1.39$ h. Two strong CAT layers induced by polarized inertia-gravity wave at $z = 14.5$ km and $z = 17.5$ km.

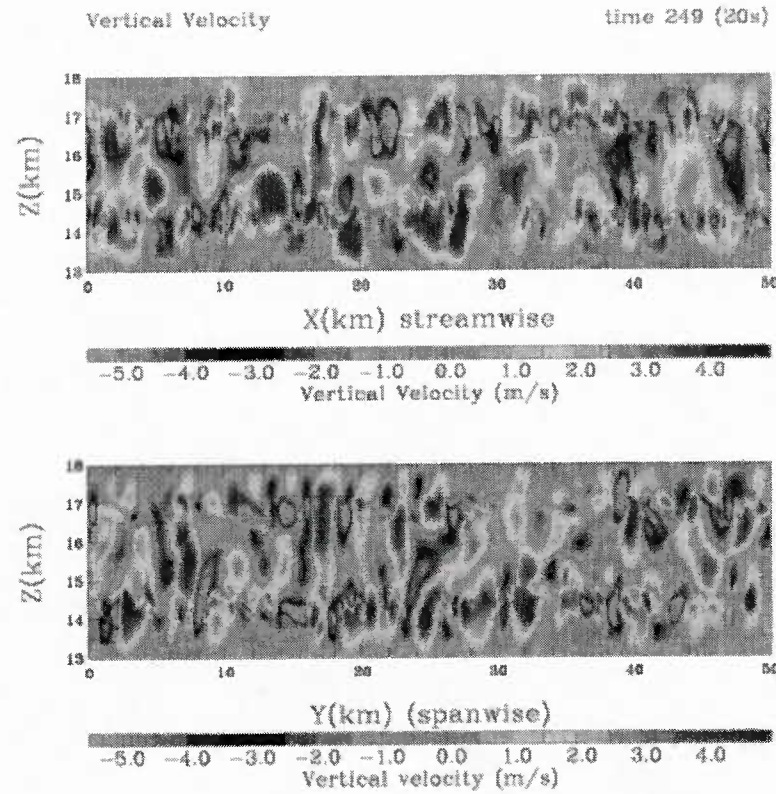
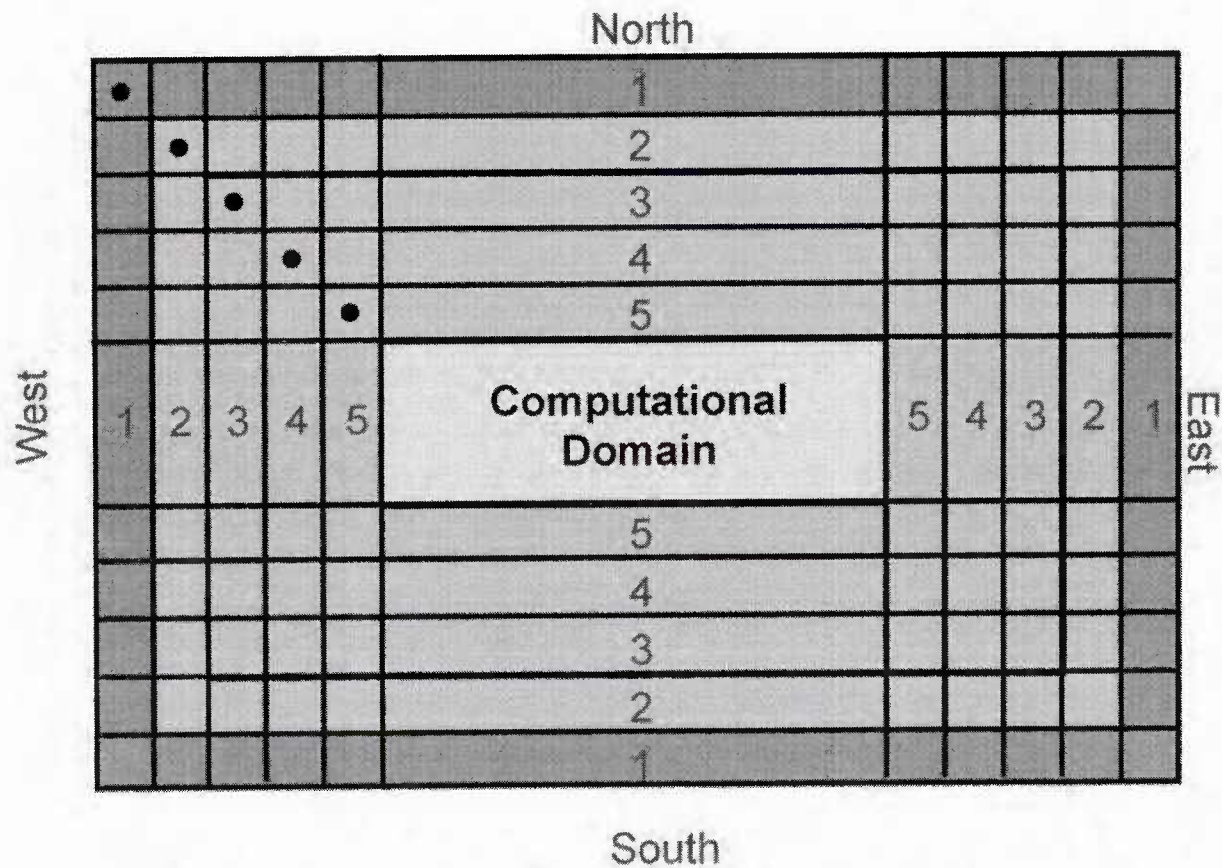





Fig. 2: upper panel: (streamwise-altitude) cross section of vertical velocity at $y=25$ km and $t=1.39$ h. lower panel: (spanwise-altitude) cross section of vertical velocity at $x=25$ km and $t=1.39$ h. Vertical velocity can jump from -10 m s^{-1} to $+10 \text{ m s}^{-1}$ within few hundred meters in the horizontal, causing pitchroll instability for the UAV.

Multiscale Modeling and Implicit Relaxation



-  BCs Specified from the coarser domain
-  BCs determined through implicit relaxation
-  Inner computational domain

The boundary relaxation schemes were implemented after each sub-step as an implicit correction. Using updated variables after each sub-time step, the relaxation is applied as a correction in a subsequent step using the relaxation flow equation (1). In the equation (1), coarse grid values are interpolated in space and to the time step $(n+1)$. For the prognostic variables located at points adjacent to the boundary, this implicit equation along the relaxation zone is solved subject to the matching boundary conditions. The outer values are specified from the parent domain, and the inner values are computed by the nested model using five and nine points wide relaxation zones. For relaxation zones with five grid points, the boundary matching conditions have the form given by (2)-(3). The subscript 0 indicates the boundary, and the subscript 4 corresponds to the last point in the relaxation zone. At each time step, the matrix equation (3) is solved in the relaxation zone. For the relaxation zone with nine grid points, the conditions are given by equations (4)-(5), where the subscript 0 indicates the boundary, and 8 is the last grid point in the relaxation zone. At each time step, the matrix equation (5) is solved in the relaxation zone. The coefficients in the matrix equation are given by equations (6)-(7). The Rayleigh (Newtonian) and diffusive relaxation times are fixed by the choice of the coefficients R and D defined in (8). Values of the computational parameters were investigated and optimized for UTLs. It was found that implicit relaxation schemes with a five-point deep relaxation zone have optimal performance for computational speed and adequate accuracy.

$$\frac{\psi_i^{n+1} - \psi_i^{n+1}}{\delta\tau} = -R_i(\psi_i^{n+1} - \psi_i^{c,n+1})$$

$$\left\{ \frac{D_i}{2\epsilon^2} (\psi_{i+1}^{n+1} - \psi_{i+1}^{c,n+1}) - 2(\psi_i^{n+1} - \psi_i^{c,n+1}) + (\psi_{i-1}^{n+1} - \psi_{i-1}^{c,n+1}) \right\} \quad (1)$$

$$\psi_4^{n+1} = \bar{\psi}_4^{n+1}, \psi_0^{n+1} = \bar{\psi}_0^{c,n+1} \quad (2)$$

$$\begin{pmatrix} b_1 & c_1 & 0 \\ a_2 & b_2 & c_2 \\ 0 & a_3 & b_3 \end{pmatrix} \times \begin{pmatrix} \psi_1^{n+1} \\ \psi_2^{n+1} \\ \psi_3^{n+1} \end{pmatrix} = \begin{pmatrix} Q_1 - a_1 \psi_0^{c,n+1} \\ Q_2 \\ Q_3 - c_3 \bar{\psi}_4^{n+1} \end{pmatrix} \quad (3)$$

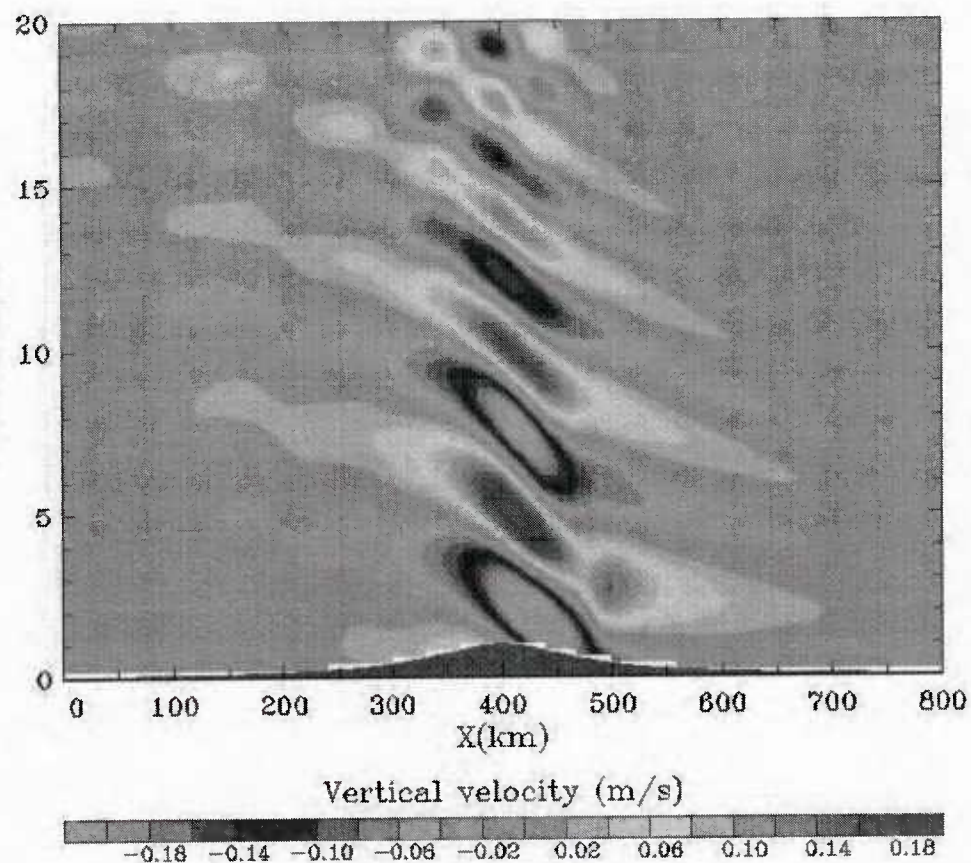
$$\psi_8^{n+1} = \bar{\psi}_8^{n+1}, \psi_0^{n+1} = \bar{\psi}_0^{c,n+1} \quad (4)$$

$$\begin{pmatrix} b_1 & c_1 & 0 & 0 & 0 & 0 & 0 \\ a_2 & b_2 & c_2 & 0 & 0 & 0 & 0 \\ 0 & a_3 & b_3 & c_3 & 0 & 0 & 0 \\ 0 & 0 & a_4 & b_4 & c_4 & 0 & 0 \\ 0 & 0 & 0 & a_5 & b_5 & c_5 & 0 \\ 0 & 0 & 0 & 0 & a_6 & b_6 & c_6 \\ 0 & 0 & 0 & 0 & 0 & a_7 & b_7 \end{pmatrix} \times \begin{pmatrix} \psi_1^{n+1} \\ \psi_2^{n+1} \\ \psi_3^{n+1} \\ \psi_4^{n+1} \\ \psi_5^{n+1} \\ \psi_6^{n+1} \\ \psi_7^{n+1} \end{pmatrix} = \begin{pmatrix} Q_1 - a_1 \psi_0^{c,n+1} \\ Q_2 \\ Q_3 \\ Q_4 \\ Q_5 \\ Q_6 \\ Q_7 - c_7 \bar{\psi}_8^{n+1} \end{pmatrix} \quad (5)$$

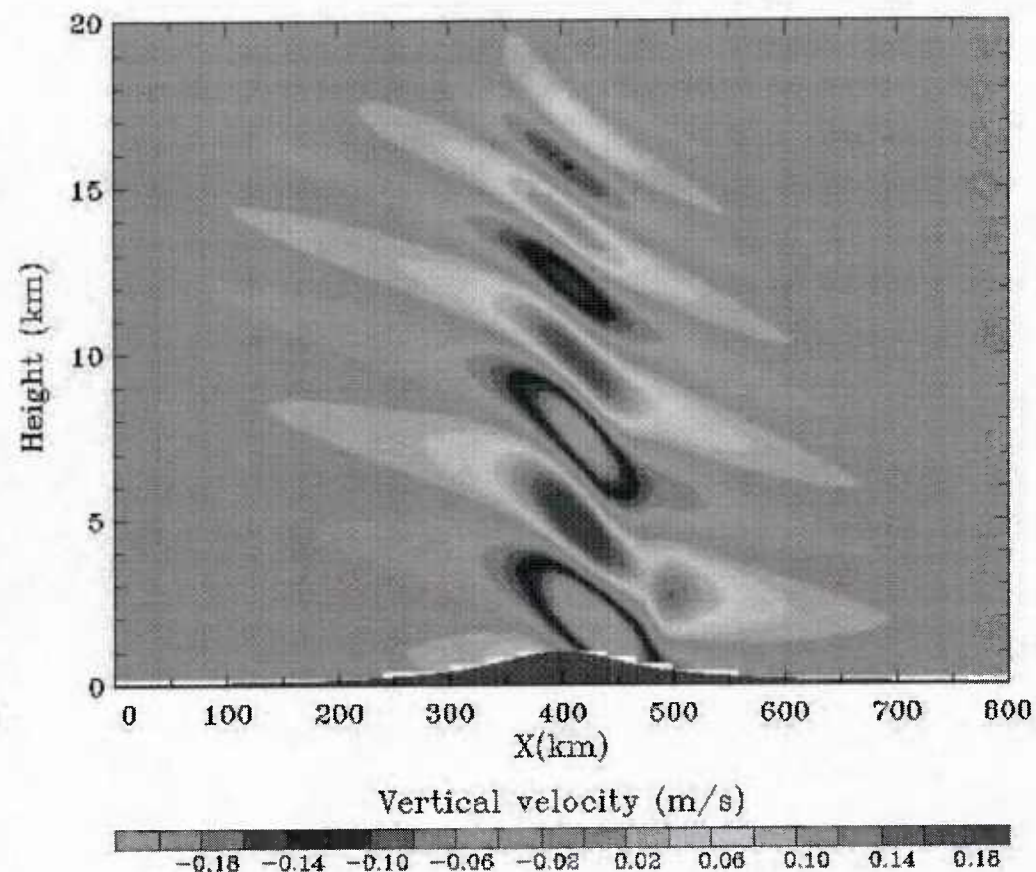
$$a_i = c_i = \frac{D_i \delta\tau}{\delta x^2}, b_i = -\left(1 + R_i \delta\tau + 2 \frac{D_i \delta\tau}{\delta x^2}\right) \quad (6)$$

$$Q_i = -\psi_i^{n+1} + \frac{D_i \delta\tau}{\delta x^2} \psi_{i-1}^{c,n+1} - \left(R_i \delta\tau + 2 \frac{D_i \delta\tau}{\delta x^2}\right) \psi_i^{c,n+1} + \frac{D_i \delta\tau}{\delta x^2} \psi_{i+1}^{c,n+1} \quad (7)$$

$$R_i = -\frac{c}{2\delta x} R_2^* R_0, D_i = -\frac{c\delta x}{2} D_2^* D_i \quad (8)$$



No relaxation

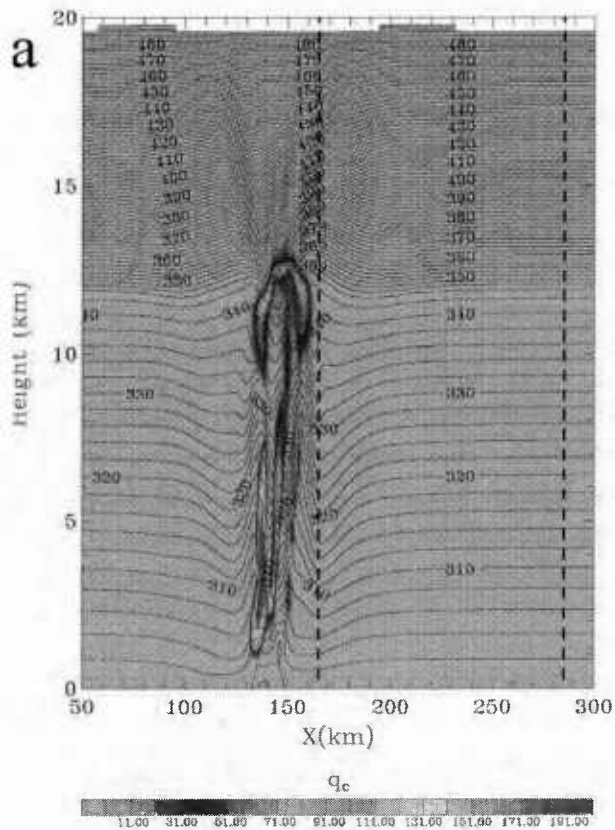


Vertical relaxation to the initial profiles

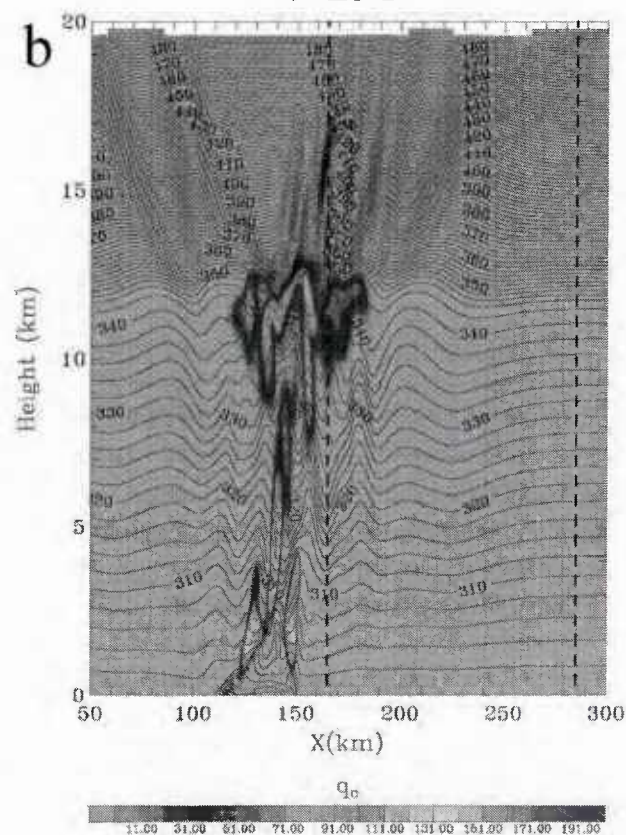
Longitude-altitude cross-section for potential temperature (contour) and vertical velocity (color).

Simulation of a cloud entering a limited area domain using implicit relaxation

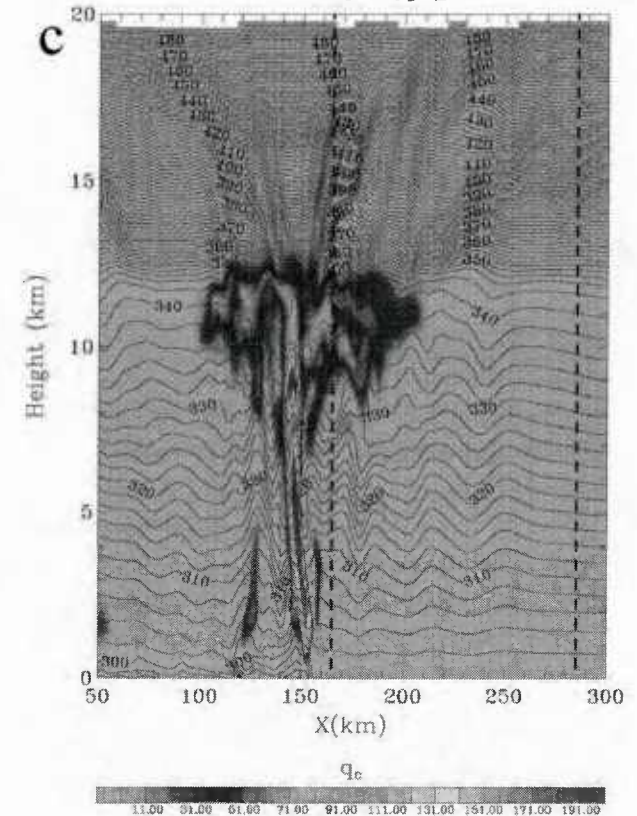
t=191



t=291



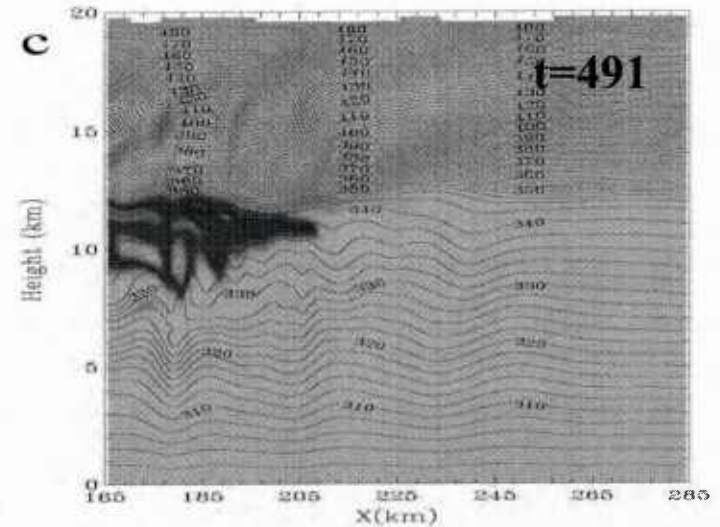
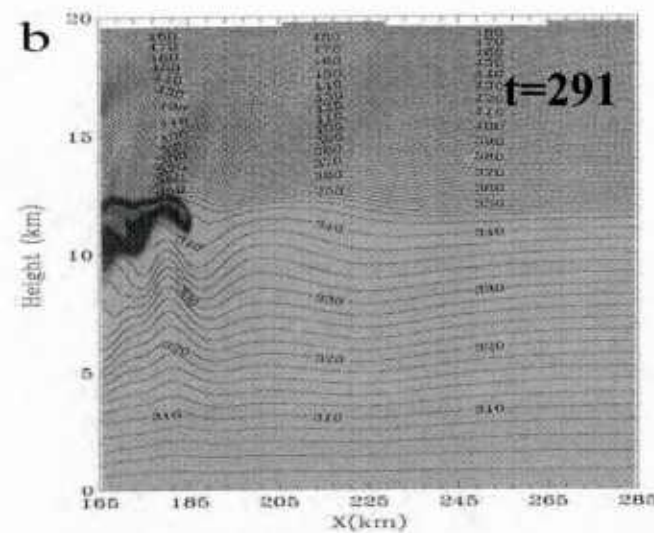
t=491



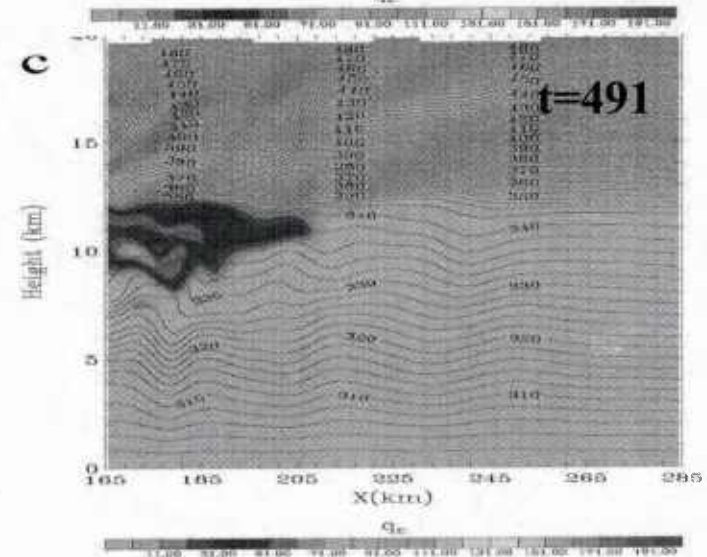
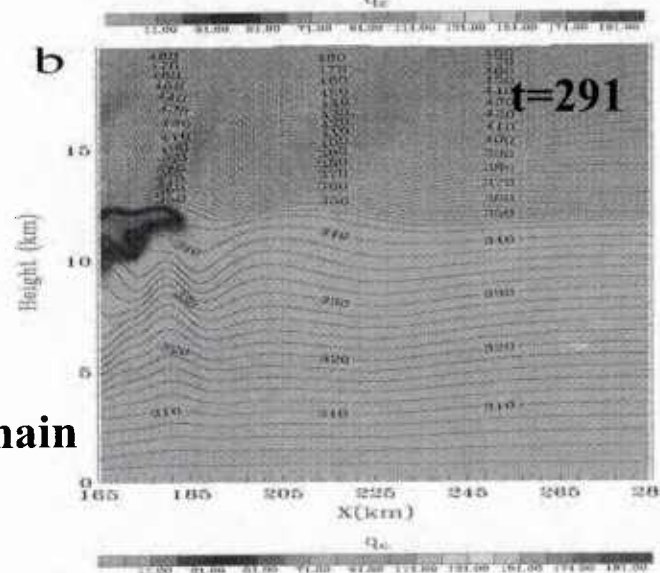
Simulation of a cloud entering a limited area domain using implicit relaxation

❖ Vertical cross sections showing water cloud and potential temperature: nested simulations with *implicit* relaxation.

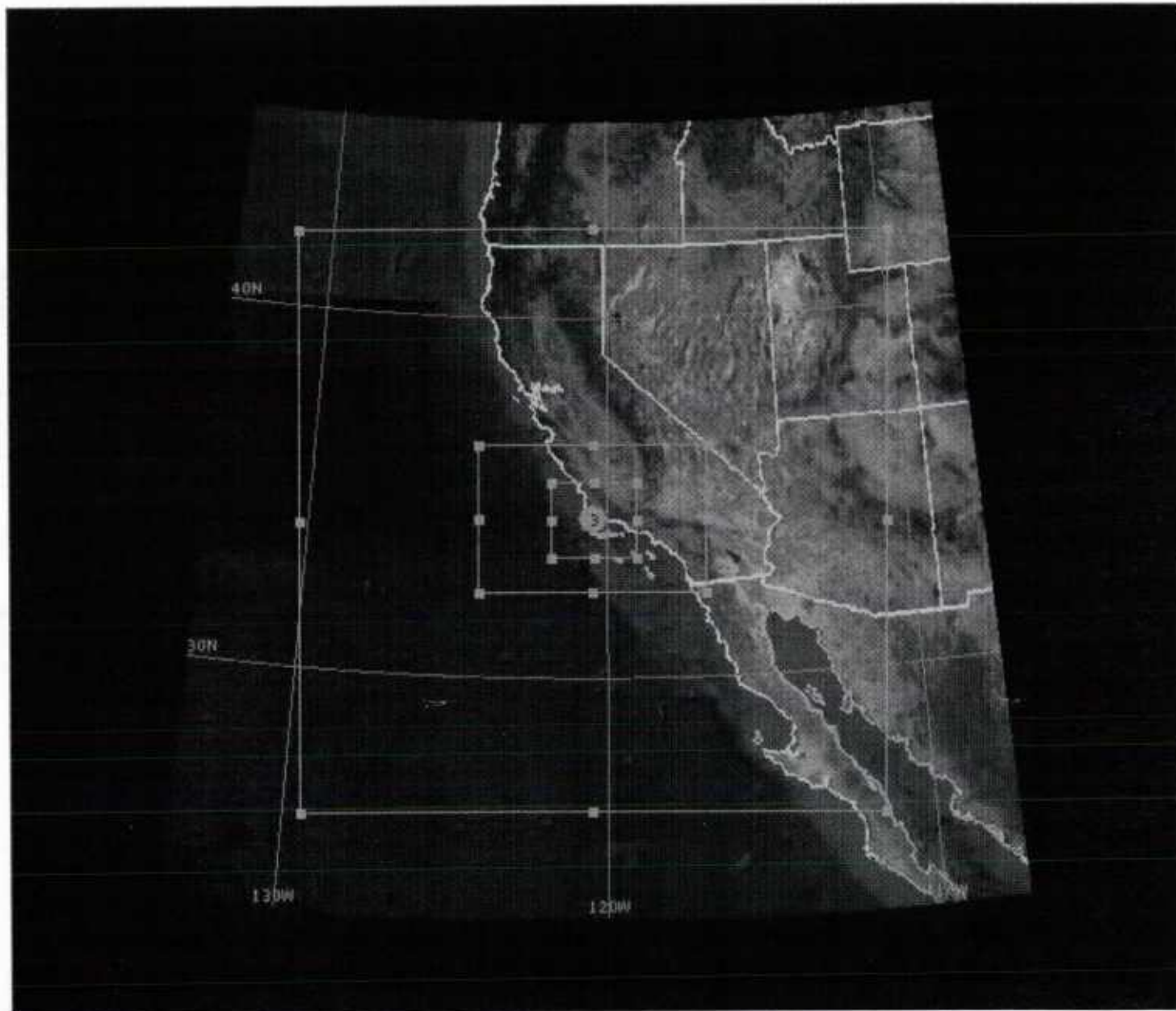
Limited area



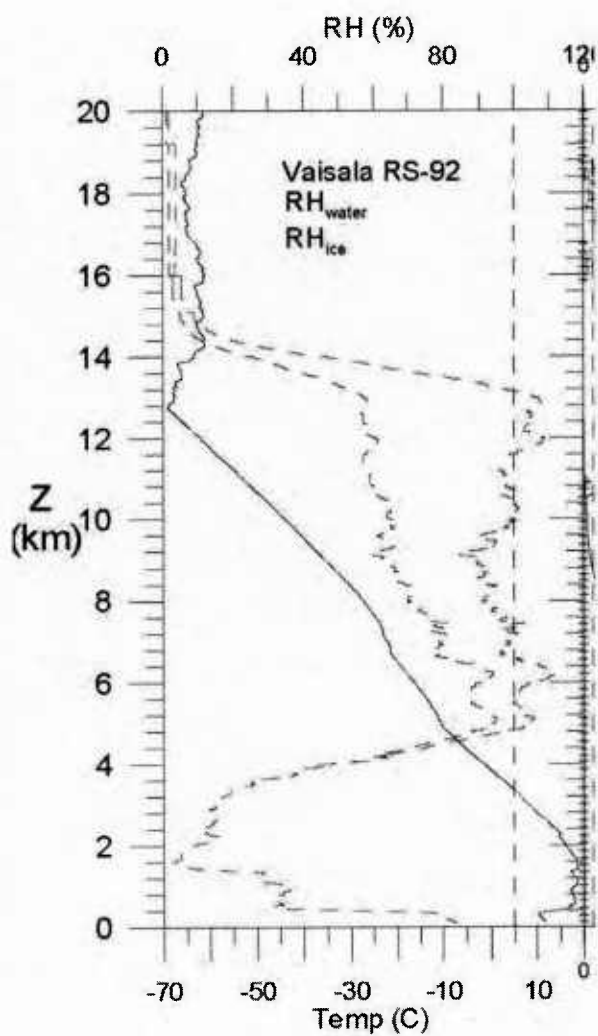
Large domain



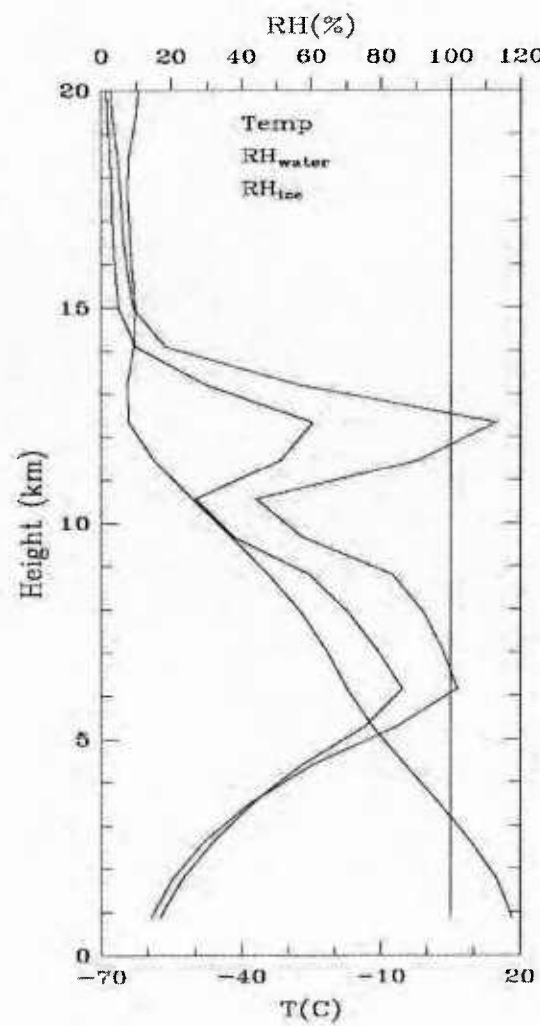
Cloud Forecasting and Comparison with Observations



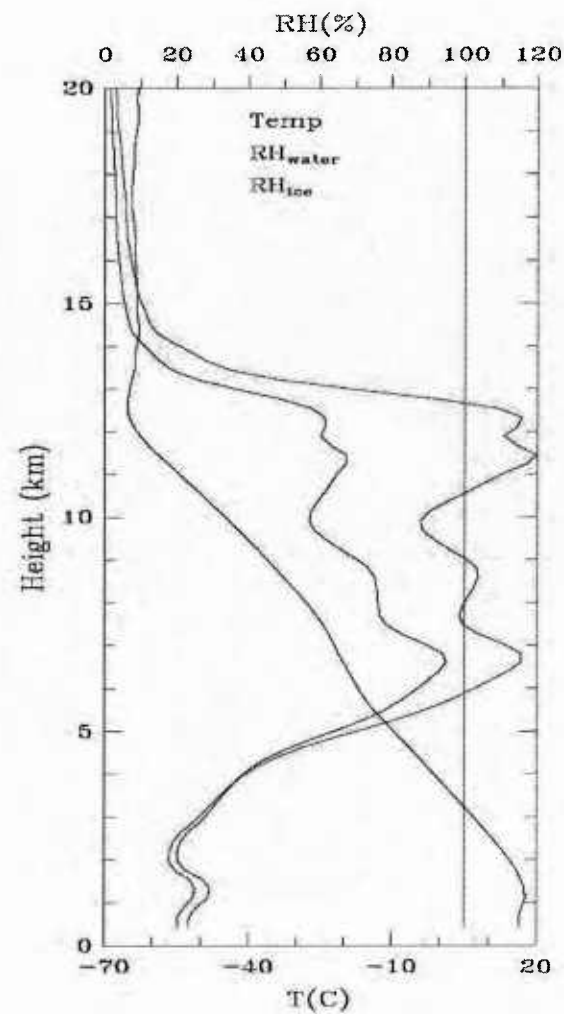
Observation



Without vertical nesting (60 vert levels)



With vertical nesting (180 vert levels)



3D Non-Hydrostatic Navier-Stokes Eqs for UTLS Dynamics

The moist equations are formulated using a terrain-following pressure coordinate:

$$\eta = \frac{(p_{dh} - p_{dht})}{\mu_d} \quad \text{where} \quad \mu_d = p_{dhs} - p_{dht}$$

$$\partial_t U + \nabla \cdot \vec{V} u + \mu_d \alpha \partial_x p + (\alpha / \alpha_d) \partial_\eta p \partial_x \phi = F_U$$

$$\partial_t V + \nabla \cdot \vec{V} v + \mu_d \alpha \partial_y p + (\alpha / \alpha_d) \partial_\eta p \partial_y \phi = F_V$$

$$\partial_t W + \nabla \cdot \vec{V} w - g \left((\alpha / \alpha_d) \partial_\eta p - \mu_d \right) = F_W$$

$$\partial_t \Theta + \nabla \cdot \vec{V} \theta = F_\Theta$$

$$\partial_t \mu_d + \nabla \cdot \vec{V} = 0$$

$$\partial_t \phi + \frac{1}{\mu_d} \left(\vec{V} \cdot \nabla \phi - g W \right) = 0$$

$$\partial_t Q_m + \nabla \cdot \vec{V} q_m = F_{Q_m}$$

3D Non-Hydrostatic Navier-Stokes Equations for UTLS Dynamics

along with the diagnostic relation for the inverse density $\partial_\eta \phi = -\alpha_d \mu_d$

and the equation of state $p = p_0 \left(\frac{R_d \theta_m}{p_0 \alpha_d} \right)^\gamma$;

$\phi = gz$ is the geopotential, $\alpha_d = \frac{1}{\rho_d}$ is the inverse density of the dry air p is the pressure,

$\vec{V} = \mu_d \vec{v} = (U, V, W)$ and $\Theta = \mu_d \theta$ are the coupled velocity vector and potential temperature.

F represents forcing terms arising from model physics, turbulent mixing, rotation, ...

$Q_m = \mu_d q_m$, $q_m = q_v, q_c, q_i, \dots$ are the coupled mixing ratios of water vapor, cloud, ice, etc.

$$\theta_m = \theta \left(1 + (R_v / R_d) q_v \right) \approx \theta (1 + 1.61 q_v)$$

$$\alpha = \alpha_d \left(1 + q_v + q_c + q_r + q_i + \dots \right)^{-1}$$

New fast and accurate time-stepping scheme for UTLS forecasting

The formulation of the fourth-order filtered time-stepping scheme has the form:

$$\frac{\psi^{n+1} - \bar{\psi}^{n+1}}{2\Delta t} = F(\psi^n) \quad (1)$$

$$\bar{\psi}^{n+1} = \bar{\psi}^{n+1} + \gamma(-\bar{\psi}^{n+3} + 4\bar{\psi}^{n+2} - 6\bar{\psi}^{n+1} + 4\psi^n - \psi^{n+1}) \quad (2)$$

where ψ^n is the approximation to the solution at the time $n\Delta t$ and $\bar{\psi}^n$ is the solution after applying a fourth-order implicit time filter using a real constant γ that determines the strength of the filter. We note that the scheme uses an implicit filter, in that both $\bar{\psi}^{n+1}$ and ψ^{n+1} in Eqs.1-2 are not known and depend on each other. Nevertheless, it is simple enough to derive the explicit expressions of both $\bar{\psi}^{n+1}$ and ψ^{n+1} .

If we let $\bar{\psi}^{n+1} = \bar{\psi}^{n+1} + \gamma(-\bar{\psi}^{n+3} + 4\bar{\psi}^{n+2} + 4\psi^n)$ the scheme can be formulated recursively as follows:

$$\bar{\psi}^{n+3} = \frac{-2\Delta t \gamma F(\psi^n) + \bar{\psi}^{n+1}}{1 + 7\gamma}, \quad \bar{\psi}^{n+1} = \frac{(1 + 6\gamma)2\Delta t F(\psi^n) + \bar{\psi}^{n+3}}{1 + 7\gamma},$$

$$\bar{\psi}^{n+1} = \bar{\psi}^{n+1} + \gamma(-\bar{\psi}^{n+3} + 4\bar{\psi}^{n+2} + 4\psi^n).$$

In this formulation, the fields of ψ that are required to solve these equations are $\bar{\psi}^{n+2}$, $\bar{\psi}^{n+1}$ and ψ^n . At the end of each time step, the storage arrays occupied by these fields are overwritten by $\bar{\psi}^{n+3}$, $\bar{\psi}^n$ and ψ^{n+1} . The scheme is implemented such that only three fields are stored per time step. Formal stability analysis shows that the new method generates amplitude errors of $O[\Delta t]^4$. The new time-stepping scheme is found to control well numerical dispersion. In addition to noticeably improving the resolution of the physical modes, the method is simple to implement and has a wider region of stability.

The amplitude errors in the new numerical time-stepping scheme are comparable to the amplitude errors of the Runge-Kutta (RK3) scheme. The new scheme, however, requires only one function evaluation per time step as opposed to the RK3 which is more expensive as it requires three evaluations for each time step. New numerical scheme is three times faster for the same accuracy than the RK3 resulting in faster forecasts.

Analyses of turbulence cases suggested by David Keller (AFWA). The selection of cases was based mostly on the height of the (severe) turbulence being at least 30,000 feet AGL. The only routine observations available are reports of turbulence provided by pilots of commercial airlines (pilot reports, PIREPs). Figure 1 shows location of reported Northwestern/Western Montana CAT cases. These CAT events occurred during the time periods from 12Z, December 5, 2012 to 00Z, December 6, 2012. UTC time is shown.

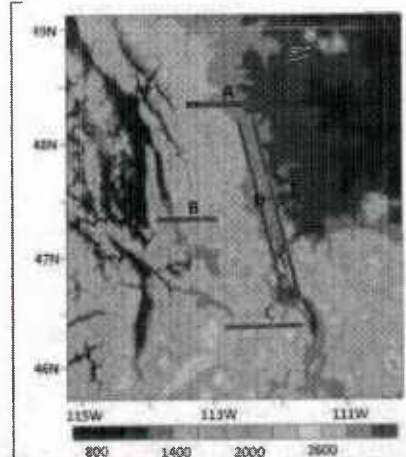


Figure 1: Northwestern/Western Montana case.

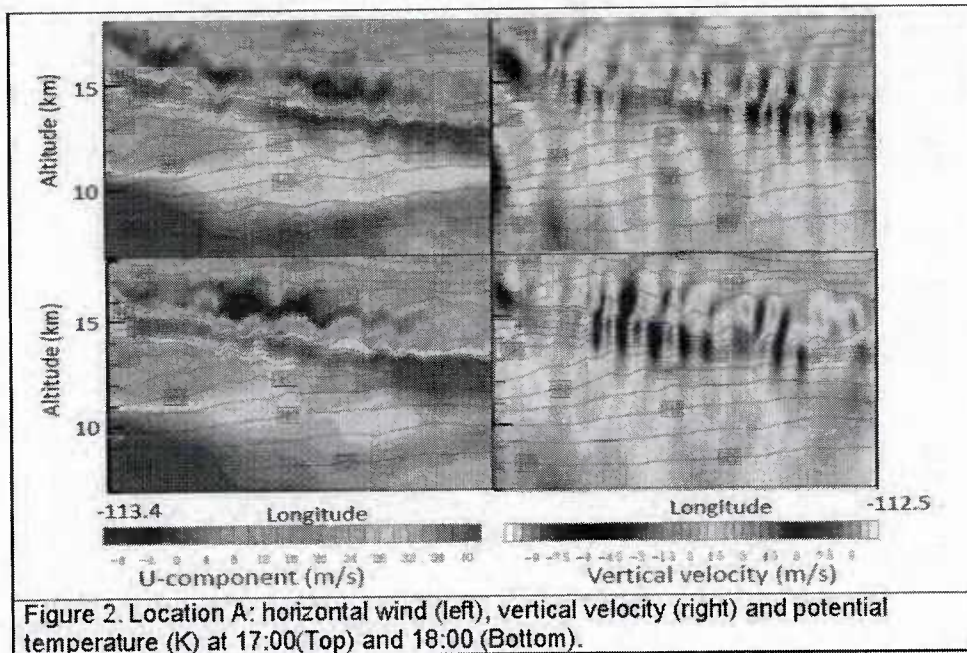
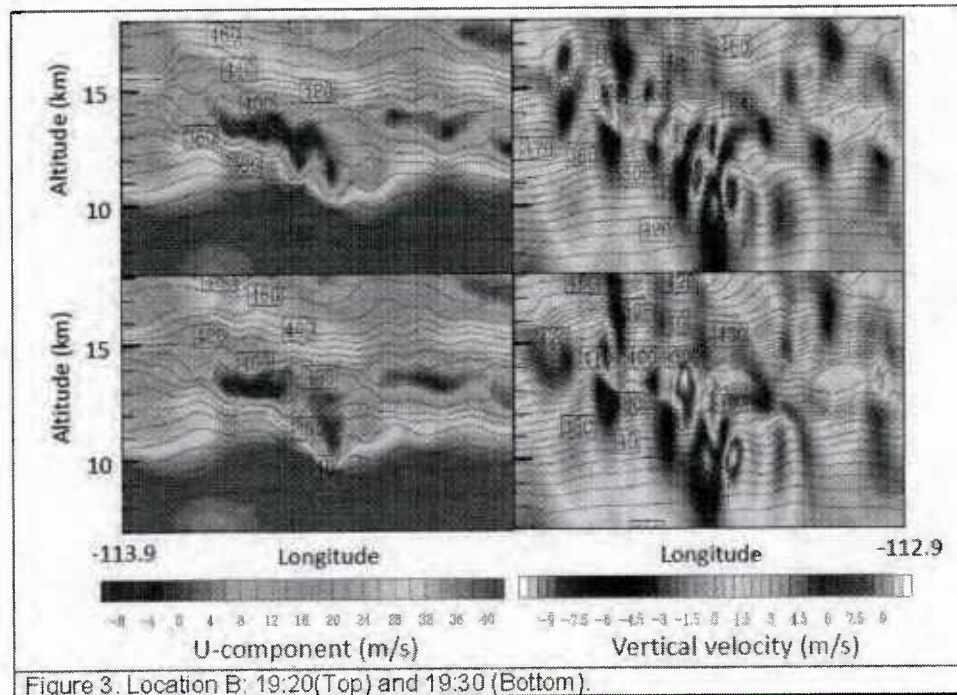


Figure 2. Location A: horizontal wind (left), vertical velocity (right) and potential temperature (K) at 17:00 (Top) and 18:00 (Bottom).

Figures 2-6 show plots of five cross-sections from microscale simulations zoomed to UTLS altitudes. Figure 2 shows the horizontal velocity U-component (m/s), vertical velocity (m/s) and potential temperature (K) contours in cross-section A (see Figure 1). Analyses of computational results indicated that the physical mechanism of CAT is associated with high vertical shear of horizontal wind components and rapid changes in direction of the horizontal wind vector with altitude in the UTLS zone.

Figure 3 is the example of the three variables' cross-section for Location B at 19:20Z and 19:30, respectively. The vertical velocity reaches values exceeding 10 m/s in both upward and downward directions (shown in the right panel of Figure 3).



Figures 4-6 are examples of the vertical variations of the horizontal velocity U-component, vertical velocity and potential temperature along the cross-section C-E, respectively. Patches of CAT in UTLS with positive/negative values of vertical velocities reaching 10m/s in magnitude were computed at these locations during 19:00 to 23:30Z time interval.

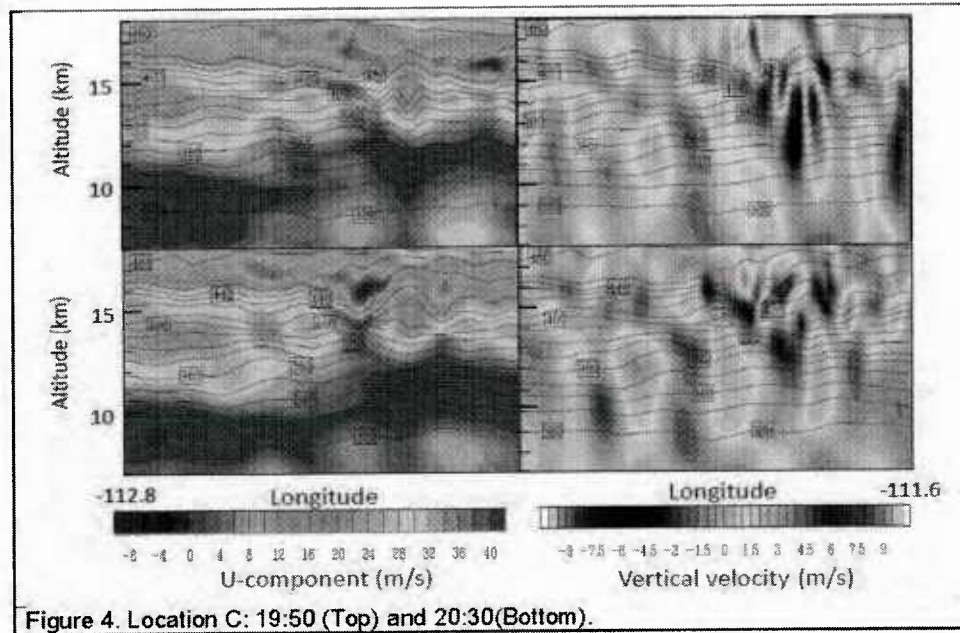


Figure 4. Location C: 19:50 (Top) and 20:30(Bottom).

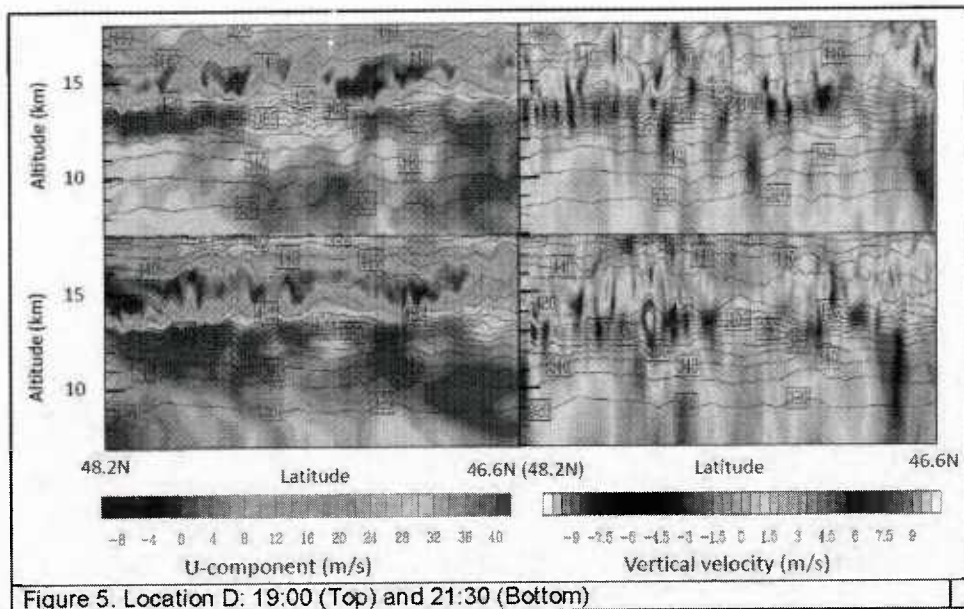


Figure 5. Location D: 19:00 (Top) and 21:30 (Bottom)

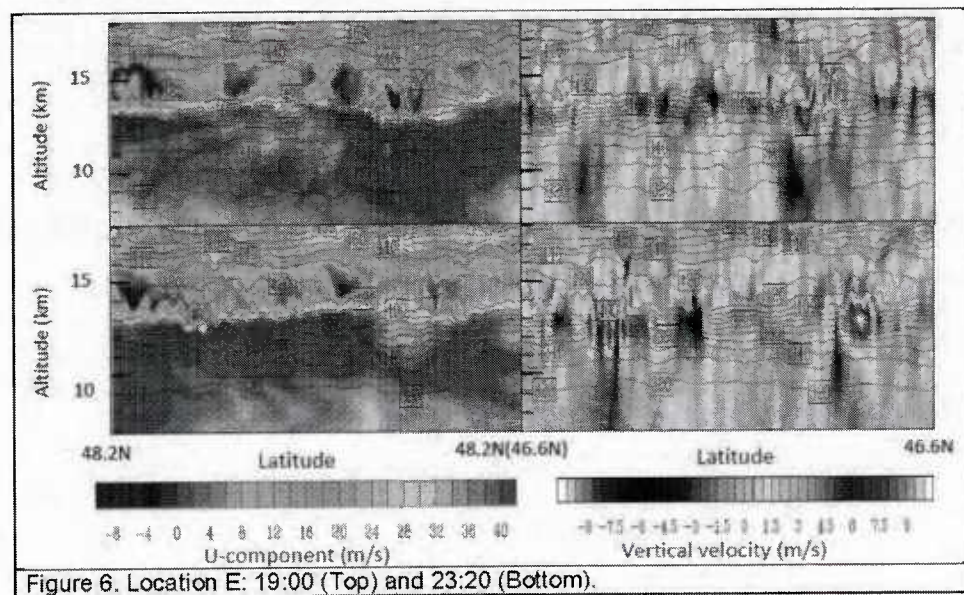


Figure 6. Location E: 19:00 (Top) and 23:30 (Bottom).

Analyses of turbulence cases included:
 (i) Northwestern/Western Montana (case 1);
 (ii) Slanted part of CA/NV border (case 2);
 (iii) Southern CA west of Las Vegas (case 3). The selection of cases was based mostly on the height of the turbulence being at least 30,000 feet AGL. The only routine observations available are reports of turbulence provided by pilots of commercial airlines (pilot reports, PIREPs). Figure 2 shows location of a CAT case reported in Montana during the time period from 12Z, December 5, 2012 to 00Z, December 6, 2012.

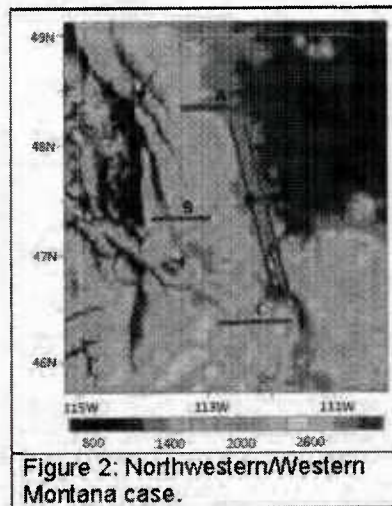
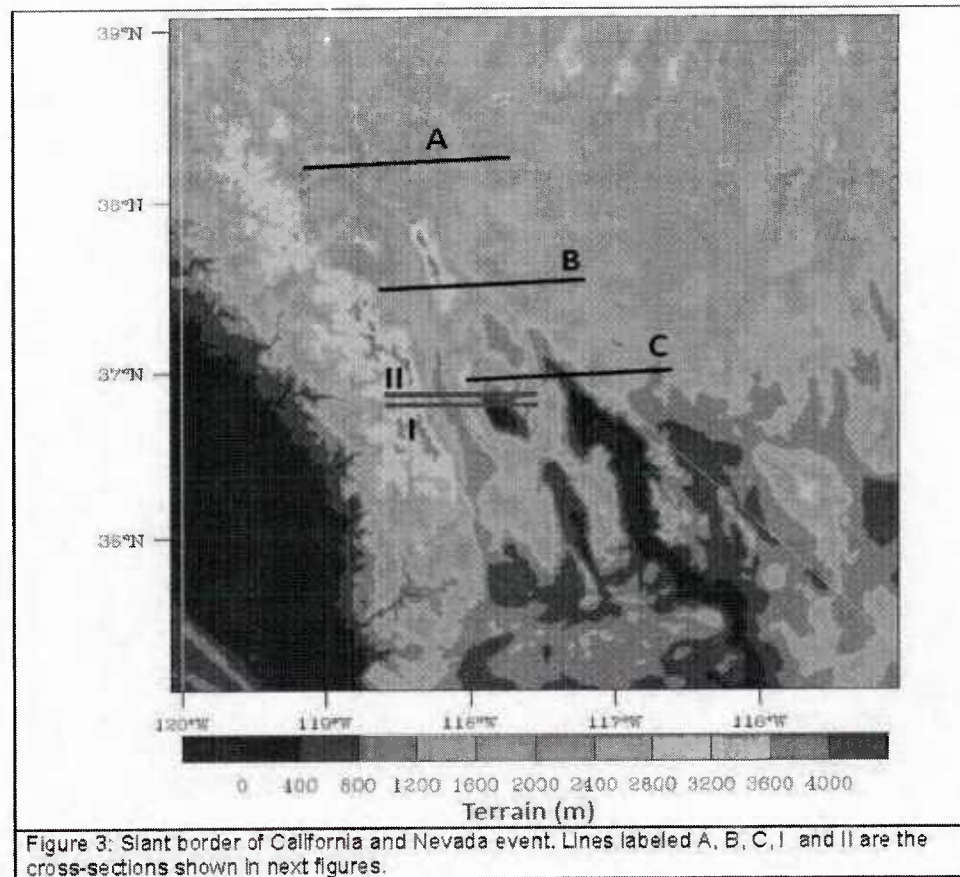
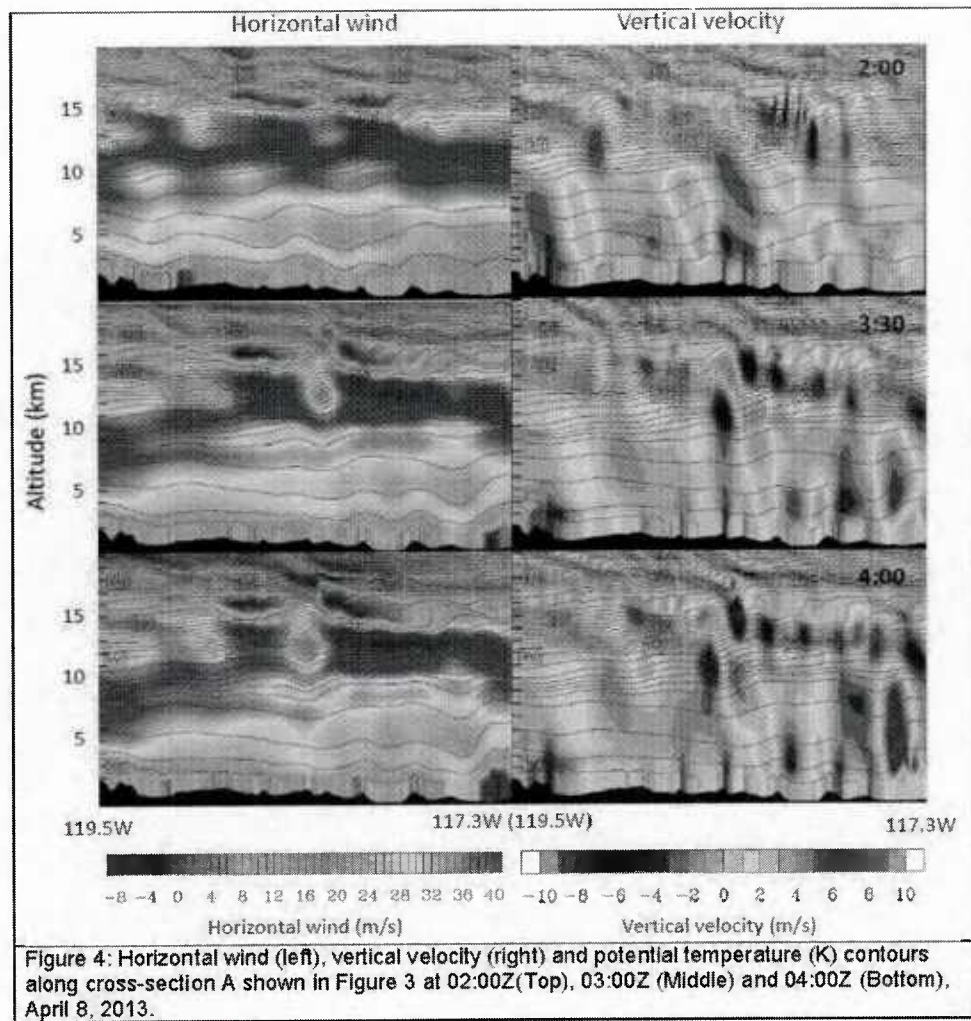


Figure 2: Northwestern/Western Montana case.

Figures 3-20 show microscale simulations of turbulence cases suggested by David Keller for slanted part of CA/NV border, and Southern CA west of Las Vegas locations (cases 2 and 3, respectively). UTC time is shown.

Figures 4-11 and Figures 13-20 are examples of the vertical variations of the horizontal velocity U-component, vertical velocity, TKE and potential temperature along the cross-sections shown in Figures 3 and 12, respectively. Patches of CAT in UTLS with positive/negative values of vertical velocities reaching 10m/s in magnitude were computed at these locations on April 8, 2013 (case 2, Figure 3) and April 15, 2013 (case 3, Figure 12). Analysis of these cases showed that many physical mechanisms of instabilities and turbulence in UTLS are similar to the ones previously studied by PI Mahalov. Complex turbulent dynamics is successfully resolved using physics-based predictive modeling and microscale nested simulations with implicit relaxation techniques.





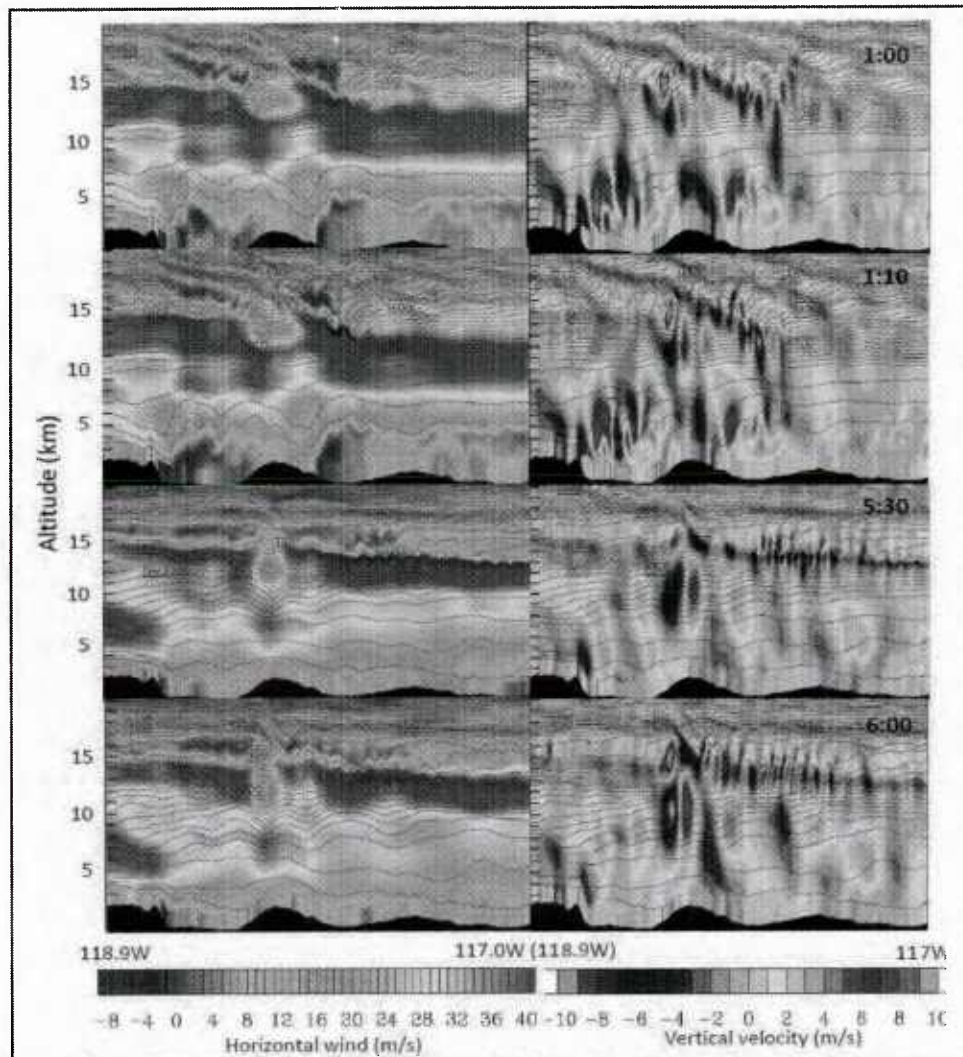


Figure 5: Horizontal wind (left), vertical velocity (right) and potential temperature (K) contours along the cross-section B (shown in Figure 3) at the time periods 01:00Z, 01:10Z, 05:30Z and 06:00Z (in the figure from Top to Bottom), April 8, 2013.

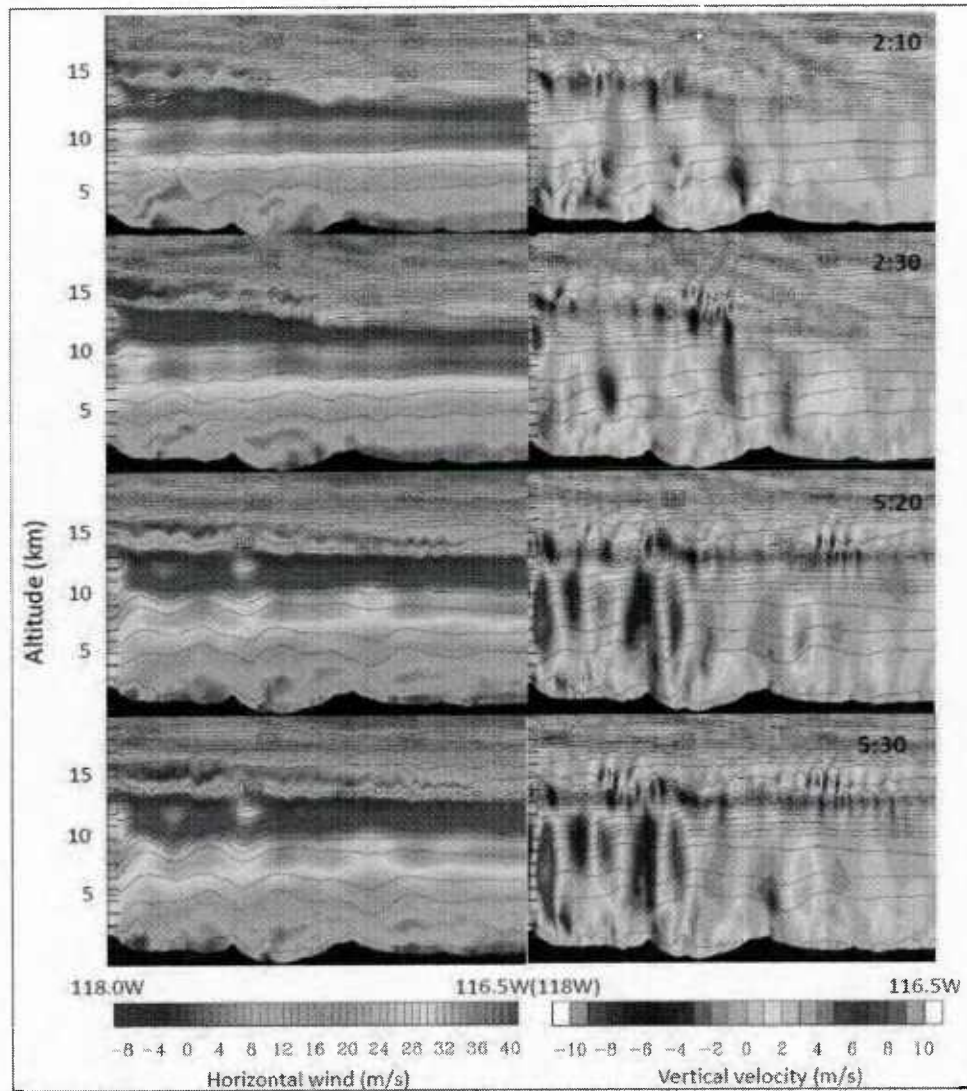


Figure 6: Horizontal wind (left), vertical velocity (right) and potential temperature (K) contours along cross-section C (shown in Figure 3) at the time periods 02:10Z, 02:30Z, 05:20Z and 05:30Z (in the figure from Top to Bottom), April 8, 2013.

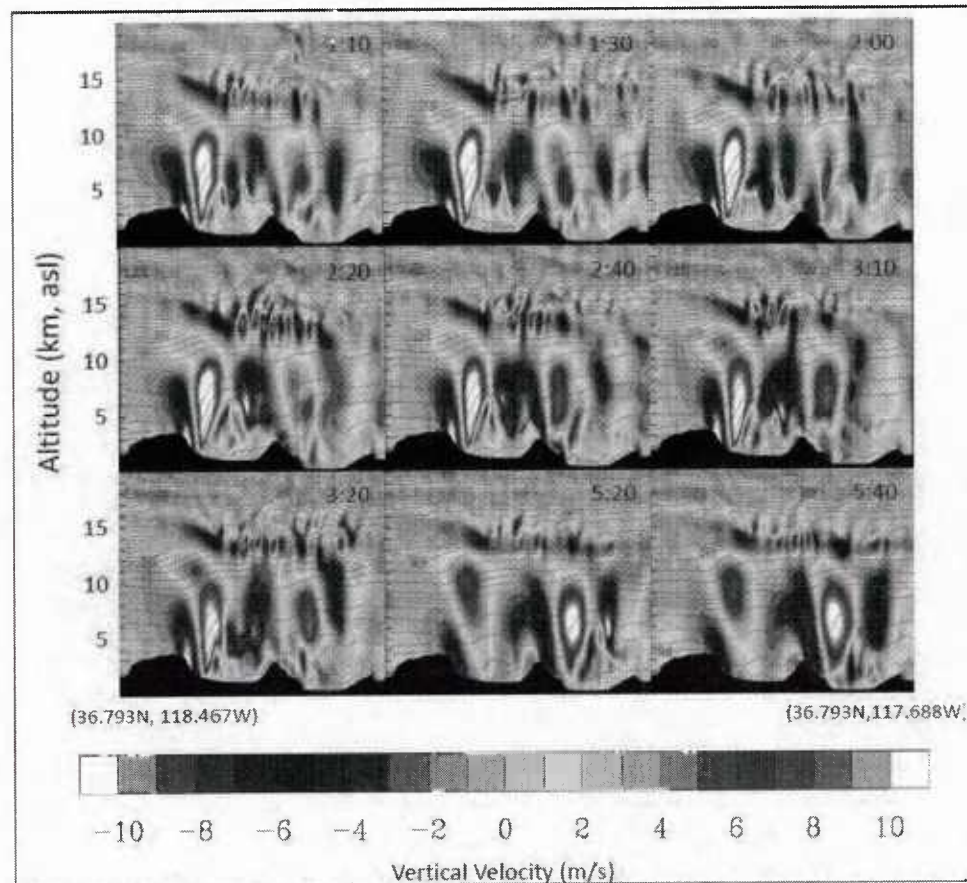


Figure 7: Vertical velocity along Line I (shown in Figure 3) at different time periods on April 8, 2013. The potential temperature is contoured at 5K intervals. The exact locations are along Line I from (36.793°N, 118.467°W) to (36.793°N, 117.688°W).

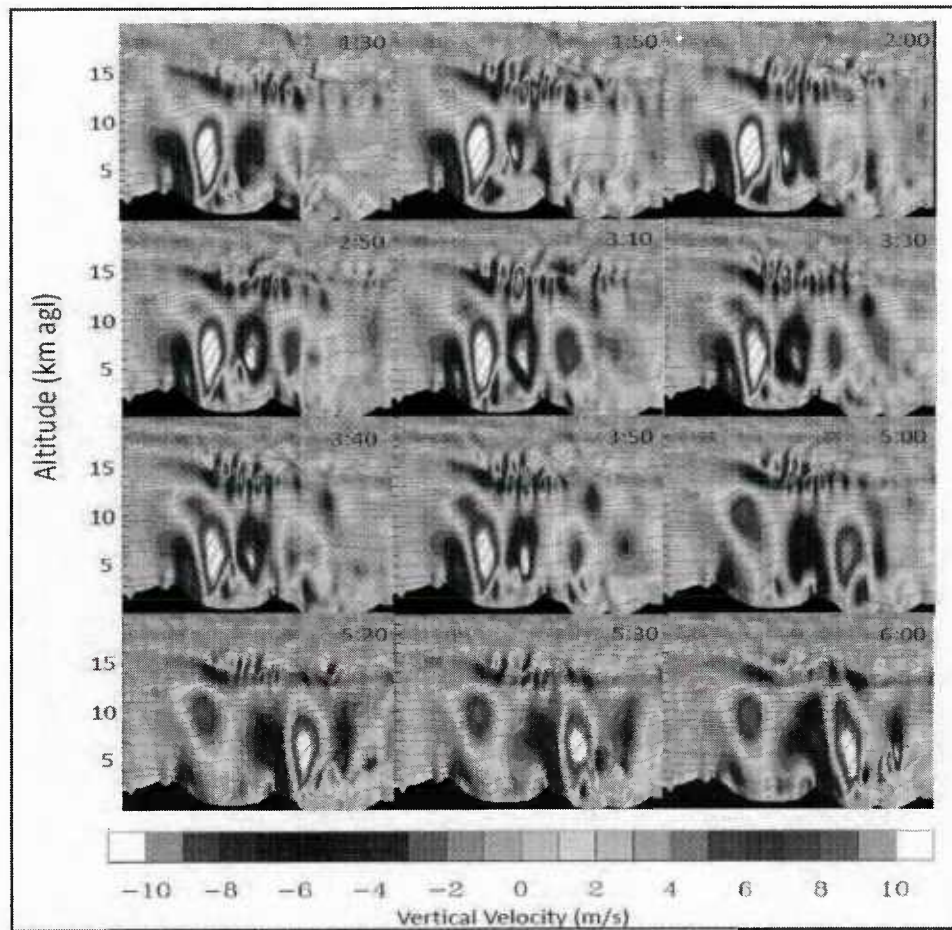


Figure 8: Vertical velocity at cross-sections along Line II (shown in Figure 3) at different time periods on April 8, 2013. The potential temperature is contoured at 5K intervals. The exact location for Line II is from (36.831°N, 118.647°W) to (36.831°N, 117.568°W).

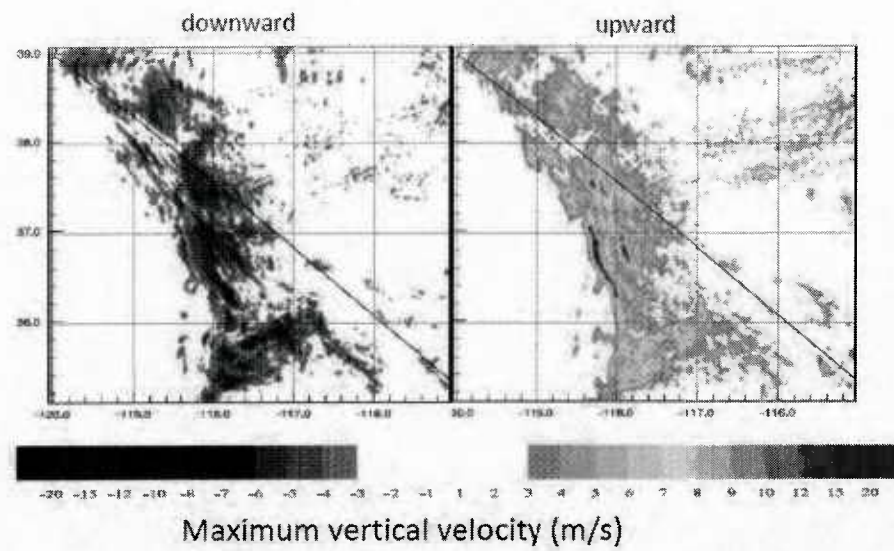
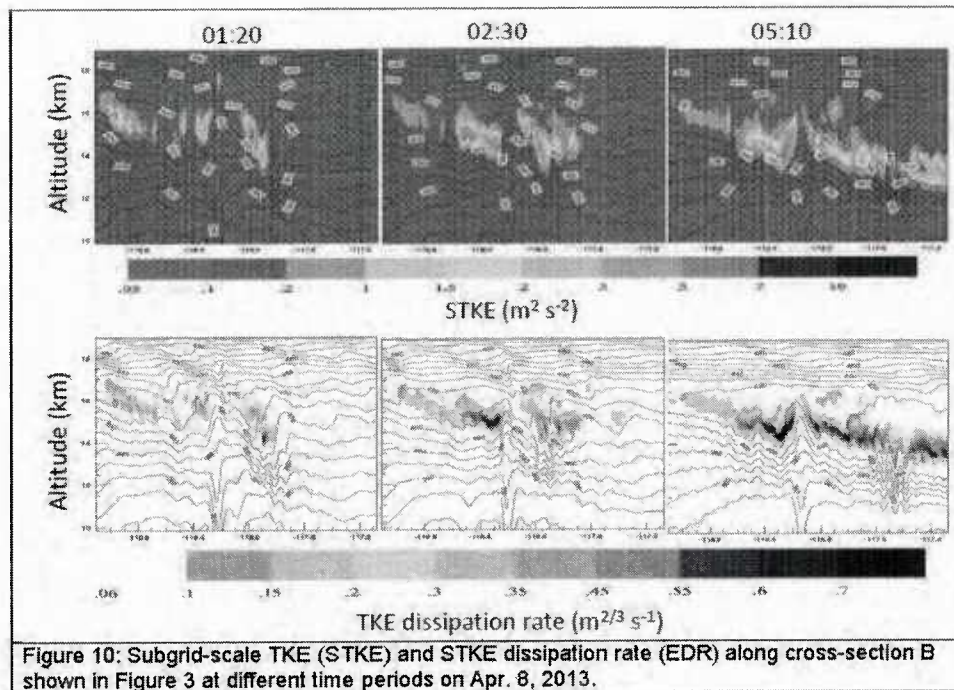


Figure 9: Maximum vertical velocity in UTLS between 7km and 15 km altitudes on Apr. 8, 2013.



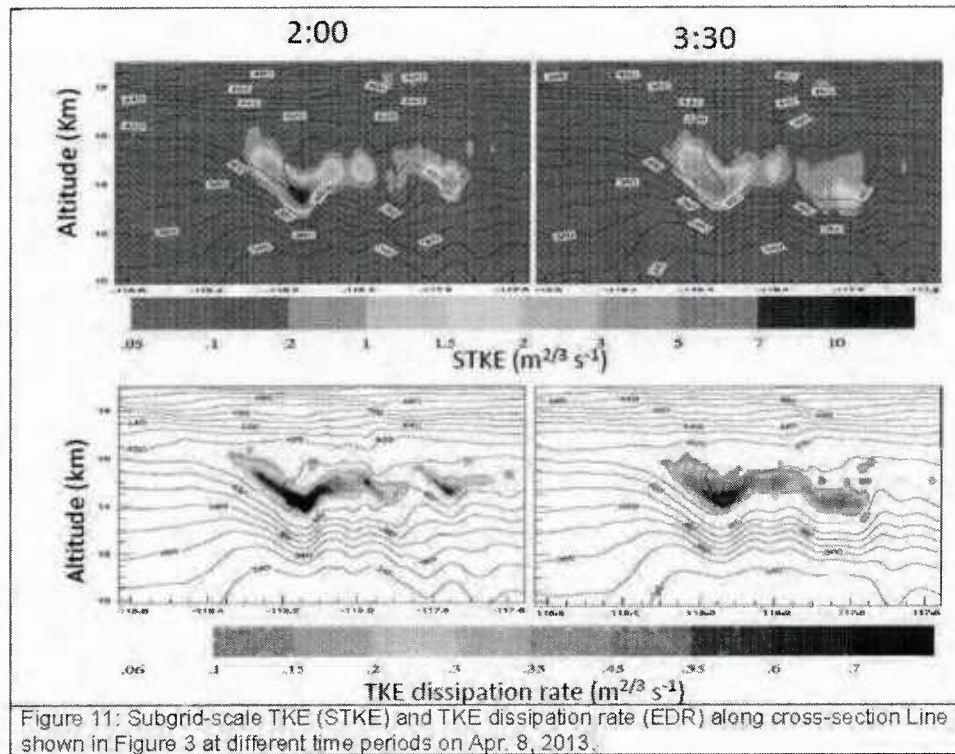
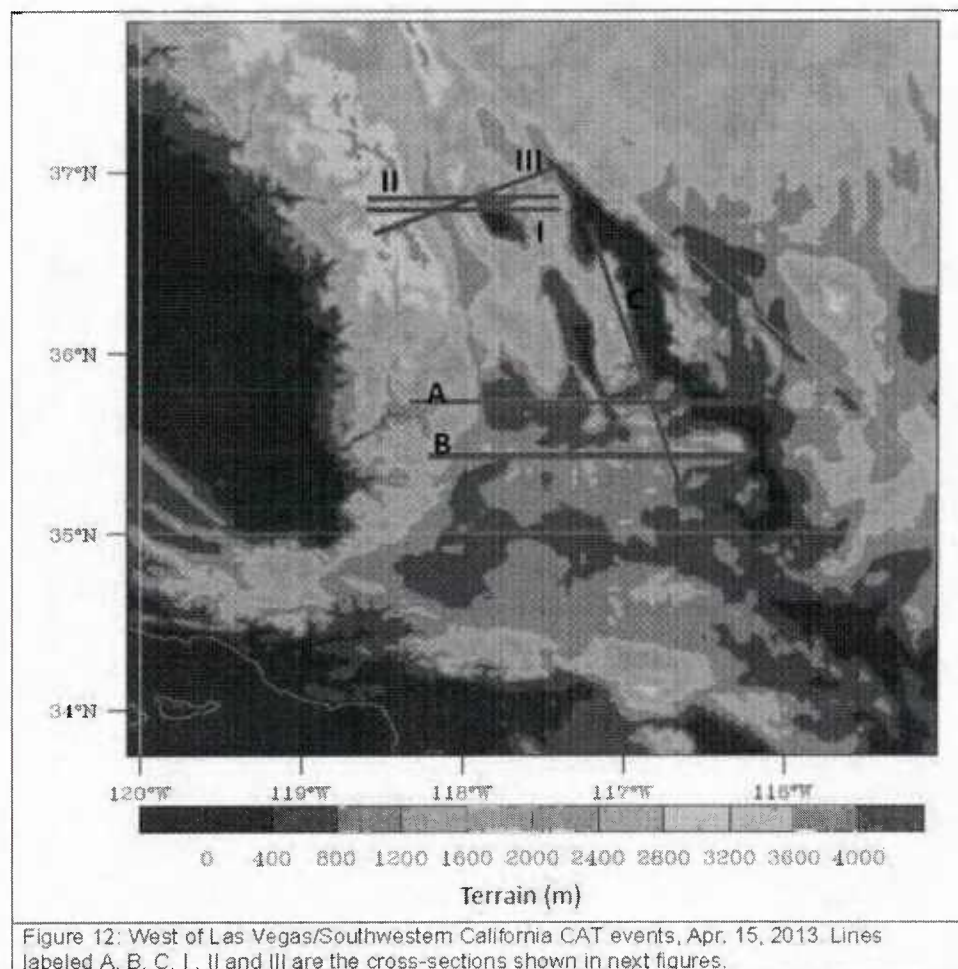


Figure 11: Subgrid-scale TKE (STKE) and TKE dissipation rate (EDR) along cross-section Line I shown in Figure 3 at different time periods on Apr. 8, 2013.



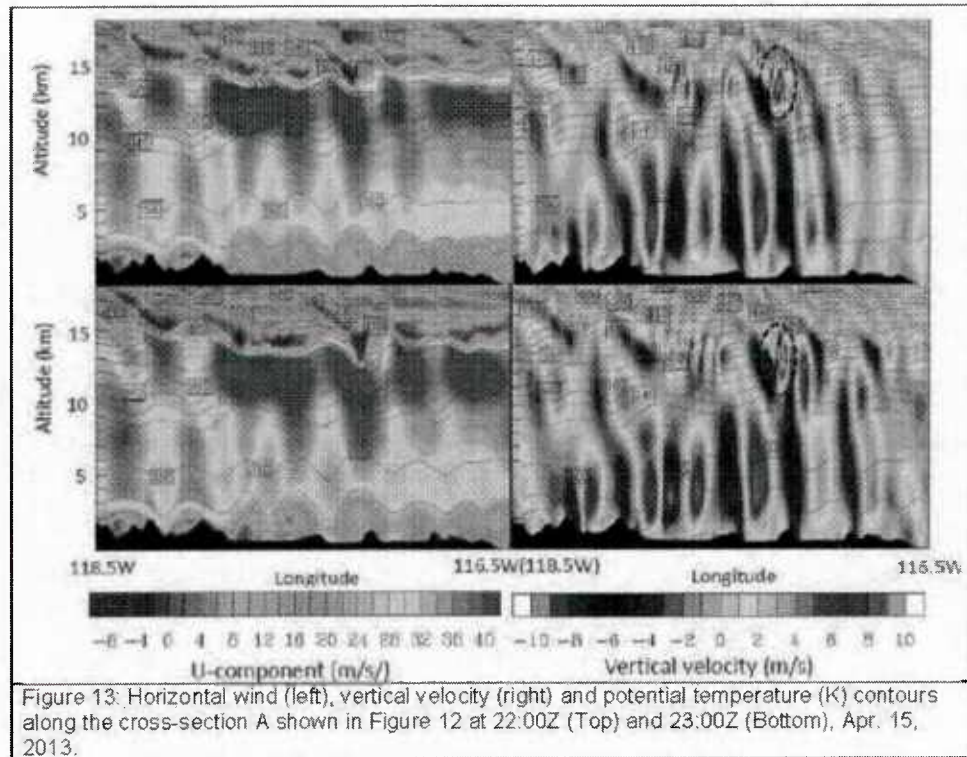


Figure 13: Horizontal wind (left), vertical velocity (right) and potential temperature (K) contours along the cross-section A shown in Figure 12 at 22:00Z (Top) and 23:00Z (Bottom), Apr. 15, 2013.

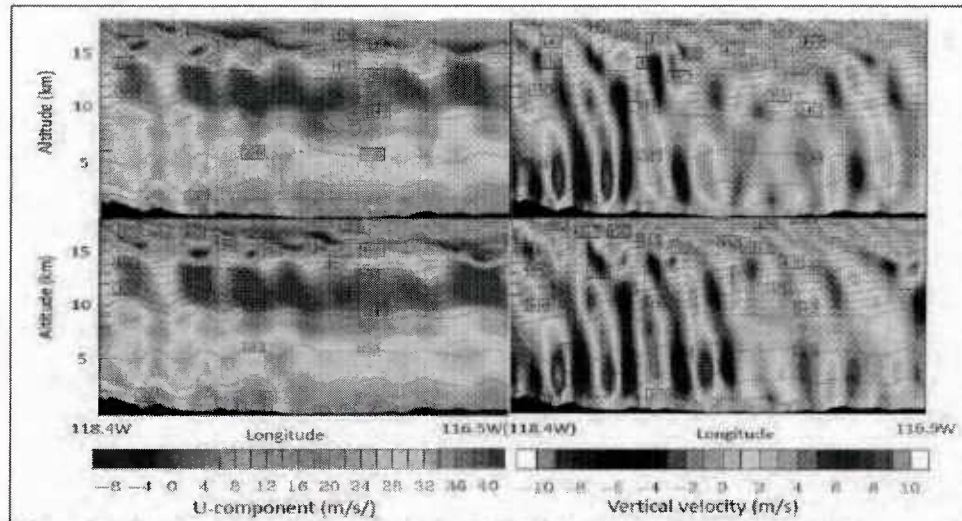


Figure 14: Horizontal wind (left), vertical velocity (right) and potential temperature (K) in contours at cross-section B shown in Figure 12 at 22:50Z (Top) and 23:00Z (Bottom), Apr. 15, 2013.

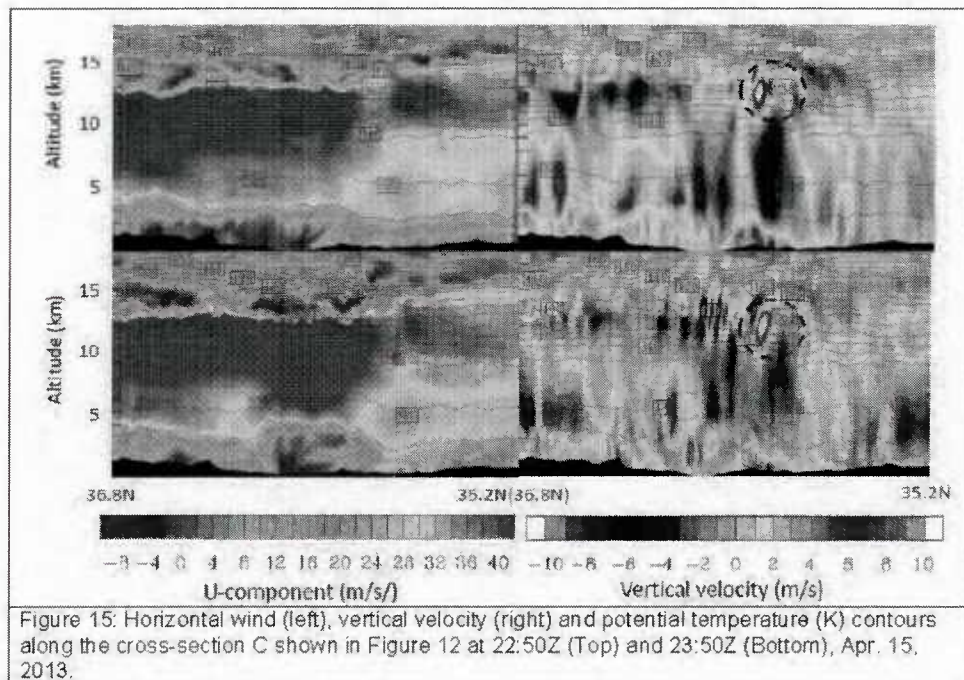
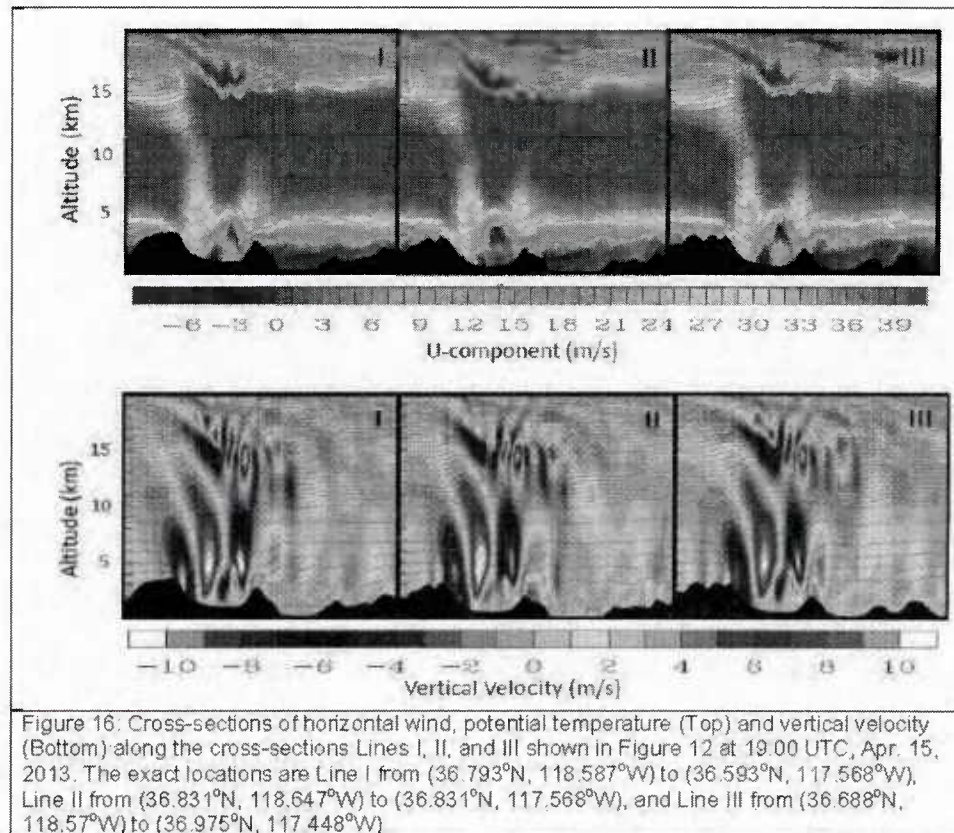
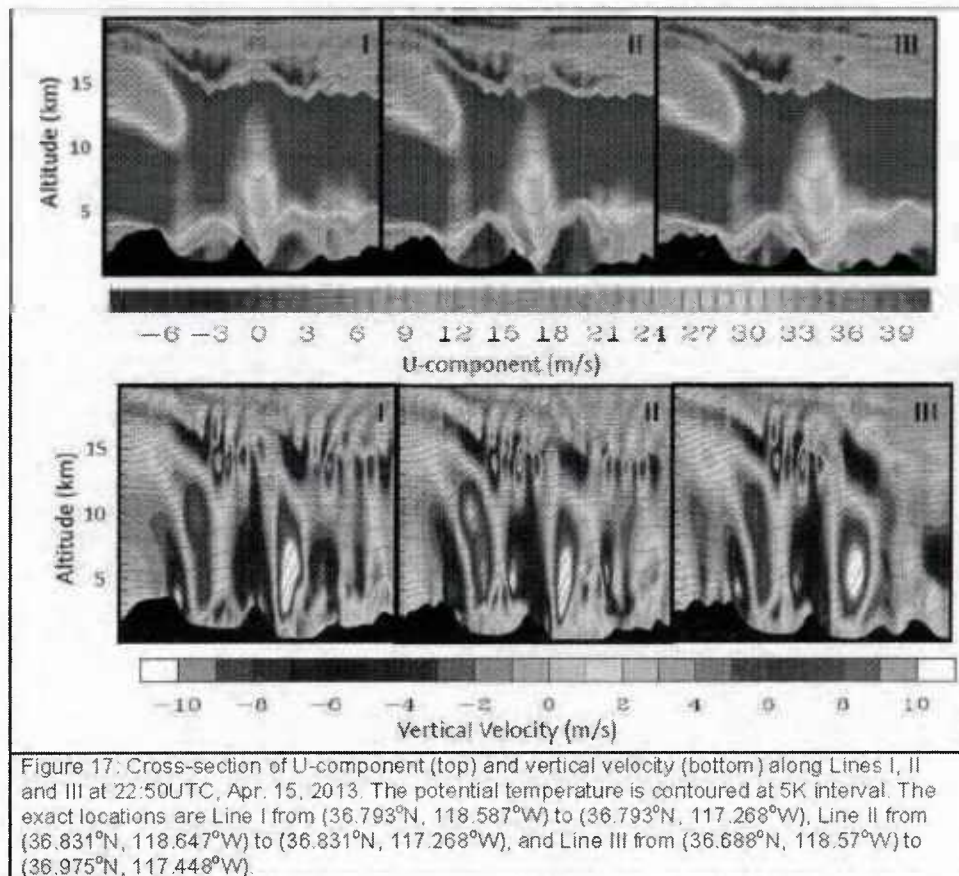


Figure 15: Horizontal wind (left), vertical velocity (right) and potential temperature (K) contours along the cross-section C shown in Figure 12 at 22:50Z (Top) and 23:50Z (Bottom), Apr. 15, 2013.





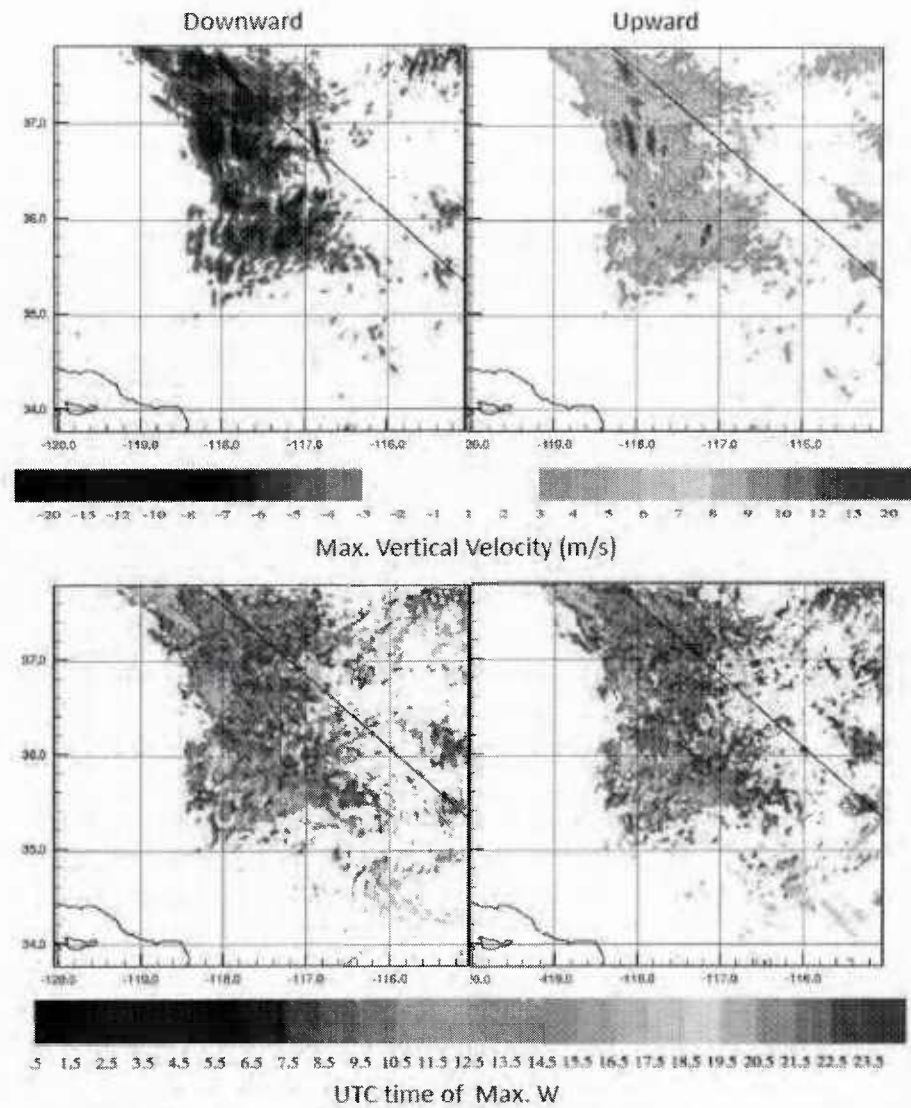


Figure 18: Maximum vertical velocity (top) between UTLS altitudes 7km to 15km and the corresponding time (bottom color bar) on Apr. 15, 2013.

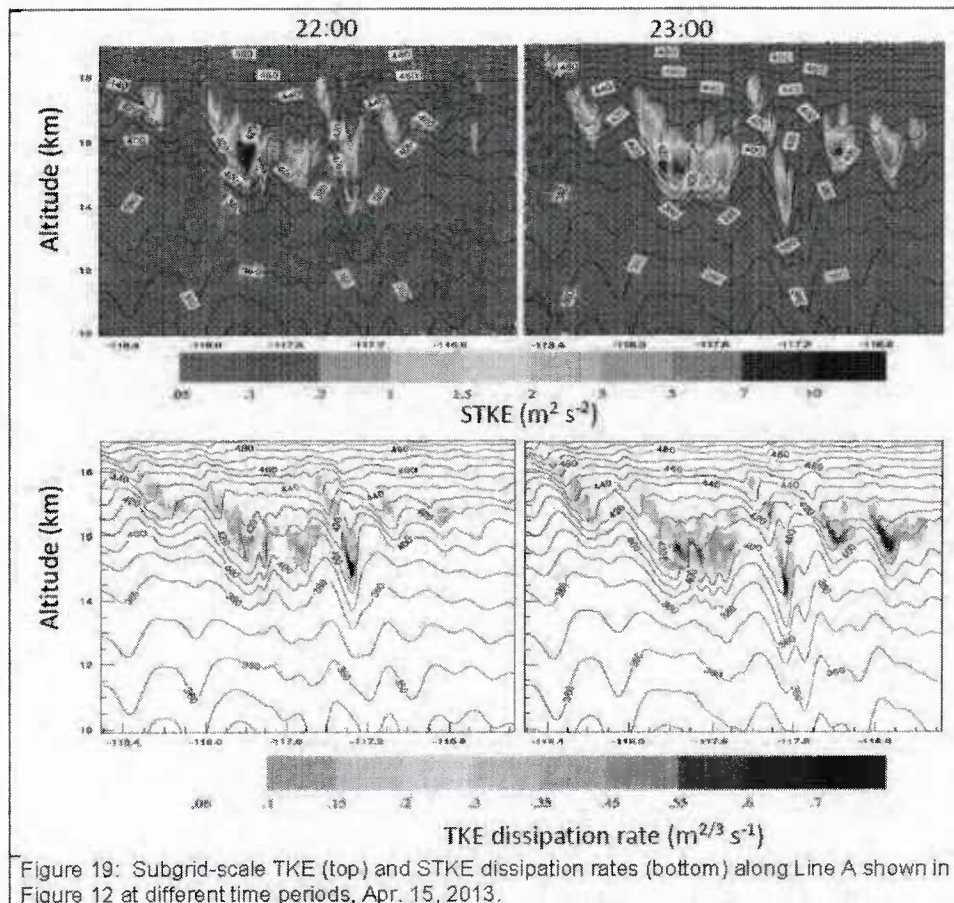


Figure 19: Subgrid-scale TKE (top) and STKE dissipation rates (bottom) along Line A shown in Figure 12 at different time periods, Apr. 15, 2013.

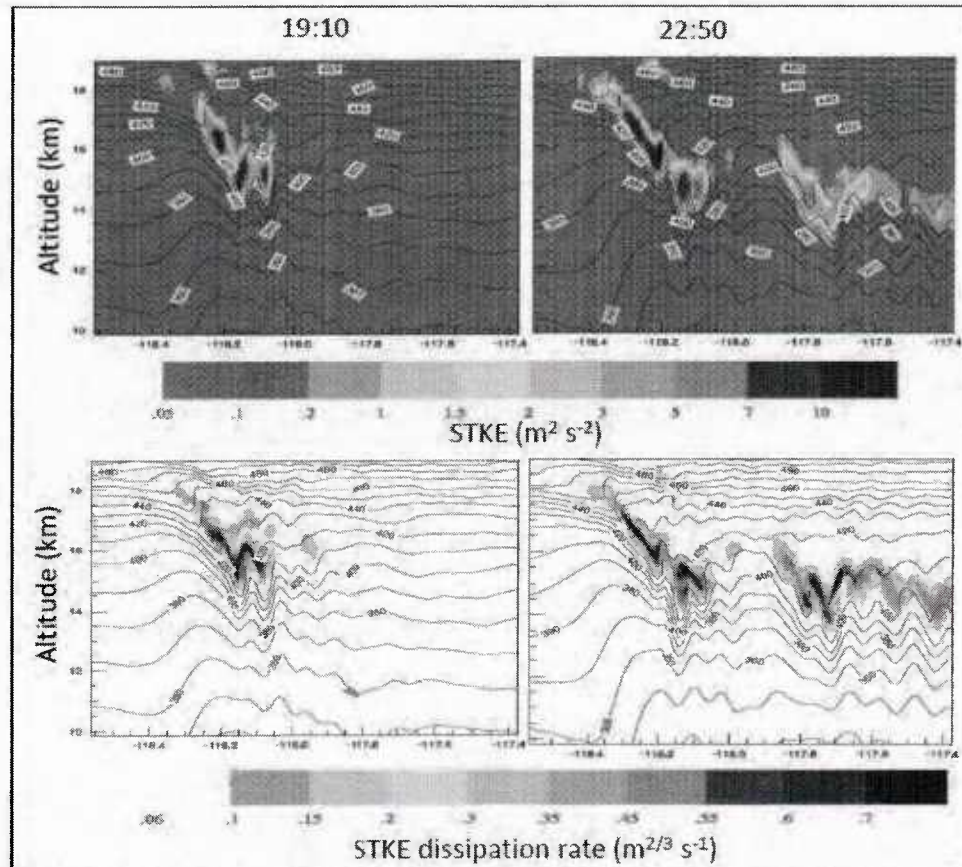


Figure 20: Subgrid-scale TKE (top) and STKE dissipation rates (bottom) along Line I shown in Figure 12 at different time periods, Apr. 15, 2013.

Sensitivity to vertical resolution:

Sensitivity of the results to vertical resolution was studied for cases from PIREP reports.

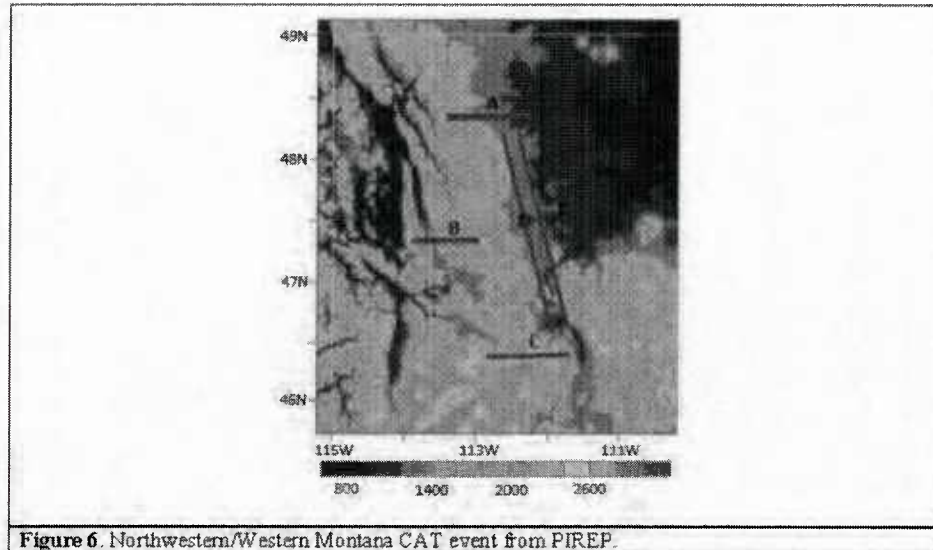


Figure 6. Northwestern/Western Montana CAT event from PIREP.

The Northwestern/Western Montana case shown in Figure 6 is characterized by the presence of well-organized patches of vertical velocity fine scale structures, which include secondary wave generation and K-H instability in the microscale nest.

Figure 7 is the cross-section showing comparisons for the CAT event computed with 135 and 162 vertical levels. The location of this cross-section, Line A, is shown in Figure 6. With 162-vertical levels, the microscale model generated well-organized vertical velocity structures with fine scales.

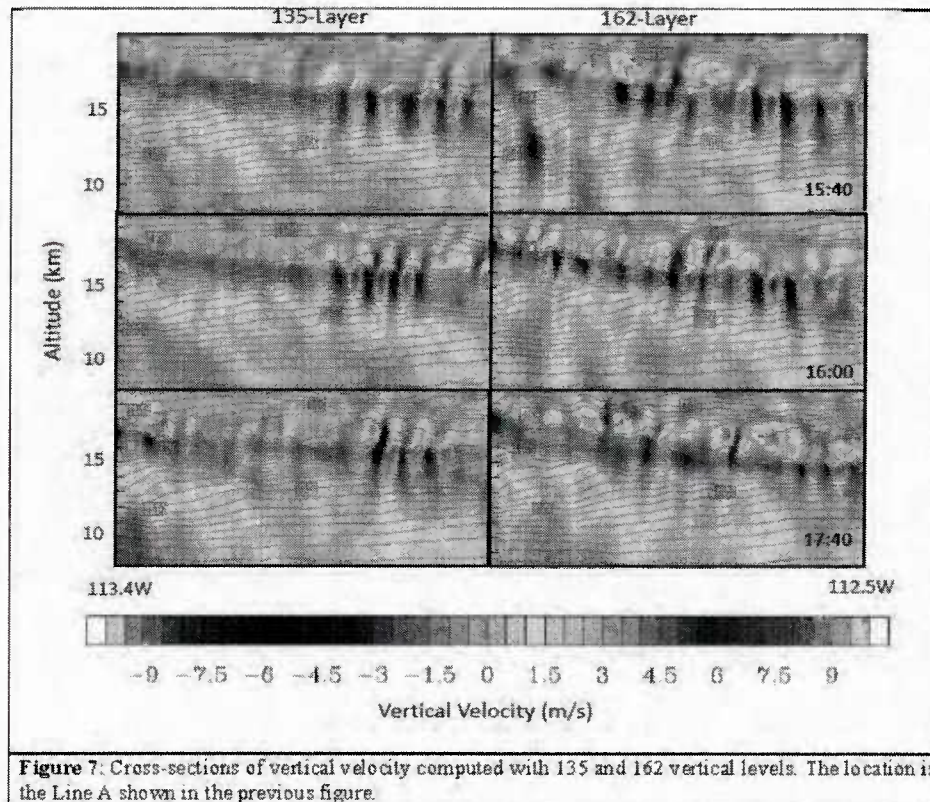


Figure 7: Cross-sections of vertical velocity computed with 135 and 162 vertical levels. The location is the Line A shown in the previous figure.

Figure 8 shows further comparisons of the horizontal wind, vertical velocity, momentum fluxes, and TKE dissipation rate at 16:00UTC along the cross-section A in Figure 6. The wind direction rotates (directional shear instabilities) above the stable layer near the jetstream.

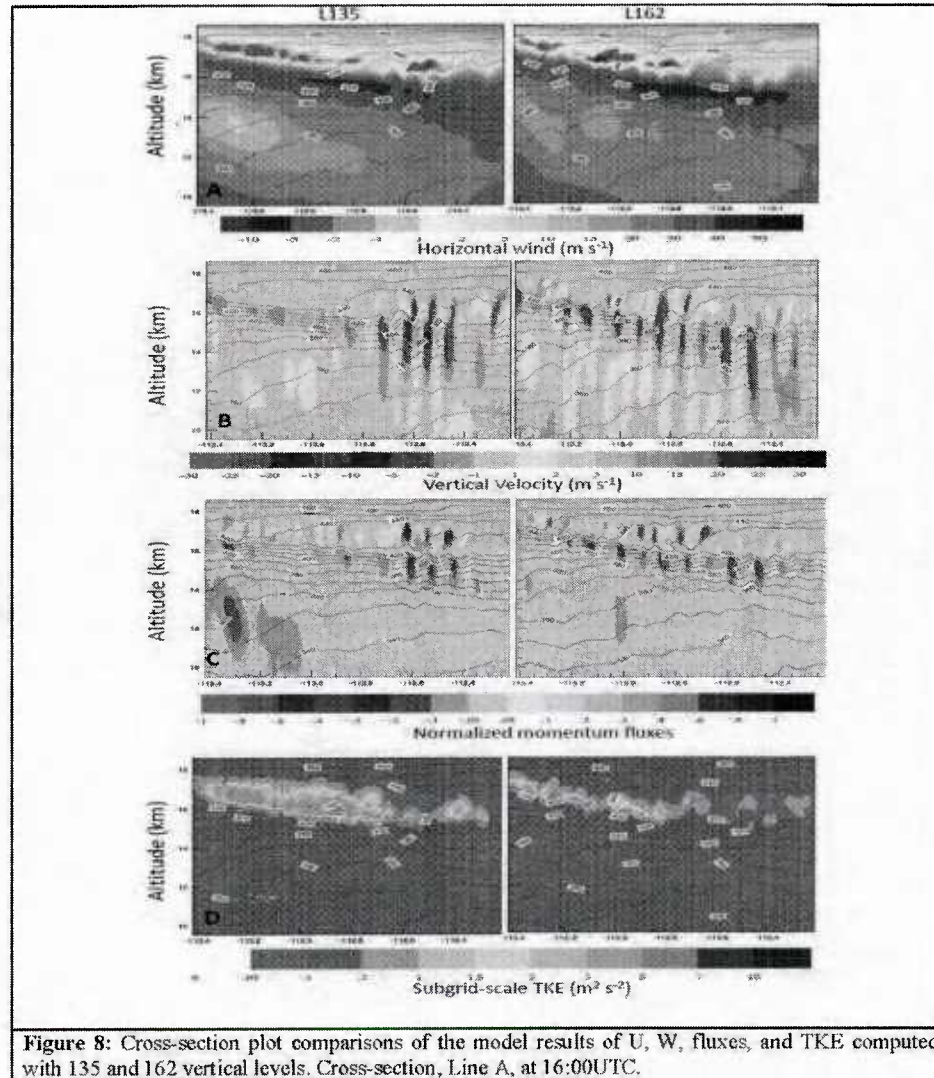


Figure 8: Cross-section plot comparisons of the model results of U, W, fluxes, and TKE computed with 135 and 162 vertical levels. Cross-section, Line A, at 16:00UTC.

Figure 9 is the cross-section along the Line B in Figure 6. Figure 9 indicates that with 162 levels, the microscale model resolved strong patches of vertical velocity.

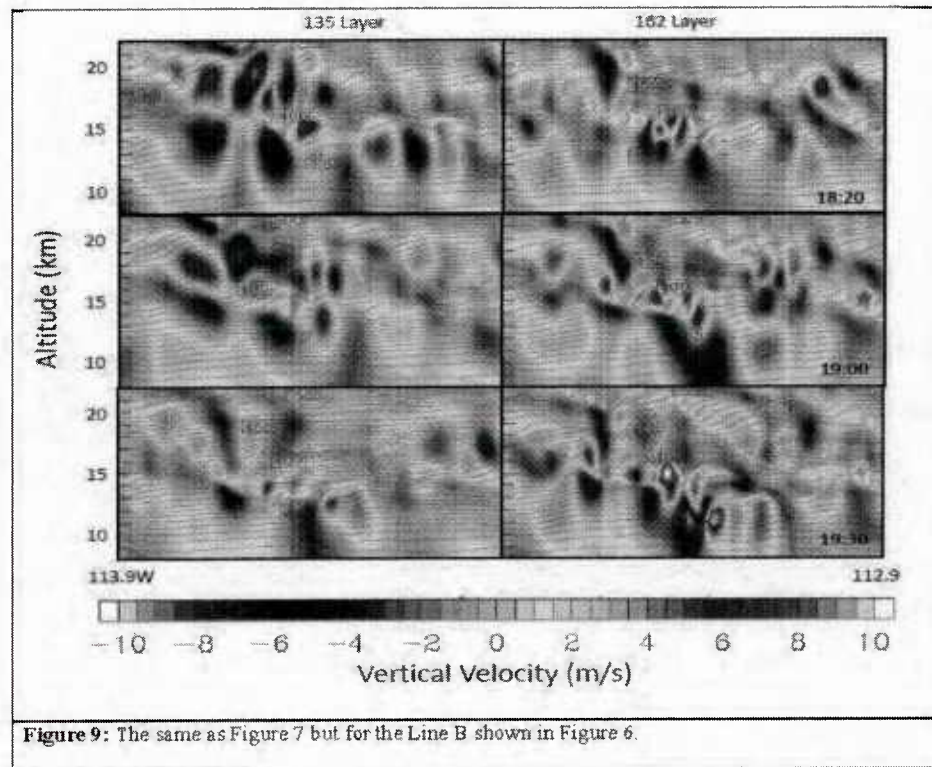


Figure 9: The same as Figure 7 but for the Line B shown in Figure 6.

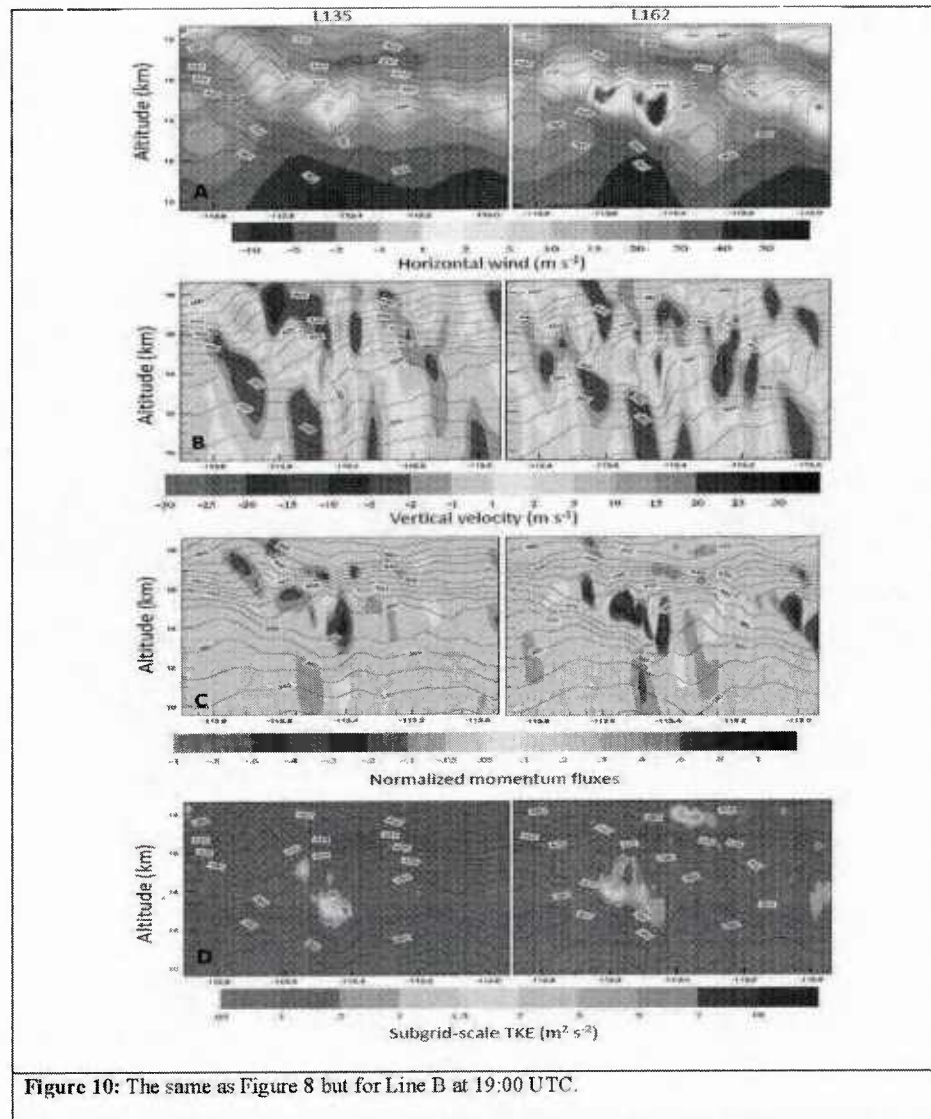


Figure 10: The same as Figure 8 but for Line B at 19:00 UTC.

Figure 10 is the same as Figure 8 but for the cross-section Line B at 19:00 UTC and the same conclusion can be made as from Figure 8.

The microscale model has predicted the right location that the reported severe turbulence occurred in the northwestern Montana. With 162-vertical levels, the microscale model resolved large upward and downward values of vertical velocity. We conclude that 160 vertical levels is desirable in the microscale nest to resolve CAT. The polarized Richardson number is the best indicator of UTLS turbulence over mountain terrains and jetstreams. It takes into account directionality of wind field, stratification and shear at every vertical level. This conclusion is further supported by many refereed publications and detailed comparisons with observations and measurements. Vertical velocity patches, fluxes, updraft/downdraft values and spacing between them are resolved in nested mesoscale/microscale simulations.

Current Operational Forecasting

Source: FAA Turbulence Impact Mitigation
Workshop, 3-4 September, 2014

Example of Current FAA Guidance

GTG

10,000 ft to FL450

0,1,2,3,6,9,12 hr lead-times

Analysis coefficients depend on
input data and resolution (tuning)

NOAA Rapid Refresh

CONUS

13.5 km grid

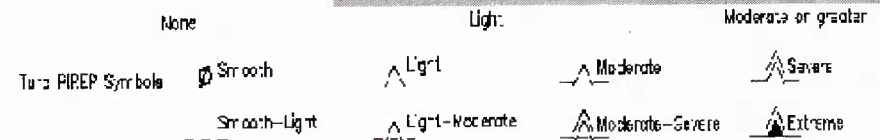
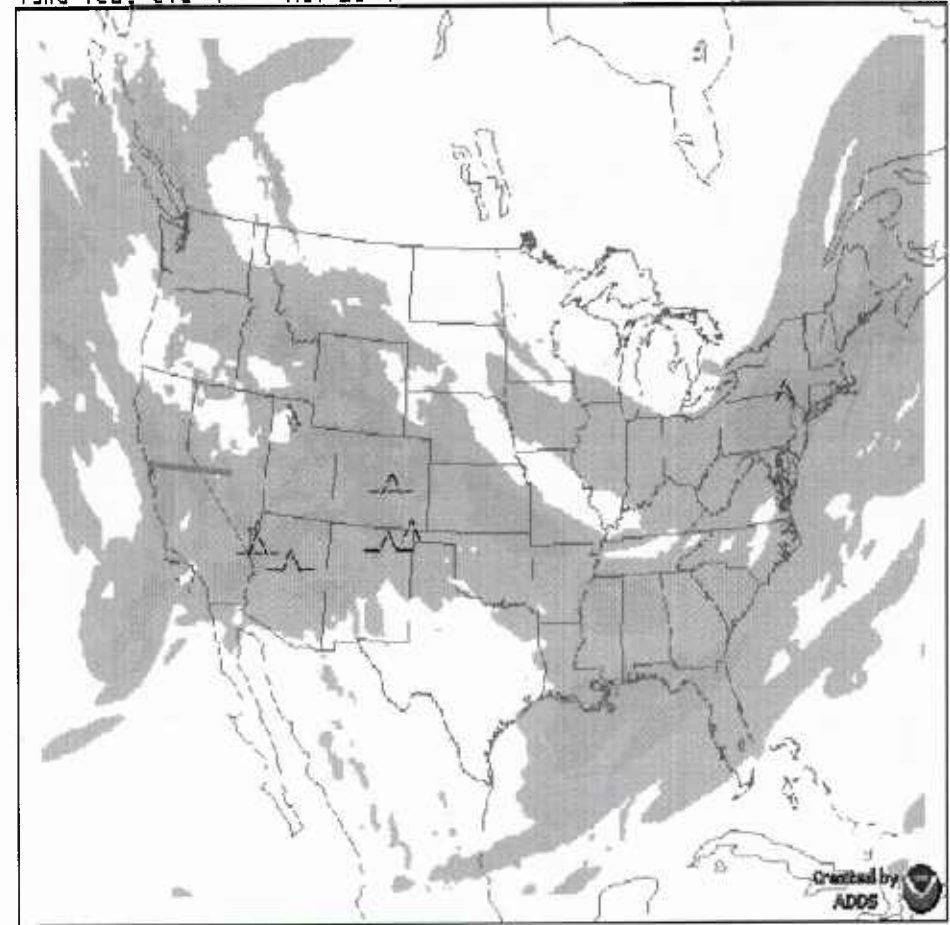
50 vertical levels

Hourly, but with delay

GTG2 - Maximum turbulence intensity (10000 ft. MSL to FL450)

Valid 1800 UTC Fri 12 Nov 2014

00-12 Forecast from 1800 UTC 14 Nov



Example of UTLS-2 v 1.0

Customer specific applications

Limited area HRMM

e.g. 1 km, 180 vertical level
Polarized Richardson Number

Resolves structure not present at 3 km

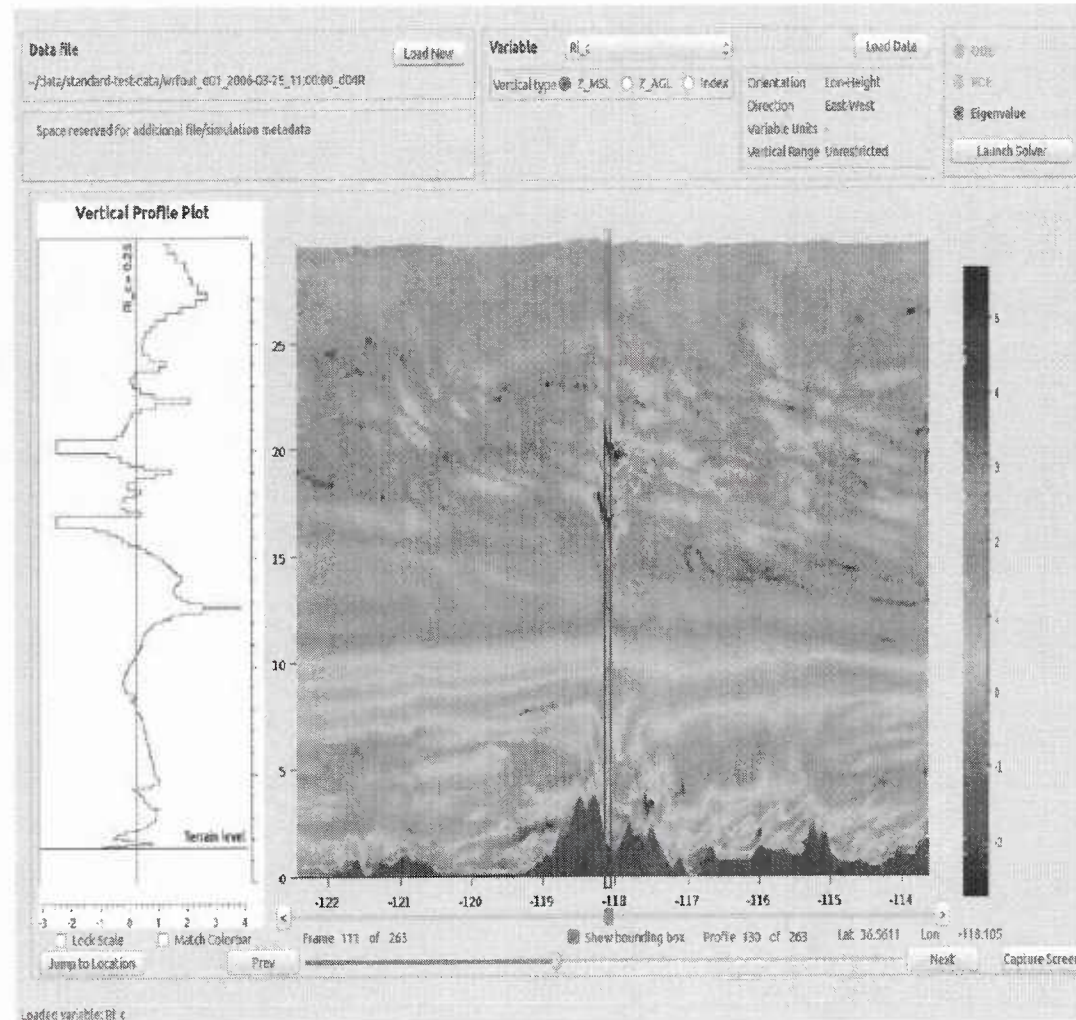
Real-time capable

User-specific analysis times

Inspection of vertical cross-sections

Inspection of specific vertical
profiles

User-defined analysis metrics



UTLS2 v1.0 CSV

FAA Weather Guidance

AC 00-45G Change 2 Aviation Weather Services

- ***Status: Final draft awaiting AFS-1 signature***
- ***Information pertinent to turbulence***
 - ***Primary/Supplementary terminology***
 - ***GTG2 description***
- ***Future change: GTG3 information***



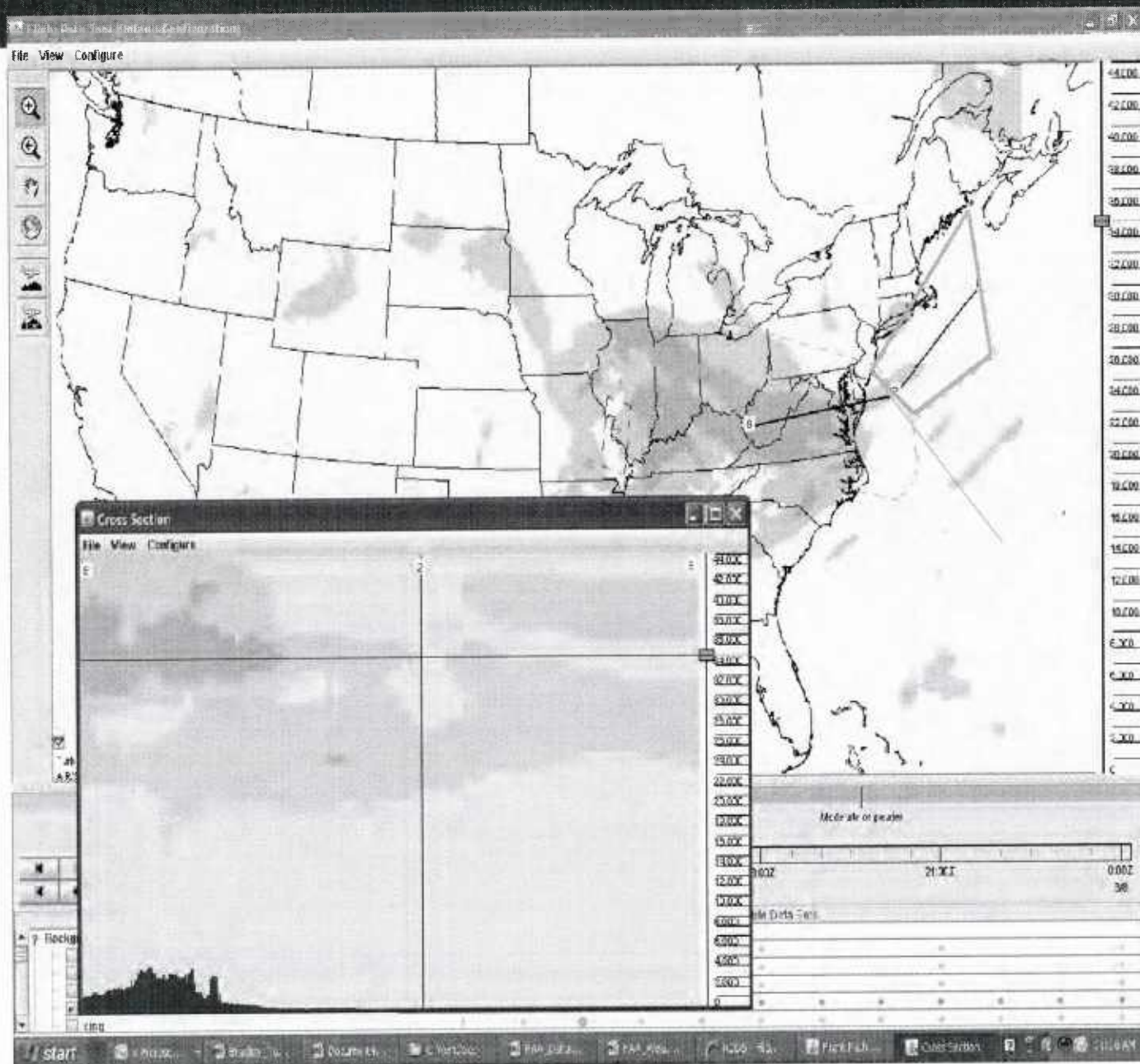
AC 00-63A Use of Displays of Digital Weather and Aeronautical Information

- ***Status: Published 4/7/14***
- ***Information pertinent to turbulence***
 - ***Authorization process for data link weather in the cockpit***



Federal Aviation
Administration

AIRMET GTG Comparison

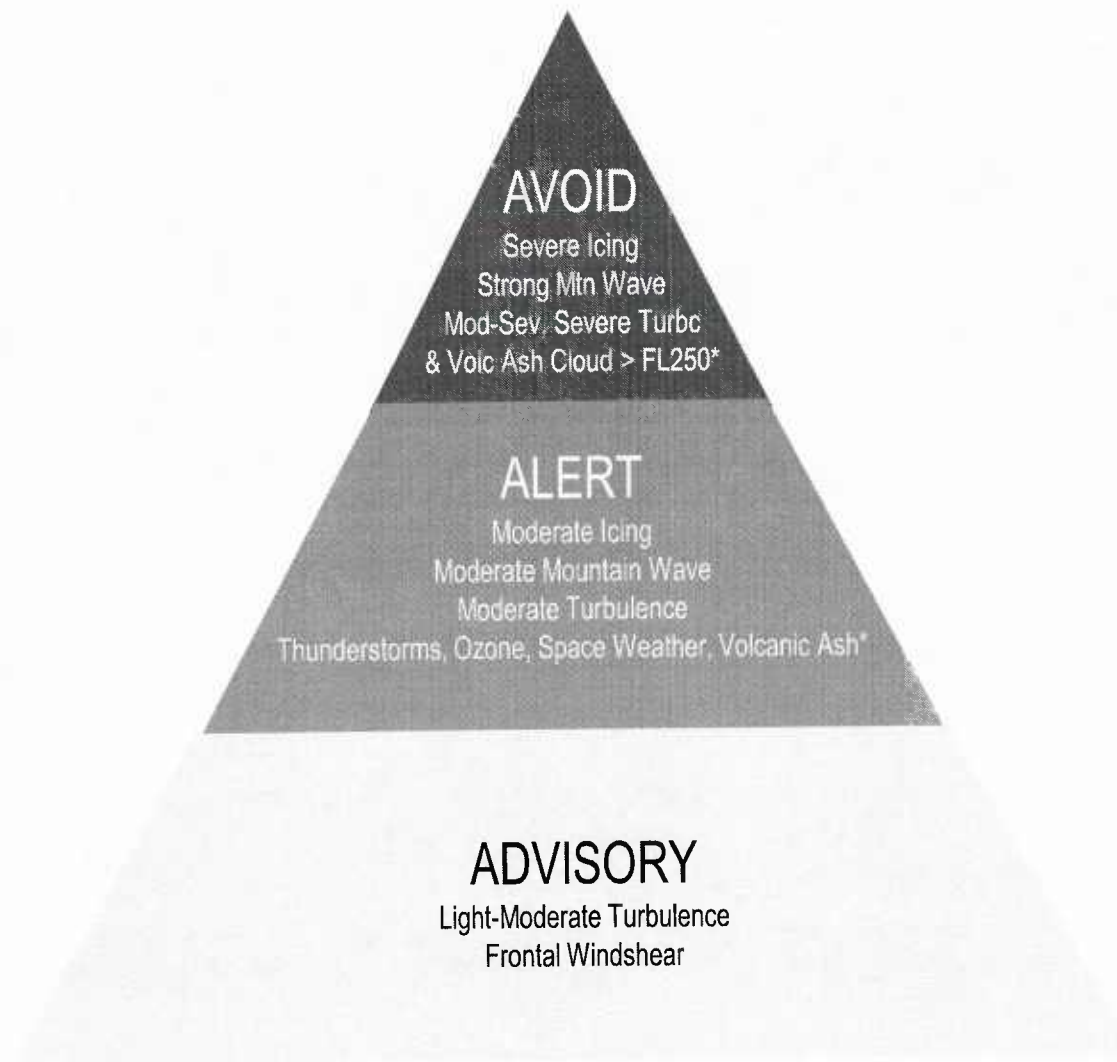


En Route Weather Hazards

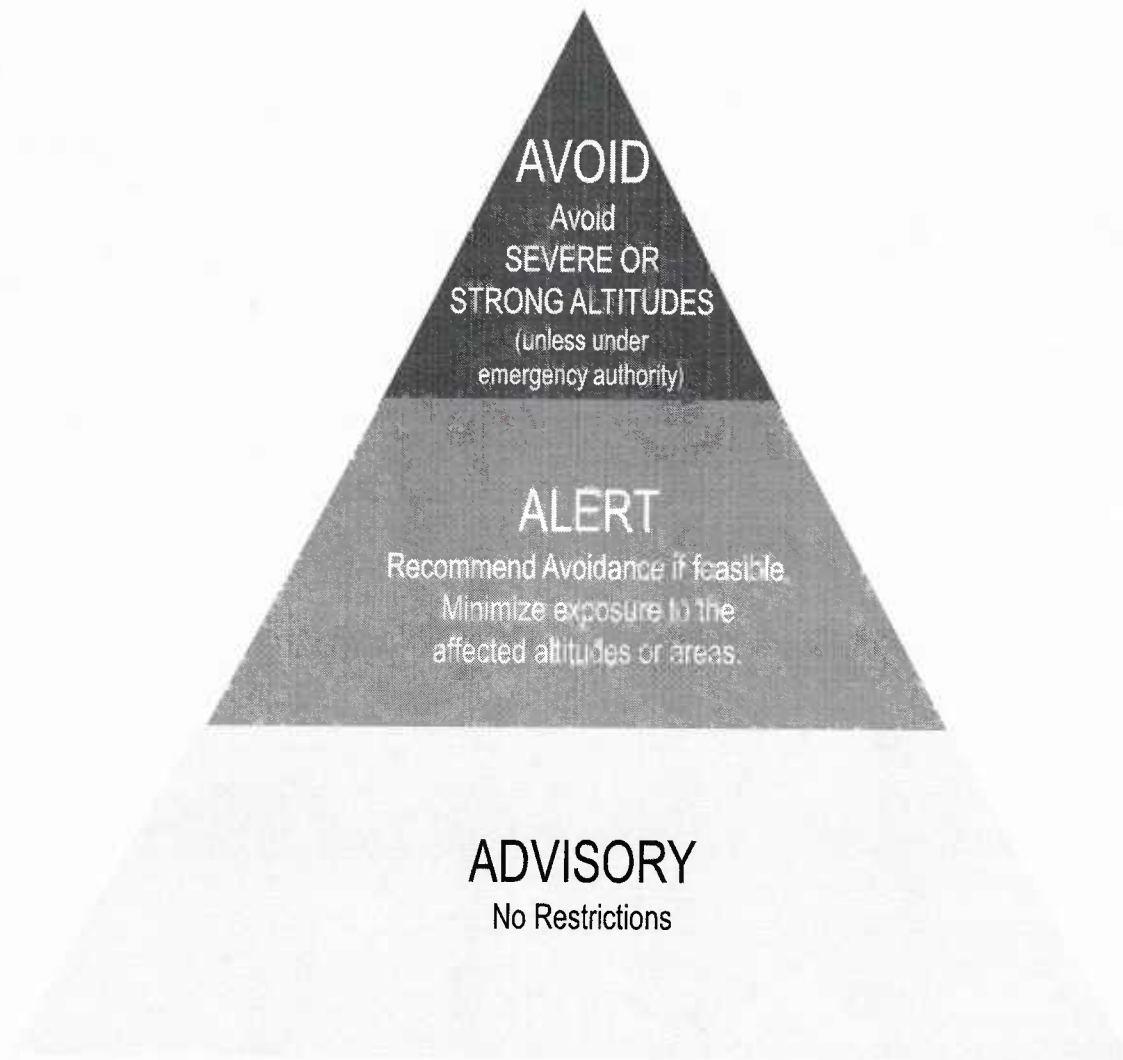
Delta has products & processes in place for these en route weather hazards:

- Turbulence
- Mountain Waves
- Thunderstorms
- Ozone
- Volcanic Ash
- Space Weather

TP Types and Hazard Intensity



Avoidance Policy and Procedures



Integrating Human & Model Forecast

Take advantage of advances in technology to move Delta into a real-time graphical world.

- Tablets in the cockpit
- Model based forecast

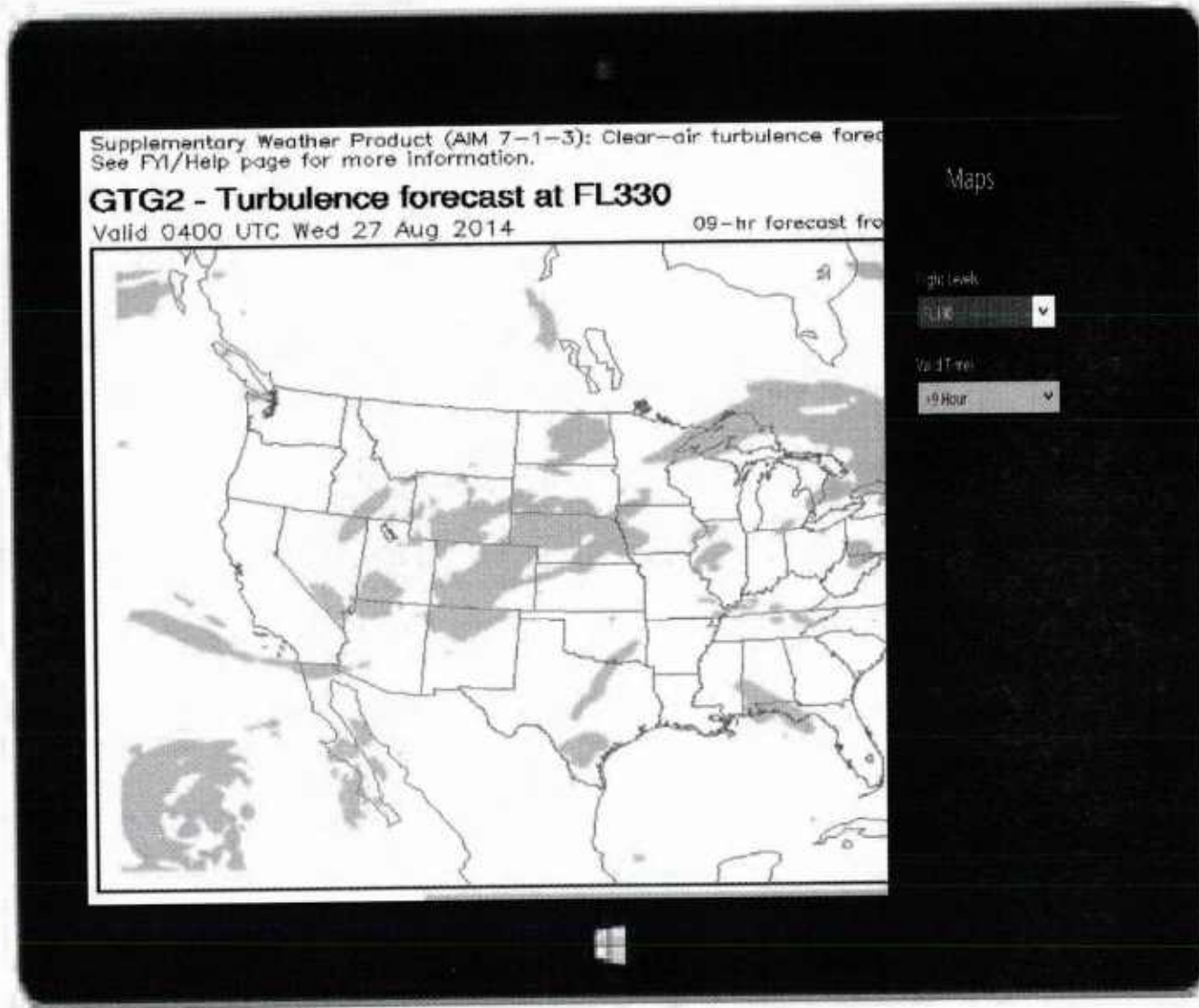


Step 1: Provide access to current products on tablet

Step 2: Enhance Products & integrate global data into dynamic display

Step 3: Transition Meteorology to over-the-loop instead of manual & in-the-loop forecast and provide flight specific graphics

Step 1: Provide Access to current products with prototype app



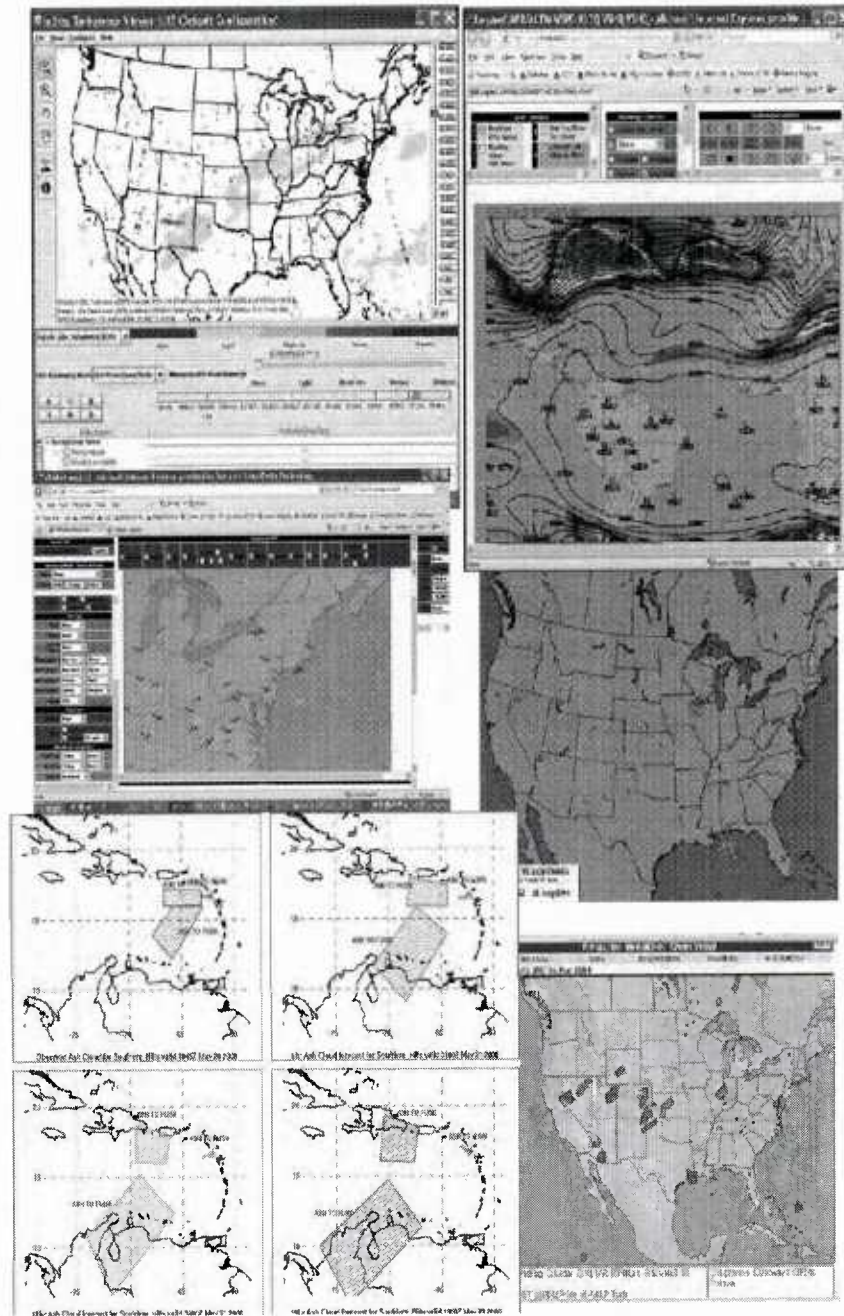
GTG Forecast available on the AWC website

Step 2: Enhance Products & Integrate Data on a Dynamic Display

Build a system that can integrate global data:

- Model data, including GTG
- TP's & Depictions
- Turbulence Reports, including traditional and auto-generated
- Satellite
- Lightning
- Radar
- SIGMETs
- Volcanic Ash Advisory

Develop tools for pilots, dispatchers & meteorologist using same data for common operation picture.



Step 3: Transition Meteorology to Human Over The Loop as Models Improve

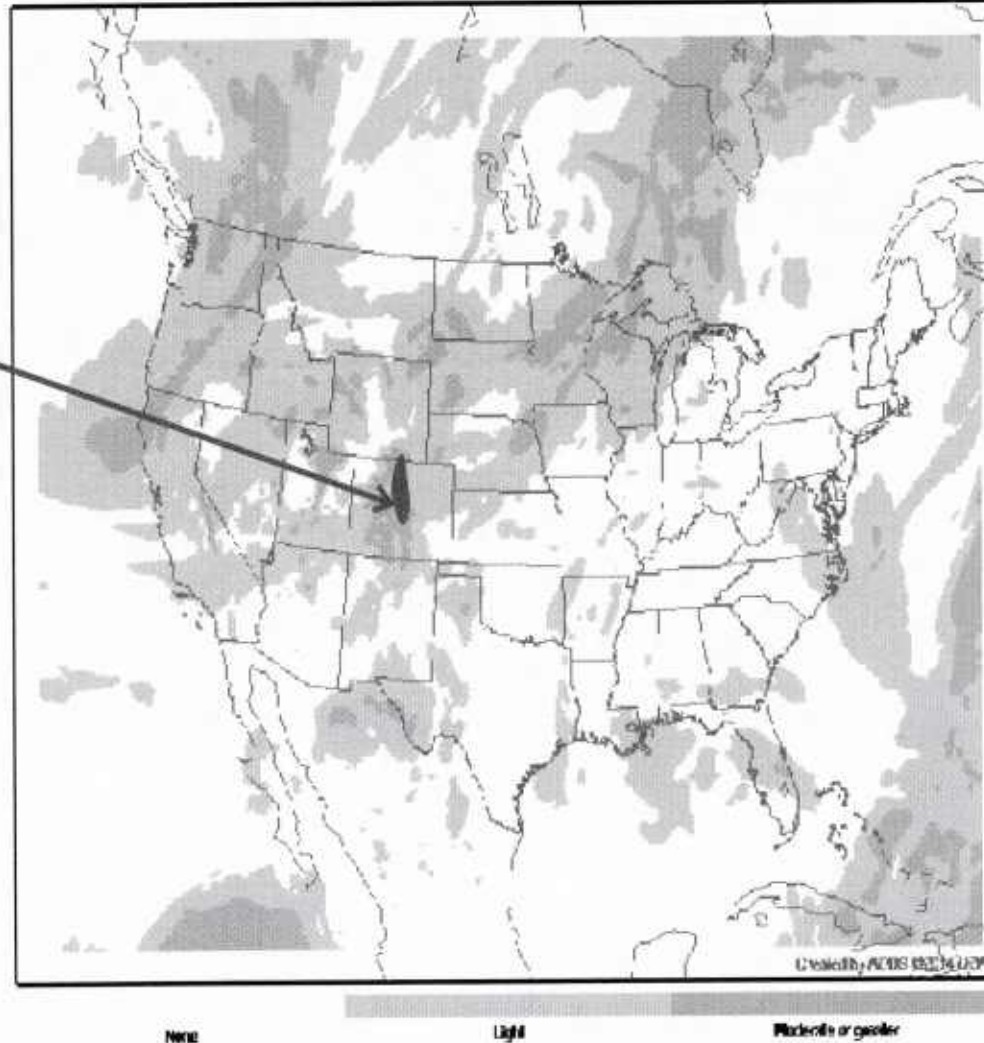
Supplementary Weather Product (ADM 7-1-8): Clear-air turbulence forecast only.
See FYI/Hep page for more information.

GIG2 - Maximum turbulence intensity (10000 ft. MSL to FL450)

Valid 1600 UTC Mon 25 Aug 2014

32-hr forecast from 1400 UTC 25 Au

Delta Meteorologist
thinks there is
potential severe
turbulence and can
increase intensity.



UTLS-2 v1.0

Technology Comparison

UTLS-2 v 1.0 Software Demonstration

STTR2: Summary of Completed Tasks

- ❖ Developed models of turbulence induced by rotational wind fields in the UTLS (polarized Richardson number).
- ❖ UTLS-2 v 1.0 software created.
- ❖ Implemented physics based subgrid scale parameterization of shear-stratified UTLS turbulence (variable turbulent Prandtl number).
- ❖ Developed multi-scale parameterizations of UTLS shear-stratified turbulence; analyzed vertical velocity-temperature fluctuations; created catalogues for a representative set of shear-stratified UTLS turbulence events.
- ❖ Performed multi-scale simulations with various horizontal and vertical resolutions and determined optimal configurations.
- ❖ Investigated how the computational results depend on the number of vertical levels. Determined the minimum number of vertical levels needed to achieve desired accuracy.

STTR2: Summary of Completed Tasks

- ❖ Developed and Implemented novel implicit relaxation techniques in limited area models of UTLS.
- ❖ Delineated physical parameters controlling the size, distribution, variability and morphology of high impact stratospheric turbulent layers. Investigated detailed temporal and spatial statistical characteristics of turbulent layers and determined optimal physical parameters in parameterization schemes.
- ❖ Tested computational domain sizes and configurations to achieve optimal performance. Selected optimal prototypes for forecasting tests.
- ❖ Developed and tested a new fast and accurate time stepping scheme for UTLS forecasting (nearly three times faster than current schemes).
- ❖ Performed high resolution multi-scale numerical simulations and analyzed high impact turbulence dynamics in UTLS. Performed validation and verification of fine scale modeling and computational results using available data bases and PIREPs.